Regulation of the Structure and Function of Skeletal Muscle and Tendon by Myostatin

by

Christopher L. Mendias

A dissertation submitted in partial fulfillment
of the requirements for the degree of
Doctor of Philosophy
(Molecular and Integrative Physiology)
in The University of Michigan
2007

Doctoral Committee:

Professor John A. Faulkner, Chair
Associate Professor Susan V. Brooks Herzog
Associate Professor Jeffrey F. Horowitz
Assistant Professor Daniel E. Michele

Acknowledgements

I would like to thank my committee for the help they have provided. My advisor, John Faulkner, has taught me so much about the process and business of science. His guidance, support, mentorship and colorful stories have been very much appreciated. I would also like to thank the other members of my committee, Susan Brooks, Jeffrey Horowitz and Daniel Michele, for their insight and advice. I appreciate the time you have taken to help in my development as a scientist.

I would also like to thank the many members of the Muscle Mechanics Lab for their invaluable assistance. In particular, I would like to express my gratitude for the assistance of two individuals, Cheryl Hassett and Dennis Claflin. Without the technical assistance of these two individuals I would not have been able to complete many of the studies in this dissertation.

I would like to thank my friends who have made my time here in Ann Arbor a blast.

And finally, I would like to thank my family for their encouragement and support from 2500 miles away, even they had no idea why I wanted to move to Michigan from Arizona.

Table of Contents

List of Figures

List of Tables

Chapter I

Introduction

Background and Hypotheses

The ability of skeletal muscle and tendon to adapt to environmental changes, injury, illness and other physiological conditions is critical in determining the overall health, mobility and athletic performance of an individual. Determining the cellular and molecular mechanisms behind the adaptation of skeletal muscle and tendon provides important insights into basic biological processes and the design of therapies for the treatment of diseases and injuries. Several cytokines have been identified as important regulators of skeletal muscle mass. One of the most potent cytokines that regulate skeletal muscle mass is myostatin (GDF-8). Myostatin is a member of the TGF-ß superfamily of cytokines and the targeted inhibition of myostatin results in an up to two-fold increase in skeletal muscle mass (54, 84). Due to the profound increase in skeletal muscle mass that occurs as a result of the deficiency of myostatin, much interest has focused on the targeted inhibition of myostatin in the treatment of muscle injuries and wasting diseases (81).

While the inhibition of myostatin results in a clear muscle mass phenotype, arguably with as great an impact on muscle mass as any other single cytokine, the full range of mechanical consequences of myostatin deficiency are not known. Using classical muscle mechanics experimental techniques in the

myostatin-deficient mouse model, along with contemporary molecular biology experimental techniques, this doctoral dissertation determined the mechanisms by which the deficiency of myostatin regulates the structure and function of skeletal muscles and of tendons. This introductory chapter describes the molecular biology of myostatin, the structure, function and adaptation of skeletal muscle and tendon tissue, and preliminary experiments that were critical for the research studies in Chapters II and III.

In Chapter II, the impact of the deficiency of myostatin on the contractile properties and extracellular matrix composition of skeletal muscle was determined. We hypothesized that the deficiency of myostatin increases the maximum tetanic force (P_o), but decreases the specific P_o (sP_o) of muscles and increases the susceptibility of muscles to contraction-induced injury. To test these hypotheses, we measured the *in vitro* contractile properties of EDL and soleus muscles from *MSTN*$^{+/+}$, *MSTN*$^{+/-}$ and *MSTN*$^{-/-}$ mice and subsequently subjected the muscles to a lengthening contraction protocol. We also determined the impact of myostatin on the connective tissue composition of skeletal muscle. We hypothesized that the deficiency of myostatin decreases the type I collagen content of muscle connective tissue. The type I collagen content of EDL and soleus muscles from *MSTN*$^{+/+}$, *MSTN*$^{+/-}$ and *MSTN*$^{-/-}$ mice was determined, as well as the expression of type I collagen in cultured skeletal muscle myotubes treated with myostatin. The results from Chapter II indicate that the deficiency of myostatin increases the P_o of muscles, increases the

susceptibility of muscles to injury and decreases the type I collagen content of skeletal muscle connective tissue.

The experiments on skeletal muscles in Chapter II lead to the exploration of the role of myostatin in the regulation of tendon structure and function in Chapter III. We hypothesized that the deficiency of myostatin results in smaller, stiffer, and more brittle tendons. To test this hypothesis, we measured the stress-strain relationships of tendons from the tibialis anterior muscles of *MSTN*$^{+/+}$ and *MSTN*$^{-/-}$ mice. We also measured the expression of structural and cell cycle regulatory genes in whole tendon tissue and in cultured tendon fibroblasts treated with myostatin. Our studies of tendons lead to the novel finding that, in addition to regulating skeletal muscle structure and function, myostatin also regulates the structure and function of tendon tissue.

Skeletal Muscle Structure and Function

Skeletal muscles consist of hundreds to thousands, and sometimes millions, of long, multinucleated fibers organized together by an extracellular matrix. There are three general layers of extracellular matrix, or connective tissue, in muscles – the outermost layer is the epimysium, the intermediate layer is the perimysium and the inner most layer is the endomysium. Understanding the structure and function of each of these three layers requires a hierarchical approach. The structure and function of the epimysium and perimysium will be discussed in a whole body and tissue level biomechanical context, whereas the structure and function of the endomysium will be discussed in the context of cellular and molecular biomechanics.

Epimysium and perimysium. The epimysium covers the surface of the muscle and has important roles in force transmission and insulation of the muscle (46). Processes from the epimysium extend into muscle tissue and form the second layer of connective tissue, the perimysium. The perimysium contains blood vessels, nerves and lymphatic ducts, and structurally divides muscle fibers into functional groups called fascicles. The orientation of fascicles are important determinants of the direction of the force a muscle can generate (55). The variation in the number of fascicles allows muscles to adopt a complex geometry and facilitate complicated movements at joints. There is a trade-off between the angle at which the fascicles are oriented and the amount of force the fascicles are able to generate. The angle at which the fascicles are oriented to the insertion is known as the angle of pennation (θ). The force that a muscle fiber can generate is proportional to the cosine of θ (50). As θ goes from 0º to 90º, the cosine of θ goes from 1 to 0. Therefore, a fascicle can generate the greatest amount of force when θ is 0º, and can generate no force when θ is 90º. An interesting feature about the angle of pennation is that, as muscle fibers undergo hypertrophy, there is an increase in θ (50). While a muscle that experiences hypertrophy is generally able to generate a greater total force, due to the cosine relationship between θ and net force development, the muscle must undergo relatively greater increases in hypertrophy to generate greater net forces across a joint.

In addition to providing a hierarchical structure to skeletal muscle fibers, the epimysium and perimysium may also protect an injured muscle from further

damage. The epimysium and perimysium are composed mostly of the fibrillar collagens, type I and type III (43). These collagens act as molecular springs and exist in parallel with the muscle fibers (9). While some debate still exists on the topic, the epimysium and perimysium are thought to protect muscle fibers against stretch induced injury by taking up the load during stretch and protecting the skeletal muscle fibers from further injury (4).

Endomysium. The innermost layer of connective tissue is the endomysium. The endomysium is composed of two layers of mostly type I and type III collagen that fuse to form a sheet-like structure that inserts into the tendon (43). The endomysium is important in transmitting forces generated within the muscle to the tendon as well as laterally to other muscle fibers (63). The endomysium is connected to the basement membrane that directly surrounds each muscle fiber. The basement membrane is composed mostly of type IV collagen (43). Unlike the fibrillar type I and type III collagen, type IV collagen forms a mesh-like network that surrounds the muscle fiber (9). Embedded within the endomysium and basement membrane are two classes of proteins that have important functions. The first class of proteins are responsible for force transmission from the sarcomeres through the intramuscular connective tissue and eventually to tendons and bone. These proteins, such as integrin and fibronectin, provide a mechanical link between the structural proteins of muscle fibers with the collagen network of the extracellular matrix (37). The second class of proteins are released from the matrix after injury and are important in initiating the recovery of muscle from injury (24, 30, 76). This second class of

proteins will be discussed in the section that focuses on contraction-induced injury.

Molecular Mechanisms of Force Transmission in Skeletal Muscle. The structure within muscle fibers that is responsible for the generation of force is the sarcomere. The sarcomere is composed of three major components – the thick filament that is surrounded by six thin filaments that are shared with the six surrounding thick filaments. The thin filaments are imbedded in the Z-disks at the end of each sarcomere (73). The thick filament contains the protein that is the molecular motor that drives muscle contraction, myosin heavy chain. The head of the myosin molecule interacts with the actin molecules on the thin filaments. The myosin binding sites on the actin molecule are regulated by the troponin protein complex. The thick filaments are anchored to the Z-disks via the proteins titin and nebulin. The Z-disks are responsible for transmitting the force generated within the sarcomere to the extracellular matrix (ECM) (11, 67). The Z-disks accomplish this by linking to structures that transmit force both laterally and longitudinally.

For the lateral transmission of force, the Z-disks link with a structure at the plasma membrane called the costamere. The Z-disk interacts with the costamere via the dystrophin class of proteins (11, 67). The dystrophin proteins link the membrane bound dystroglycan complex, which is in turn linked to the extracellular matrix via laminin and fibronectin. Longitudinal force transmission is accomplished via a mechanical linkage between the Z-disk and the actin cytoskeleton of the muscle cell (55). This force is transmitted to the ends of the

fibers at the location where the fibers insert into tendons. This linkage comes about due to the association between the actin cytoskeleton with vinculin and talin (12). Vinculin and talin transmit force across the plasma membrane using the fibronectin receptor that is bound to fibronectin in the ECM (3, 12). The contraction of a muscle is therefore dependent upon the effective transmission of the forces generated by the interaction between actin and myosin molecules through structural proteins, out to the endomysium and eventually to tendons that link the muscles to bone.

Skeletal Muscle Contraction. There are three general types of skeletal muscle contractions. The contractions are defined by the change in fiber length that occurs subsequent to muscle activation (18). During a shortening contraction, the force generated by the muscle is greater than the load placed on the muscle. Consequently, the distance between the distal and proximal ends of a muscle decrease and positive work is performed. During an isometric contraction, the force generated by the muscle is equal to the load on the muscle. Consequently, the length of the muscle fiber does not change significantly and no net work is done. The amount of force a muscle can generate is greatest during an isometric contraction and is referred to as the maximum isometric tetanic force (P_o). The specific maximum tetanic force (sP_o) is the value P_o normalized to the CSA. During a lengthening contraction, the load on the muscle is greater than the force generated by the muscle. Consequently, the distance between the ends of the muscle increases and there is net negative work done. Contraction-induced injury occurs during lengthening

contractions when the magnitude of the opposing force is sufficient to disrupt the ultrastructure of individual or groups of sarcomeres (18). Clinically, contraction-induced injuries are commonly referred to as muscle strains.

Tendon Structure and Function

Tendons are connective tissue structures responsible for the transmission of the force developed by muscles to bones, and in doing so, enable the contraction of muscles to lead to joint movements and locomotion. Force transmission may also occur in the opposite direction, from bone through tendon to muscle. The transmission of force in this direction allows for the storage of elastic energy within the tendon and muscle, but may also lead to damage to the muscle. During a lengthening contraction, tendons may protect muscle from injury by limiting the strain placed on muscle fibers (23).

Tendon Structure. Tendon tissue is arranged in an hierarchical order, similar to skeletal muscle. Fibroblasts are the major cellular component of tendons and consequently are responsible for the maintenance, repair, modification of the tendon ECM (37). The fundamental anatomical structure in tendons is the tendon fiber (31, 82). The tendon fiber is composed of collagen fibrils and other structural proteins and is wrapped in a layer of connective tissue that carries nerve endings, capillaries and lymphatic ducts. Fibers coalesce to form fascicles, that are surrounded by a second connective tissue layer that contains arterioles, venules and axons of nerve cells. Tendon fascicles are surrounded by a third connective tissue structure called the epitenon. The synovial sheath surrounds the epitenon and secretes synovial fluid that helps to

cushion the tendon and reduce friction from adjacent tissues as the tendon is stretched and relaxed. Early damage to tendon tissue can result in an overproduction of tendon synovial fluid (42). Swelling in the synovium is referred to as tenosynovitis and is an early clinical diagnostic sign that tendon tissue is injured. Tendons are linked to muscle tissue by myotendinous junctions located at the ends of the tendon (82). Many muscles have an aponeurosis or internal tendon, that is an extension of the tendon into the muscle tissue. At the other end, tendons are connected to bone by strong fibrous structures called entheses (6).

Tendon Mechanical Properties. The proteins and molecules that make up the tendon can be divided into two categories, based upon the mechanical properties they impart to tendon – stiffness and viscoelasticity. The stiffness of a tendon is an important determinant of the ability of the tendon to store elastic energy. Type I and type III collagens are the major proteins that determine the stiffness of a tendon (37). Both type I and type III collagens are triple helical molecules (9). The amino acid residues that face the inner core of the triple helix are able to form hydrogen bonds with each other, and it is this hydrogen bonding that provides much of the molecular basis for the stiffness material property of tendons (45). As the tendon is stretched the hydrogen bonds between amino acid residues are broken and the breaking of these bonds gives off energy in the form of heat (61). The tendon must be able to dissipate this heat energy, because if the energy is not properly dissipated, the structural covalent bonds of molecules in the tendon can be broken and this will lead to tendon rupture.

The second category of molecules impart the viscoelastic properties of tendons. Viscoelasticity is important because this allows the tendon to resume its original shape after the application of a strain (37). This second category of molecules is comprised of elastin, proteoglycans and glycosaminoglycans. These molecules are highly hydrophilic, and their ability to bind water molecules allows for them to transfer the heat produced by the breaking of hydrogen bonds within collagen to the water molecules, that are further able to dissipate heat energy into surrounding tissues (61).

An additional factor that is an important determinant of the mechanical properties of tendons is the covalent cross-linking between collagen molecules. Cross-linking reduces the friction between collagen molecules as they are stretched (61). The consequence of greater cross-linking between collagen molecules is that the tendon becomes stiffer and can store mechanical energy more efficiently without losing this energy in the form of heat. Cross-linking between collagen molecules can occur via an enzymatic or a non-enzymatic mechanism. The lysyl oxidase enzyme generates aldehyde groups on lysine residues in collagen molecules (19). These highly reactive aldehyde groups can form stable covalent bonds with other lysine residues. Non-enzymatic cross-linking can occur when the amino group on the side-chains of amino acid residues come into contact with a reducing sugar (65). In addition to cross-linking amino acid residues between collagen molecules, this reaction generates compounds called advanced glycation end products (AGEs) (65). These AGEs

accumulate in the tissue and can disrupt the hierarchical structure of tendons and lead to tissue damage.

The structural and mechanical properties of tendons change with aging and physical activity. Compared with younger tendons, aged tendon is stiffer (60), has a lower rate of type I collagen synthesis (59) and is more prone to rupture (33, 60). The density of fibroblasts in tendon is highest at birth and steadily declines throughout the lifespan (56, 59). While conflicting reports have been published (40, 79), tendon typically adapts to chronic physical activity by increasing CSA, stiffness, peak stress, peak strain, type I collagen synthesis and fibroblast activity (34, 47, 48, 72, 80, 86, 87).

Regulation of Muscle Growth and Atrophy

The regulation of muscle growth and atrophy involves a sensitive balance between protein synthesis and degradation. Minor damage to muscle fibers causes an adaptive response in which damaged proteins are removed and new proteins are synthesized (20). With repetitive minor damage, such as the damage that occurs during exercise sessions that involve repeated lengthening contractions, there is a net increase in protein synthesis (17). This increase in protein synthesis increases both the size and P_o of individual fibers. However, if the damage to muscle is of sufficient magnitude, such as the damage that occurs following a muscle "strain", there is a robust activation of proteolytic enzymes that cause the breakdown of both damaged proteins and healthy, functional proteins (21, 30). The premature breakdown of functional proteins leads to muscle atrophy and a decrease in both the size and P_o of individual fibers.

Understanding the mechanical, cellular and molecular mechanisms that control muscle growth and atrophy is critical in improving the current treatments available for muscle injuries and diseases, as well as enhancing athletic performance and maximizing strength gains in exercise programs.

Mechanical damage to muscle fibers can initiate a series of events that lead to muscle hypertrophy and an increase in P_o. Sarcomeres are usually damaged only during lengthening contractions (10, 51, 52). The process of mechanical damage to sarcomeres is best explained in terms of the length-tension relationship of the sarcomere. The tension a muscle fiber can develop is proportional to the amount of overlap between the thick and thin filaments (74). The point of maximum tension occurs when the muscle is at a length at which the maximum number of cross bridges can be formed. This is the point at which the load opposing the muscle contraction is equal to the tension generated by the muscle, an isometric contraction. As an actively contracting muscle is lengthened, the available cross bridge binding sites steadily decreases. The forces transmitted to the sarcomeres from the external load can damage the ultrastructure of the sarcomere, and this disruption of sarcomere ultrastructure is responsible for the immediate decrease in force production following injury (10, 16, 41). In addition to damaging the sarcomeres, lengthening contractions can lead to disruption of the plasma membrane and endomysium due to shear forces generated during the lengthening contraction (14, 44). This process of sarcomere and membrane damage initiates a response that eventually leads to repair of damaged structures and hypertrophy of the damaged muscle fiber.

Cellular Regulation of Muscle Growth and Atrophy. The nuclei within skeletal muscle fibers are arrested at the G_1 cell cycle checkpoint and are unable to replicate (36). Following injury to a muscle fiber, the nuclei in the damaged area undergo apoptosis (7, 70). Skeletal muscle stem cells, referred to as satellite cells or myoblasts, reside in a space between the sarcolemma and the basal lamina (58). Satellite cells, that normally exist in a quiescent state, become activated, migrate to the site of injury, proliferate, and fuse with the damaged fiber to repopulate the nuclei lost as a result of injury (24). Damage to the endomysium releases inactive hepatocyte growth factor (HGF) (76). Reactive oxygen species, produced by the nitric oxide synthase (NOS) enzyme, activate HGF (77). Activated HGF binds to the c-met receptor on the plasma membrane of satellite cells. HGF signaling activates the satellite cells from the quiescent state and initiates the migration of satellite cells to the site of injury (76).

As satellite cells migrate to the site of injury, they also undergo proliferation. The initiation of proliferation is brought on by an increase in the expression of the basic helix-loop-helix (bHLH) transcription factor MyoD (24). MyoD is one of four members of myogenic regulatory factor (MRF) family, that include Myf-5, myogenin and MRF-4. The MRF family of transcription factors initiate the "myogenic program" in these proliferating satellite cells (24). The myogenic program changes the cellular morphology of satellite cells from a fibroblastic type morphology to a muscle like morphology (75). Once in proximity of the damaged muscle fiber, satellite cells fuse with each other to form multinucleated structures called myotubes. These myotubes fuse with the

existing, damaged muscle fiber and can help bridge the gap between ruptured ends of a muscle fiber. As the myotubes fuse with the muscle fiber, the nuclei within the myotubes arrest in G_1 (25, 36). A certain population of satellite cells that underwent proliferation do not form myotubes, but instead resume a sub-basal lamina position and return to quiescence (24). In addition to satellite cells, fibroblasts and immune cells are attracted to the site of injury. The presence of these cells helps to remove cellular debris and repair the ECM. If there is a severe disruption of the ECM, fibroblasts can respond with an overproduction of ECM (27). This overproduction of ECM results in the clinical condition of fibrosis, or scar tissue accumulation. The mechanisms behind the formation of scar tissue are of particular interest to clinicians, as this scar tissue is generally disruptive to the proper function of muscle tissue and, once formed, is relatively permanent (30).

Once the myotubes have fused with the damaged muscle fiber, the nuclei from these myotubes occupy a centrally located position in the muscle fiber (24, 52). While nuclei in an uninjured fiber are typically located just beneath the sarcolemma, taking up a central location presumably allows for greater surface area contact of the nucleus with ribosomes and endoplasmic reticulum and thus enhance the ability of muscle fibers to synthesize new proteins. During the repair stages, the majority of proteins that are synthesized are responsible for repairing the damaged fiber (26). While it is not clear exactly why the nuclei take up a subsarcolemmal location after repair, the nuclei do not need as close a direct association with endoplasmic reticulum, as mRNA that encodes sarcomeric

proteins is trafficked directly to the sarcomere, where translation and processing occur (35). This strategy is likely in place as sarcomeric proteins are relatively large, translation at the sarcomere minimizes the need for the muscle fiber to have an elaborate protein trafficking system in place. The location of the nuclei within the cytosol therefore provides a way to track the progress of repair in skeletal muscle tissue.

Molecular Regulation of Muscle Growth and Atrophy. While the satellite cells are undergoing migration, proliferation and fusion, the muscle fiber is initiating the underlying processes that are responsible to begin the repair process. Damage to the plasma membrane causes a persistent increase in intracellular calcium levels (78). The influx of calcium initiates the persistent activation of sarcomeres distal to the site of injury, and is likely the mechanism behind the "muscle spasm" that is observed clinically after a muscle injury. This influx of calcium also activates the proteolytic systems of muscle tissue (5, 29). By three days following injury, the plasma membranes of the muscle fibers are largely sealed off (64) and calcium homeostasis is restored (5).

The ubiquitin-proteasome proteolytic system is important in regulating skeletal muscle mass and protein turn-over. Atrogin-1 (MAFbx) is a ubiquitin ligase protein expressed in skeletal muscle (20, 32). Atrogin-1 directs the polyubiquination of proteins (8). Once a protein is tagged with ubiquitin, that protein is targeted to the proteasome organelle. The amount of ubiquitin tags on a protein appears to be directly related to the speed at which the doomed protein is degraded. Upon reaching the proteasome, the protein is broken down and its

constituent amino acids for recycled for use in the synthesis of new proteins. The expression of atrogin-1 is regulated by the Forkhead box O (Foxo) family of transcription factors (20, 32). The promoter region of the atrogin-1 gene contains binding sites for the Foxo3 transcription factor that acts as a co-activator of atrogin-1 transcription (68). Phosphorylation of Foxo3 by Akt inhibits the ability of Foxo3 to enter the nucleus and thus blocks the ability of Foxo3 to act as a transcription factor.

Regulation of Muscle Growth and Atrophy by Myostatin

Myostatin is a negative regulator of muscle mass (38, 39, 54, 84, 85, 90). The myostatin gene consists of three exons, the first two of which encode a propeptide, and the third encodes the mature, active form of myostatin (Figure 1.1). Compared with *MSTN*$^{+/+}$ mice, the *MSTN*$^{+/-}$ mice used in this study have a 20% reduction in circulating myostatin levels, and *MSTN*$^{-/-}$ mice have no detectable myostatin (Figure 1.2). While the masses of the male *MSTN*$^{+/+}$, *MSTN*$^{+/-}$ and *MSTN*$^{-/-}$ mice are similar until 9 months of age, following this time point, the masses of the *MSTN*$^{-/-}$ mice are noticeably greater than *MSTN*$^{+/+}$ and *MSTN*$^{+/-}$ mice (Figure 1.3). The masses of female *MSTN*$^{+/+}$, *MSTN*$^{+/-}$ and *MSTN*$^{-/-}$ mice do not differ from one another (Figure 1.3). Myostatin deficiency increases the CSA (cross-sectional area) of muscle fibers from EDL and soleus muscles, and also increases the whole muscle CSA (Figure 1.4). Myostatin deficiency does not change the relative myofibrillar protein content of EDL or soleus muscles (Figure 1.5).

Molecular Signaling Pathways. Myostatin signal transduction is mediated through the activin family of serine/threonine kinase receptors. Myostatin is secreted as a 25 kDa dimer, bound to its 37 kDa propeptide (54). Upon dissociation from its latent complex, myostatin binds the type IIb activin receptor (ActRIIB or ACVR2B) (38). This binding promotes the recruitment and phosphorylation of the type Ib activin co-receptor (ActRIB or ACVRB) (38). The activated ActRIIB-ActRIB complex activates Smad2 and Smad3 transcription factors, and TAK1, via phosphorylation (Figure 1.6) (62). Phosphorylation of Smad2 and Smad3 allows for these proteins to oligomerize and enter the nucleus (57). Specifically, Smad2 and Smad3 can form homodimers, heterodimers and heterotrimers with themselves and an additional transcription factor, Smad4 (57). The Smad oligomers interact with other transcription factors and recruit co-activators or co-repressors of gene transcription (57). The activated TAK1 kinase activates the downstream kinases p38 MAPK and Erk1/2 via MKK3/6 (62, 88). p38 MAPK and Erk1/2 are able in turn to regulate the activity of various transcription factors via phosphorylation. While the myostatin-deficient mice have a very clear hypermuscular phenotype, the downstream gene targets of myostatin-mediated signal transduction, remain largely unknown.

Unlike myostatin, IGF-1 (insulin like growth factor-1) is a positive regulator of muscle mass. IGF-1 binds to the IGF-1 receptor that activates PI3K via IRS-1 (1). PI3K activates Akt/PKB that activates several downstream transcription factors via phosphorylation (1). Akt appears to regulate muscle mass both by promoting satellite cell proliferation and by decreasing protein degradation (20).

Akt promotes satellite cell proliferation, at least in part, by increasing the expression of MyoD (20). To inhibit protein degradation, Akt phosphorylates the Foxo3 transcription factor that keeps Foxo3 localized in the cytosol (20, 69). Foxo3 is a potent activator of atrogin-1, and in the absence of a nuclear localized Foxo3 transcription factor, atrogin-1 expression declines (20). The myostatin and IGF-1 pathways can inhibit each other. Activation of ActRIIB by myostatin blocks the IGF-1 mediated phosphorylation of PI3K and Akt (89). Akt binds and prevents the nuclear localization of Smad3 (13).

Induction of Muscle Atrophy by Myostatin. The deficiency of myostatin results in a profound increase in skeletal muscle mass (38, 39, 54, 84, 85, 90) and overexpression of myostatin results in muscle atrophy (66, 91). While the deficiency of myostatin increases protein synthesis (83), it was not known if myostatin also increase protein breakdown. Our preliminary studies of the regulation of atrogin-1 by myostatin indicated that, despite no difference in relative myofibrillar protein content (Figure 1.5), compared with $MSTN^{+/+}$ mice, the EDL muscles of $MSTN^{-/-}$ mice had a noticeable decrease in ubiquitin tagged myosin heavy chain (Figure 1.7A) and a 40% decrease in atrogin-1 expression (Figure 1.7C). For soleus muscles, $MSTN^{-/-}$ mice had only a minor decrease in ubiquitin tagged myosin heavy chain (Figure 1.7B) and no difference in atrogin-1 expression (Figure 1.7D). The decreased ubiquitination of myosin heavy chain, in conjunction with the decrease in atrogin-1 expression, suggests that there is a decrease in protein degradation in $MSTN^{-/-}$ EDL muscles. This may explain why, compared with soleus muscles, the deficiency of myostatin leads to a greater

relative increase in EDL muscle mass (further discussed in Chapter II). While sarcomeric proteins must first be liberated from the sarcomere by calpain mediated proteolysis of titin, these results do indicate that myostatin deficiency leads to a functional decrease in protein degradation. Determining the expression of the calpain proteases will provide greater insight into this mechanism.

Myostatin increases the expression of atrogin-1 in C_2C_{12} myotubes (53). We determined if myostatin could increase the expression of atrogin-1 in primary myotubes, and which arm of the myostatin signaling pathway was involved in this process. When primary myotubes were treated with myostatin, there was a dose-dependent increase in atrogin-1 expression (Figure 1.8). Inhibition of both the p38 MAPK and Smad2/3 pathways blocked the myostatin-mediated increase in atrogin-1 expression, suggesting that both arms of the myostatin signal transduction pathway are important in the regulation of atrogin-1. While the p38 MAPK mediated induction of atrogin-1 expression is not clear, Foxo3 can directly bind Smad3 to promote gene transcription (22, 69), and the interaction between Foxo3 and Smad3 may therefore be necessary for the regulation of atrogin-1 by myostatin.

Methods

Animals. All experiments were conducted in accordance with the guidelines of the University of Michigan Committee on the Use and Care of Animals. Mice were housed in specific-pathogen-free conditions and were provided food and water *ad libidum*. The *MSTN*$^{-/-}$ mice are of a C57Bl/6

background and were a kind gift of Dr. Se-Jin Lee (54). The null *MSTN* allele was generated by replacing a portion of the third exon of the *MSTN* gene that encodes the C-terminal region of the mature myostatin protein with a *neo* cassette (Figure 1.1A). The genotype of mice was determined by PCR-based analysis of DNA samples obtained via tail biopsy (Figure 1.1B).

ELISA Quantification of Myostatin in Serum. Approximately 1mL of blood was withdrawn from 6 month old male $MSTN^{+/+}$, $MSTN^{+/-}$, and $MSTN^{-/-}$ mice, allowed to clot and spun at 10,000 × g for 10 minutes to separate serum. Serum was briefly treated with 0.1N HCl to dissociate myostatin from its carrier proteins and was subsequently diluted 1:2 in RIPA buffer. Samples were then subjected to sandwich ELISA (R&D Systems) in triplicate.

Cell Culture. Satellite cells were isolated from 6 month old male $MSTN^{+/+}$ mice using the methods described by Allen and his colleagues (2). Mice were anesthetized with intraperitoneal injection of Avertin (400 mg/kg) and sacrificed by cervical dislocation. The hindlimb muscles were quickly removed, minced and digested in protease solution (1.0 mg/mL of Type XIV Proteinase in PBS, Sigma) for 1 hour at 37ºC. Satellite cells were separated from muscle fiber fragments and from tissue debris by differential centrifugation and then plated on fibronectin coated 35mm tissue culture plates (BD Biosciences). Cultures were maintained in a humidified environment maintained at 37ºC and 5% CO_2.

Satellite cells were grown in DMEM + 20% FBS + 1% antibiotic-antimycotic (AbAm) until reaching 80% confluence, at which time the media was changed to DMEM + 2% horse serum + 1% AbAm to induce differentiation into

myotubes. Myotubes were maintained in culture for 5 days and then serum starved for 24 hours by replacing the differentiation media with DMEM + Insulin-Transferrin-Selenium Supplement (Invitrogen) + 1% AbAm. Recombinant murine myostatin was produced in NS0 mouse myeloma cells (R & D Systems) and dissolved into the starvation media at a final concentration of 250 or 500 ng/mL. Stock solutions of the p38 MAPK inhibitor SB-203580 (15) and the Smad2/3 inhibitor SB-431542 (28) were prepared by dissolving these solid anhydrous compounds in DMSO at a concentration of 10mM. SB-203580 and SB-431542 stock solutions were then added to starvation media containing myostatin and 0.5% DMSO at a final concentration of 10μM for SB-203580 and 5μM for SB-431542. Cells were pretreated with SB-203580 or SB-431542 for 1 hour prior to treatment with myostatin for 12 hours.

Myofibrillar Protein Content. Myofibrillar proteins were extracted from EDL and soleus muscles using the methods of Solaro (71), modified to include the addition of Leupeptin (Sigma). The protein content of the isolated myofibrils was determined using a DC Protein Assay (Bio-Rad) and normalized to the wet mass of the muscle.

SDS-PAGE and Immunoblot. Whole EDL and soleus muscles were removed from anesthetized 6 month old *MSTN*$^{+/+}$ and *MSTN*$^{-/-}$ mice, flash frozen in liquid nitrogen and stored at -80ºC until use. Muscles and myotubes were homogenized in Laemmli's sample buffer with 1:20 β-mercaptoethanol, 1:20 protease inhibitor cocktail (Sigma) and 1:40 phosphatase inhibitor cocktail (Sigma) and then placed in boiling water for 5 minutes. Protein concentration of

the samples was determined using an RC DC Protein Assay (Bio-Rad). Equal amounts of protein were loaded into 4% stacking, 7.5% resolving polyacrylamide gels and subjected to electrophoresis. To detect total myosin heavy chain, gels were stained with Coomassie Brilliant Blue (Bio-Rad). To detect ubiquitinated myosin heavy chain, proteins were transferred from gels to a 0.45 μm nitrocellulose membrane and stained with Ponceau S to verify equal protein transfer. Membranes were blocked using casein (Vector Labs), incubated with an HRPO tagged anti-ubiquitin antibody (Santa Cruz) and developed with SuperSignal West Dura enhanced chemiluminescent reagents (Pierce Biotechnology) and visualized using a FluorChem chemiluminescent documentation system (Alpha Innotech).

RT-qPCR. RNA was isolated from samples using an RNeasy Fibrous Tissue kit (Qiagen) and treated with DNase I. Poly-A mRNA was reverse transcribed using an Omniscript RT system (Qiagen) and oligo$(dT)_{15}$ primers. cDNA was amplified using primers for atrogin-1 (forward: 5'-ATTCTACACTGGCAGCAGCA-3'; reverse: 5'- TGTAAGCACACAGGCAGGTC-3') and β2-microglobulin (forward: 5'-ATGGGAAGCCGAACATACTG-3'; reverse: 5'-CAGTCTCAGTGGGGGTGAAT-3') using a SYBR Green I PCR system (Qiagen) with Uracil DNA Glycosylase (Invitrogen) in an Opticon 2 real-time thermal cycler (Bio-Rad). qPCR reactions were conducted in quadruplicate for each sample. C(t) values for atrogin-1 were normalized to β2-microglobulin using the $2^{-\Delta\Delta C(t)}$ method. β2-microglobulin was selected as a normalizing gene based on its stable expression in skeletal muscle tissue (49) and because its

expression did not differ between groups. The presence of single amplicons from qPCR reactions were verified by melting curve analysis as well as electrophoresis using a 2% agarose gel. Genomic DNA contamination was not detected in qPCR reactions.

Statistical Analysis. Results are presented as means ± SE. KaleidaGraph 4.02 software was used to conduct statistical tests. For ELISA, histology and gene expression data from cell culture experiments, differences between groups were tested with a one-way ANOVA with $\alpha = 0.05$. Fisher's least significant post hoc test was used to identify specific differences when significance was tested. For all other data, differences between groups were tested with Student's t-test with $\alpha = 0.05$.

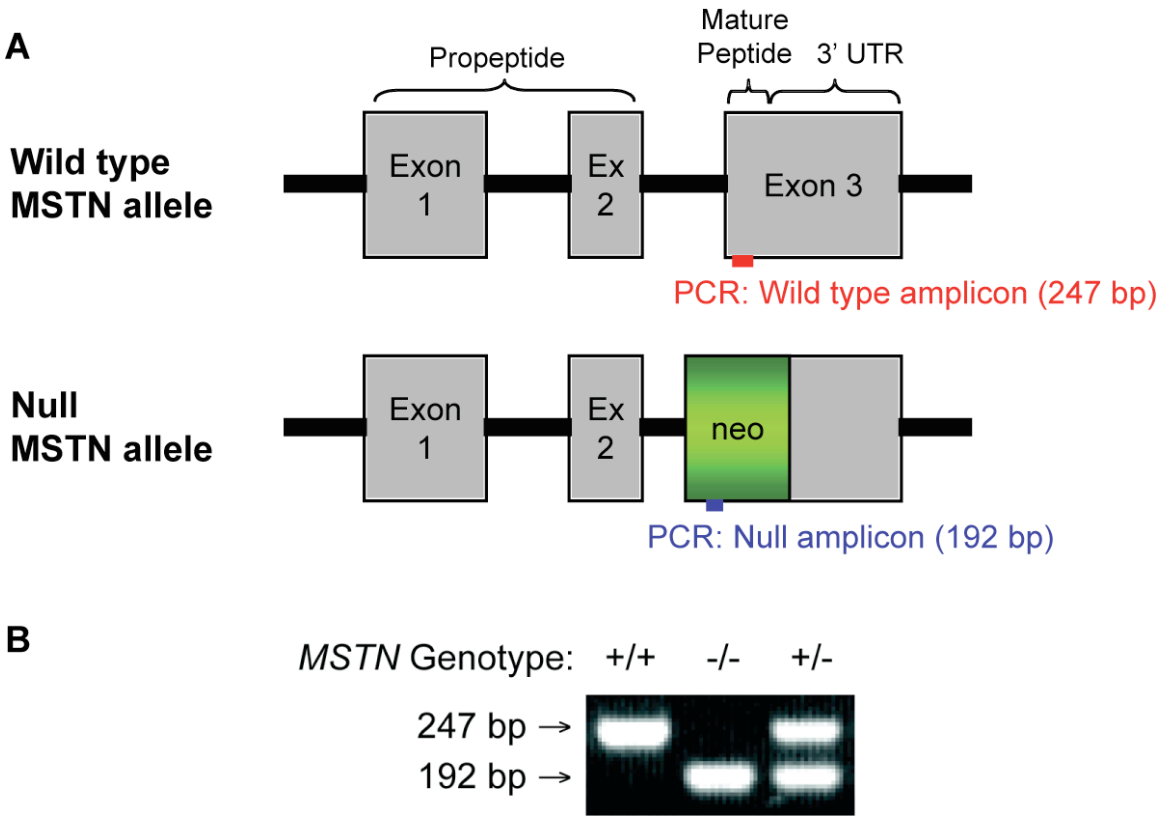

Figure 1.1. (A) Structure of wild type and null MSTN alleles. (B) PCR based detection of myostatin alleles.

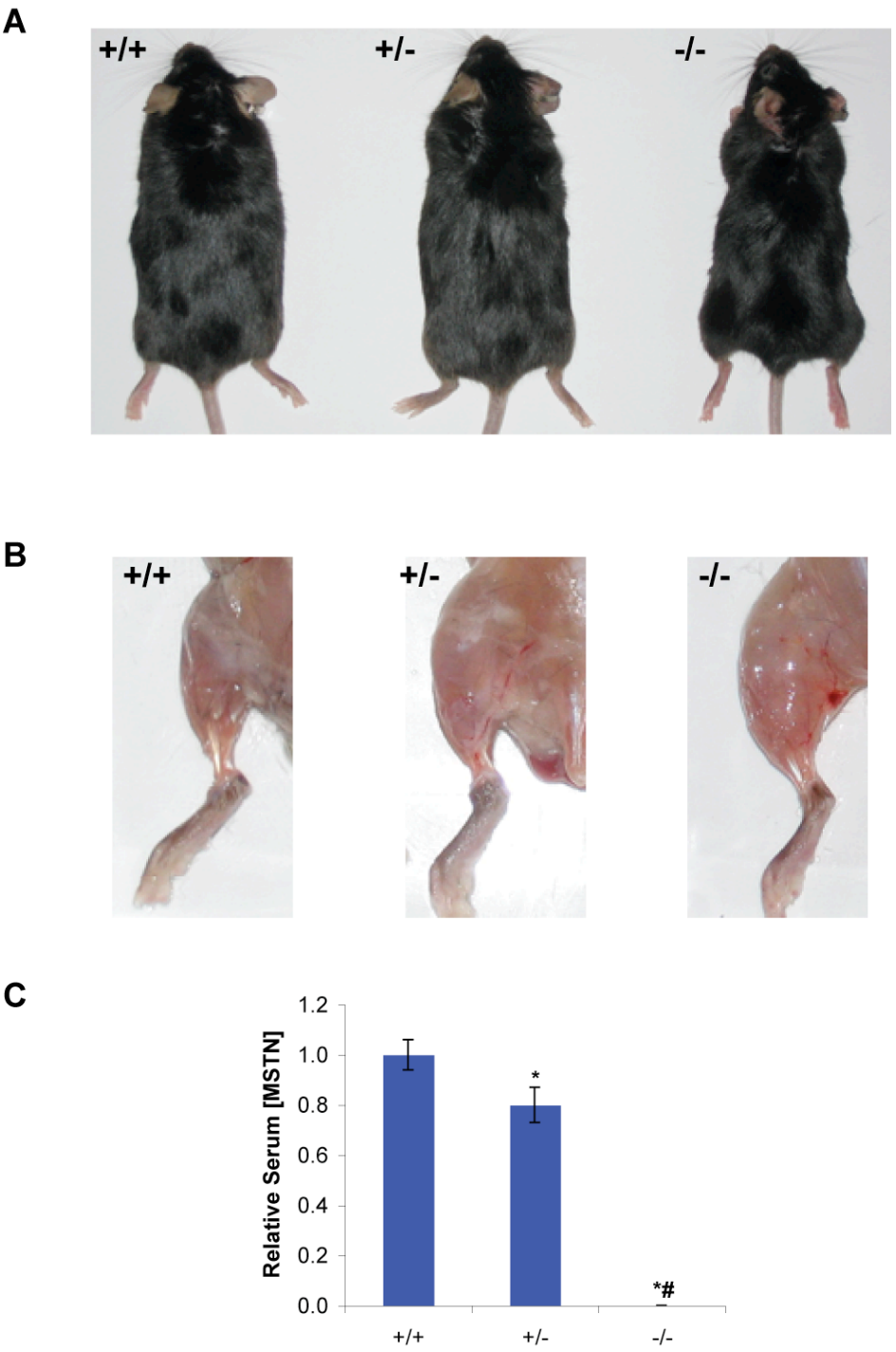

Figure 1.2. Mouse models used in the current study. Picture of (A) whole mouse carcasses and (B) hind limb musculature. (C) Relative myostatin concentration in plasma measured by ELISA. N = 6 mice. *, significantly different from $MSTN^{+/+}$ at $P < 0.05$, #, significantly different from $MSTN^{+/-}$ at $P < 0.05$.

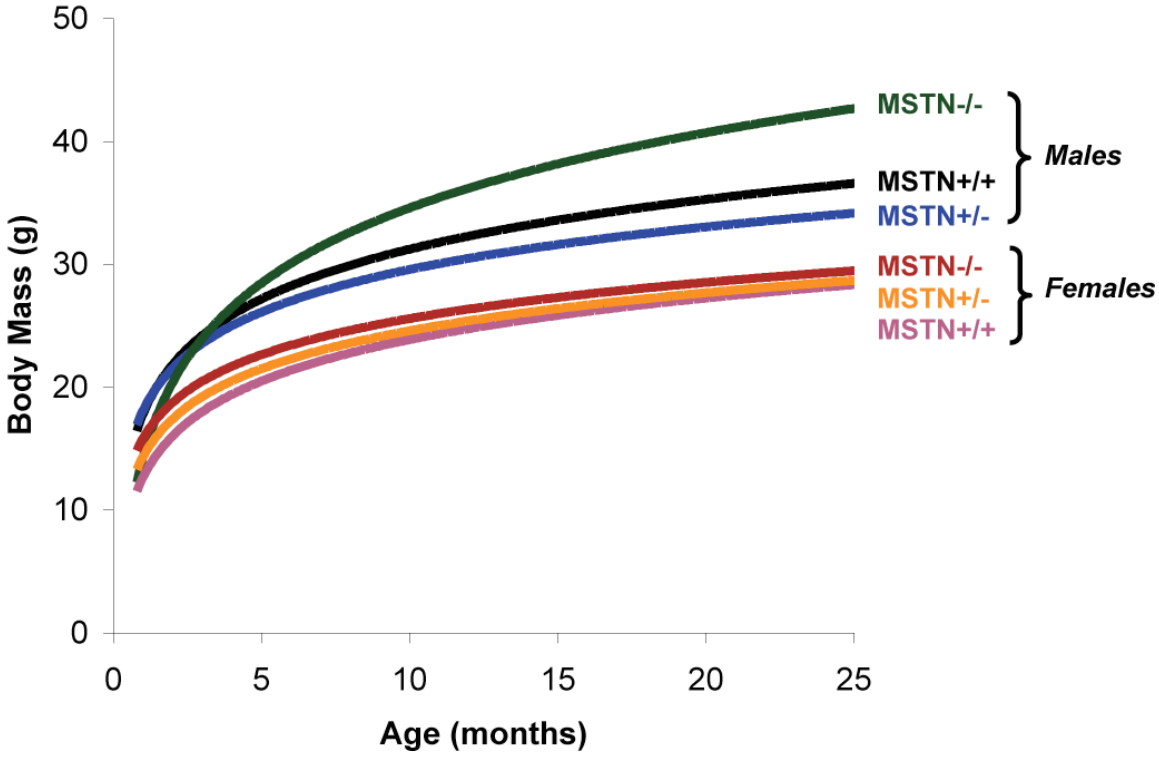

Figure 1.3. Growth curves of male and female *MSTN*$^{+/+}$, *MSTN*$^{+/-}$ and *MSTN*$^{-/-}$ mice.

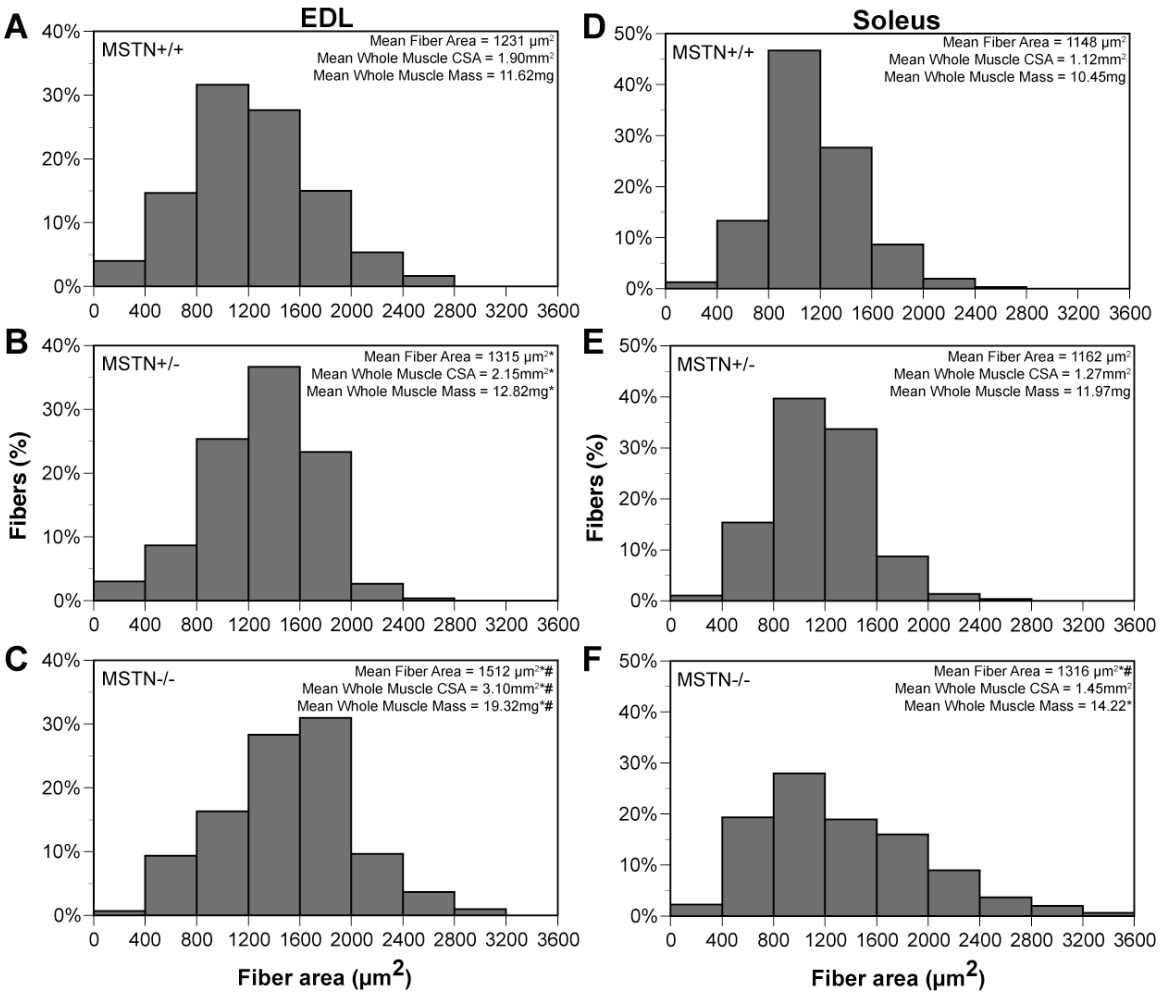

Figure 1.4. Muscle fiber CSA distributions. EDL muscles of (A) *MSTN*$^{+/+}$, (B) *MSTN*$^{+/-}$ and (C) *MSTN*$^{-/-}$ mice. Soleus muscles of (D) *MSTN*$^{+/+}$, (E) *MSTN*$^{+/-}$ and (F) *MSTN*$^{-/-}$ mice. N = 3 muscles from each genotype. *, significantly different from *MSTN*$^{+/+}$ at $P < 0.05$, #, significantly different from *MSTN*$^{+/-}$ at $P < 0.05$.

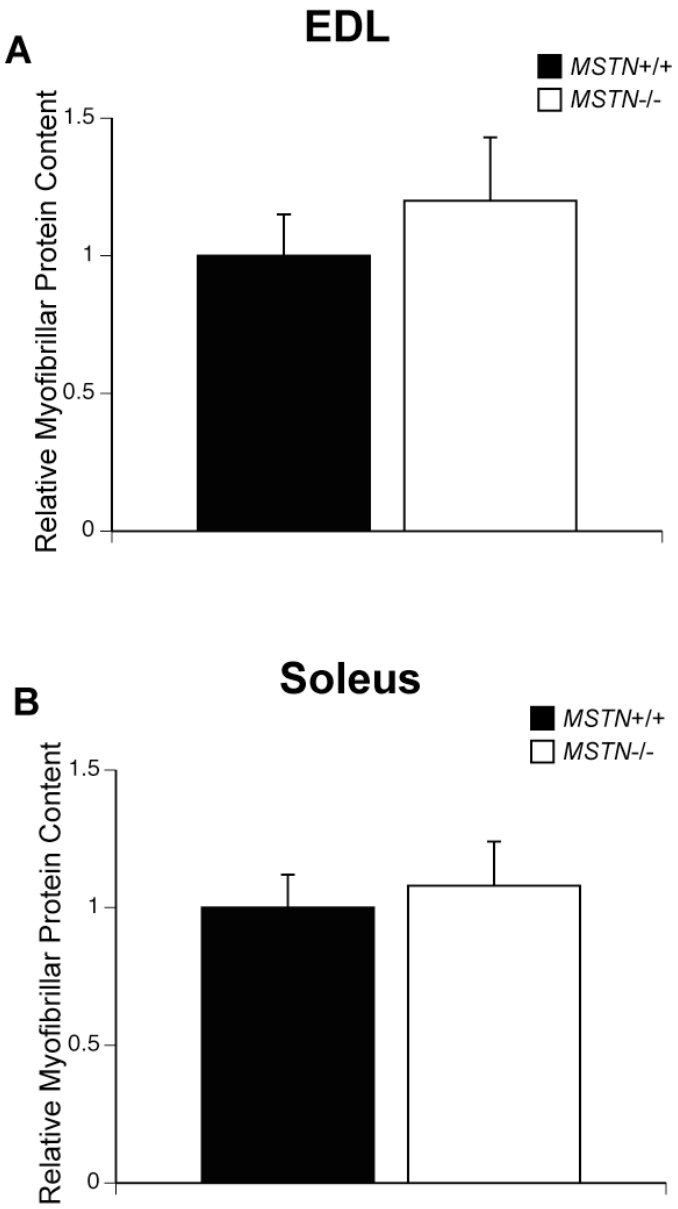

Figure 1.5. Relative myofibrillar protein content of (A) EDL and (B) soleus muscles of *MSTN*$^{+/+}$ and *MSTN*$^{-/-}$ mice. (A) There was no difference between the myofibrillar protein content (normalized first to muscle mass, and then to levels in *MSTN*$^{+/+}$ mice) between *MSTN*$^{+/+}$ and *MSTN*$^{-/-}$ mice for (A) EDL and (B) soleus muscles. N = 3 muscles.

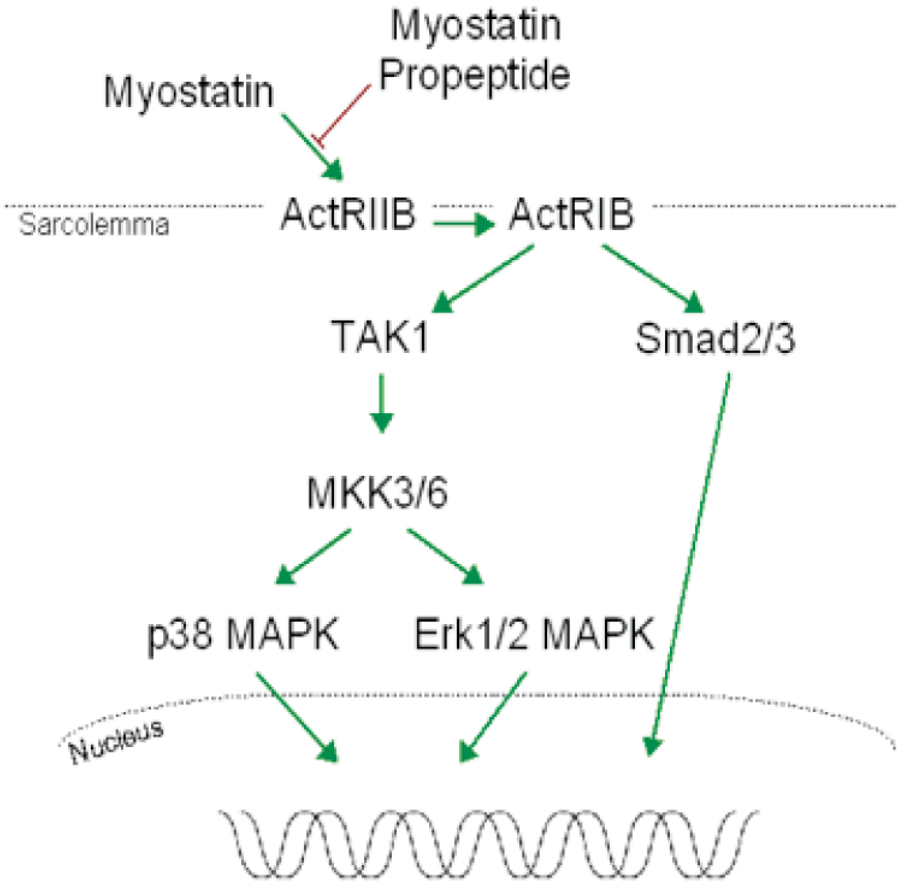

Figure 1.6. Myostatin signal transduction pathways.

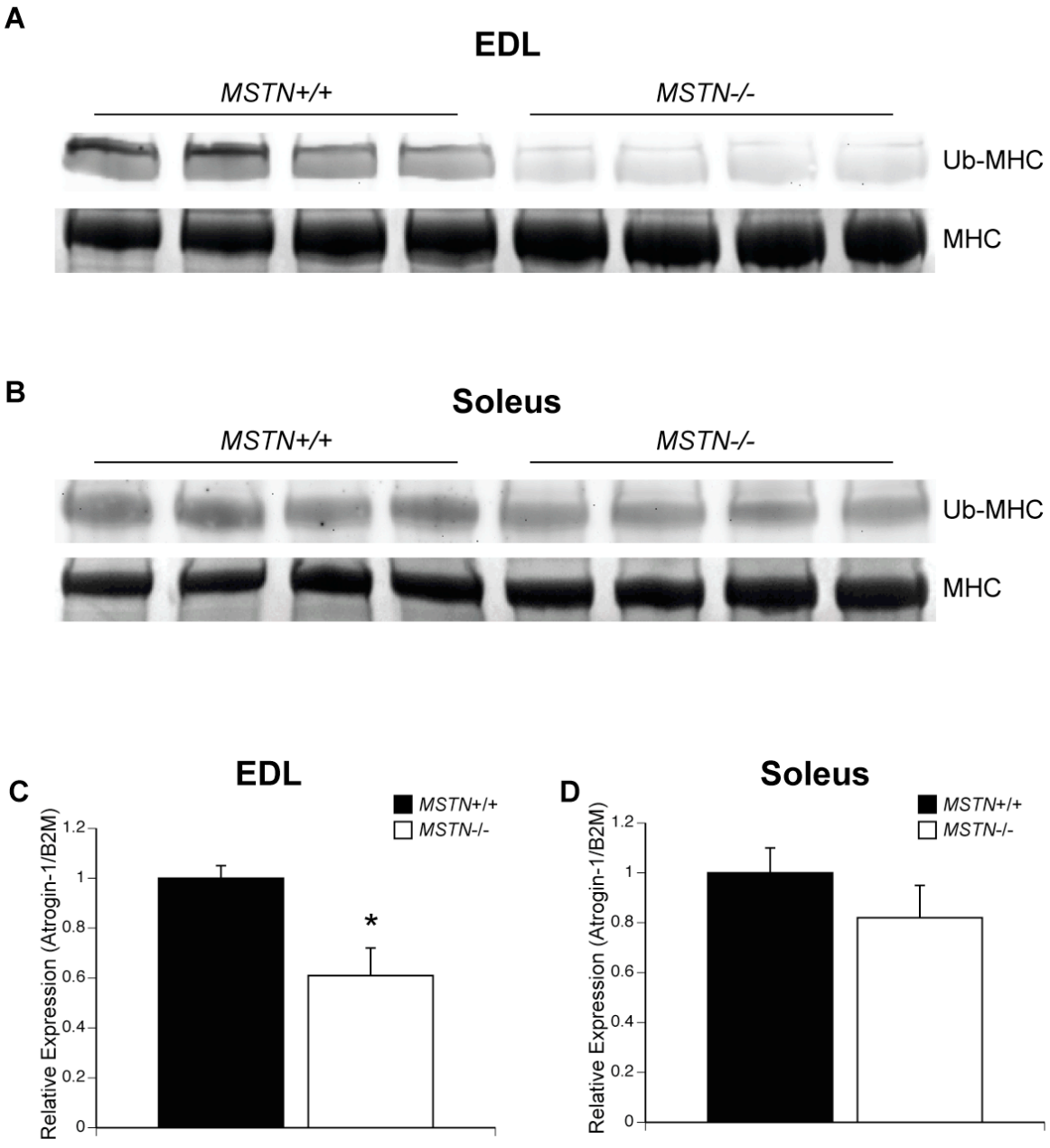

Figure 1.7. Ubiquitinated myosin heavy chain (Ub-MHC) protein and atrogin-1 expression from EDL and soleus muscles of *MSTN*$^{+/+}$ and *MSTN*$^{-/-}$ mice. *MSTN*$^{-/-}$ mice have less Ub-MHC than *MSTN*$^{+/+}$ mice in (A) EDL, but there is only a minimal difference between genotypes in (B) soleus muscles. There is a decrease in the relative expression of atrogin-1, normalized to β2-microglobulin, in (C) EDL muscles of *MSTN*$^{-/-}$ mice, but no differences in (D) soleus muscles. N = 4 muscles.

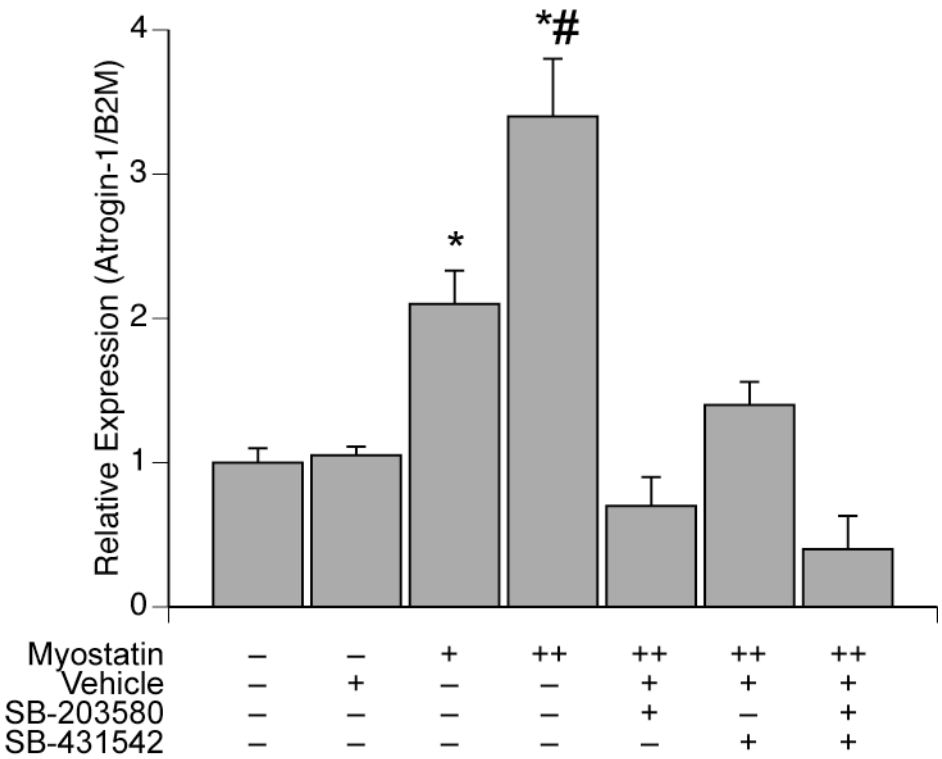

Figure 1.8. Atrogin-1 expression in primary myotubes treated with myostatin. Treatment of primary myotubes with myostatin for 12h increases the relative expression of atrogin-1, normalized to β2-microglobulin. +, 250ng/mL of myostatin. ++, 500ng/mL of myostatin. *, significantly different from control group at $P < 0.05$. #, significantly different from 250ng/mL group at $P < 0.05$. N = 3 independent experiments.

References

1. Adams G. Invited Review: Autocrine/paracrine IGF-I and skeletal muscle adaptation. *J Appl Physiol* 93: 1159-1167, 2002.
2. Allen RE, Temm-Grove CJ, Sheehan SM, and Rice G. Skeletal muscle satellite cell cultures. *Methods Cell Biol* 52: 155-176, 1997.
3. Anastasi G, Cutroneo G, Santoro G, and Trimarchi F. The non-junctional sarcolemmal cytoskeleton: the costameres. *Ital J Anat Embryol* 103: 1-11, 1998.
4. Arruda E, Mundy K, Calve S, and Baar K. Denervation does not change the ratio of collagen I and collagen III mRNA in the extracellular matrix of muscle. *Am J Physiol Regul Integr Comp Physiol* 292: R983-987, 2007.
5. Belcastro AN, Shewchuk LD, and Raj DA. Exercise-induced muscle injury: a calpain hypothesis. *Mol Cell Biochem* 179: 135-145, 1998.
6. Benjamin M, Kumai T, Milz S, Boszczyk B, Boszczyk A, and Ralphs J. The skeletal attachment of tendons--tendon "entheses". *Comp Biochem Physiol, Part A Mol Integr Physiol* 133: 931-945, 2002.
7. Biral D, Jakubiec-Puka A, Ciechomska I, Sandri M, Rossini K, Carraro U, and Betto R. Loss of dystrophin and some dystrophin-associated proteins with concomitant signs of apoptosis in rat leg muscle overworked in extension. *Acta Neuropathol (Berl)* 100: 618-626, 2000.
8. Bodine S, Latres E, Baumhueter S, Lai V, Nunez L, Clarke B, Poueymirou W, Panaro F, Na E, Dharmarajan K, Pan Z, Valenzuela D, DeChiara T, Stitt T, Yancopoulos G, and Glass D. Identification of ubiquitin ligases required for skeletal muscle atrophy. *Science* 294: 1704-1708, 2001.
9. Brinckmann J. Collagen - Primer in Structure, Processing and Assembly. *Top Curr Chem* 247: 1-229, 2005.
10. Brooks SV, Zerba E, and Faulkner JA. Injury to muscle fibres after single stretches of passive and maximally stimulated muscles in mice. *J Physiol* 488 (Pt 2): 459-469, 1995.
11. Capetanaki Y, Bloch RJ, Kouloumenta A, Mavroidis M, and Psarras S. Muscle intermediate filaments and their links to membranes and membranous organelles. *Exp Cell Res* 313: 2063-2076, 2007.
12. Chopard A, Arrighi N, Carnino A, and Marini JF. Changes in dysferlin, proteins from dystrophin glycoprotein complex, costameres, and cytoskeleton in human soleus and vastus lateralis muscles after a long-term bedrest with or without exercise. *Faseb J* 19: 1722-1724, 2005.
13. Conery AR, Cao Y, Thompson EA, Townsend CM, Jr., Ko TC, and Luo K. Akt interacts directly with Smad3 to regulate the sensitivity to TGF-beta induced apoptosis. *Nat Cell Biol* 6: 366-372, 2004.
14. Consolino CM, and Brooks SV. Susceptibility to sarcomere injury induced by single stretches of maximally activated muscles of mdx mice. *J Appl Physiol* 96: 633-638, 2004.
15. Cuenda A, Rouse J, Doza Y, Meier R, Cohen P, Gallagher T, Young P, and Lee J. SB 203580 is a specific inhibitor of a MAP kinase homologue which is stimulated by cellular stresses and interleukin-1. *FEBS Lett* 364: 229-233, 1995.

16. Devor ST, and Faulkner JA. Regeneration of new fibers in muscles of old rats reduces contraction-induced injury. *J Appl Physiol* 87: 750-756, 1999.
17. Evans WJ. Protein nutrition and resistance exercise. *Can J Appl Physiol* 26 Suppl: S141-152, 2001.
18. Faulkner JA, Brooks SV, and Opiteck JA. Injury to skeletal muscle fibers during contractions: conditions of occurrence and prevention. *Phys Ther* 73: 911-921, 1993.
19. Gerriets J, Curwin S, and Last J. Tendon hypertrophy is associated with increased hydroxylation of nonhelical lysine residues at two specific cross-linking sites in type I collagen. *J Biol Chem* 268: 25553-25560, 1993.
20. Glass D. Molecular mechanisms modulating muscle mass. *Trends in molecular medicine* 9: 344-350, 2003.
21. Glass DJ. Skeletal muscle hypertrophy and atrophy signaling pathways. *Int J Biochem Cell Biol* 37: 1974-1984, 2005.
22. Gomis R, Alarcón C, He W, Wang Q, Seoane J, Lash A, and Massagué J. A FoxO-Smad synexpression group in human keratinocytes. *Proc Natl Acad Sci USA* 103: 12747-12752, 2006.
23. Griffiths RI. Shortening of muscle fibres during stretch of the active cat medial gastrocnemius muscle: the role of tendon compliance. *J Physiol* 436: 219-236, 1991.
24. Hawke T, and Garry D. Myogenic satellite cells: physiology to molecular biology. *J Appl Physiol* 91: 534-551, 2001.
25. Hawke TJ, Meeson AP, Jiang N, Graham S, Hutcheson K, DiMaio JM, and Garry DJ. p21 is essential for normal myogenic progenitor cell function in regenerating skeletal muscle. *Am J Physiol Cell Physiol* 285: C1019-1027, 2003.
26. Herndon DN, Dasu MR, Wolfe RR, and Barrow RE. Gene expression profiles and protein balance in skeletal muscle of burned children after beta-adrenergic blockade. *Am J Physiol Endocrinol Metab* 285: E783-789, 2003.
27. Huard J, Li Y, and Fu F. Muscle injuries and repair: current trends in research. *The Journal of bone and joint surgery American volume* 84-A: 822-832, 2002.
28. Inman G, Nicolás F, Callahan J, Harling J, Gaster L, Reith A, Laping N, and Hill C. SB-431542 is a potent and specific inhibitor of transforming growth factor-beta superfamily type I activin receptor-like kinase (ALK) receptors ALK4, ALK5, and ALK7. *Mol Pharmacol* 62: 65-74, 2002.
29. Jackman R, and Kandarian S. The molecular basis of skeletal muscle atrophy. *Am J Physiol, Cell Physiol* 287: C834-843, 2004.
30. Järvinen T, Järvinen T, Kääriäinen M, Kalimo H, and Järvinen M. Muscle injuries: biology and treatment. *The American journal of sports medicine* 33: 745-764, 2005.
31. Józsa LG, and Kannus P. *Human tendons : anatomy, physiology, and pathology*. Champaign, IL: Human Kinetics, 1997, p. ix, 574 p.
32. Kandarian S, and Jackman R. Intracellular signaling during skeletal muscle atrophy. *Muscle Nerve* 33: 155-165, 2006.

33. Kannus P, and Józsa L. Histopathological changes preceding spontaneous rupture of a tendon. A controlled study of 891 patients. *The Journal of bone and joint surgery American volume* 73: 1507-1525, 1991.
34. Kiiskinen A. Physical training and connective tissues in young mice--physical properties of Achilles tendons and long bones. *Growth* 41: 123-137, 1977.
35. Kiri A, and Goldspink G. RNA-protein interactions of the 3' untranslated regions of myosin heavy chain transcripts. *J Muscle Res Cell Motil* 23: 119-129, 2002.
36. Kitzmann M, and Fernandez A. Crosstalk between cell cycle regulators and the myogenic factor MyoD in skeletal myoblasts. *Cell Mol Life Sci* 58: 571-579, 2001.
37. Kjaer M. Role of extracellular matrix in adaptation of tendon and skeletal muscle to mechanical loading. *Physiol Rev* 84: 649-698, 2004.
38. Lee S, and McPherron A. Regulation of myostatin activity and muscle growth. *Proc Natl Acad Sci USA* 98: 9306-9311, 2001.
39. Lee S, Reed L, Davies M, Girgenrath S, Goad M, Tomkinson K, Wright J, Barker C, Ehrmantraut G, Holmstrom J, Trowell B, Gertz B, Jiang M, Sebald S, Matzuk M, Li E, Liang L, Quattlebaum E, Stotish R, and Wolfman N. Regulation of muscle growth by multiple ligands signaling through activin type II receptors. *Proc Natl Acad Sci USA* 102: 18117-18122, 2005.
40. Legerlotz K, Schjerling P, Langberg H, Brüggemann G, and Niehoff A. The effect of running, strength, and vibration strength training on the mechanical, morphological, and biochemical properties of the Achilles tendon in rats. *J Appl Physiol* 102: 564-572, 2007.
41. Lieber R, Woodburn T, and Fridén J. Muscle damage induced by eccentric contractions of 25% strain. *J Appl Physiol* 70: 2498-2507, 1991.
42. Lin T, Cardenas L, and Soslowsky L. Biomechanics of tendon injury and repair. *Journal of biomechanics* 37: 865-877, 2004.
43. Listrat A, Picard B, and Geay Y. Age-related changes and location of type I, III, IV, V and VI collagens during development of four foetal skeletal muscles of double-muscled and normal bovine animals. *Tissue & cell* 31: 17-27, 1999.
44. Lovering RM, and De Deyne PG. Contractile function, sarcolemma integrity, and the loss of dystrophin after skeletal muscle eccentric contraction-induced injury. *Am J Physiol Cell Physiol* 286: C230-238, 2004.
45. Lucero HA, and Kagan HM. Lysyl oxidase: an oxidative enzyme and effector of cell function. *Cell Mol Life Sci* 63: 2304-2316, 2006.
46. MacIntosh BR, Gardiner PF, and McComas AJ. *Skeletal muscle : form and function*. Champaign, IL: Human Kinetics, 2006, p. 423 p.
47. Maganaris C, Narici M, and Reeves N. In vivo human tendon mechanical properties: effect of resistance training in old age. *Journal of musculoskeletal & neuronal interactions* 4: 204-208, 2004.
48. Magnusson S, Hansen P, and Kjaer M. Tendon properties in relation to muscular activity and physical training. *Scandinavian journal of medicine & science in sports* 13: 211-223, 2003.

49. Mahoney D, Carey K, Fu M, Snow R, Cameron-Smith D, Parise G, and Tarnopolsky M. Real-time RT-PCR analysis of housekeeping genes in human skeletal muscle following acute exercise. *Physiol Genomics* 18: 226-231, 2004.
50. Maxwell L, Faulkner J, and Hyatt G. Estimation of number of fibers in guinea pig skeletal muscles. *Journal of applied physiology* 37: 259-264, 1974.
51. McCully KK, and Faulkner JA. Characteristics of lengthening contractions associated with injury to skeletal muscle fibers. *J Appl Physiol* 61: 293-299, 1986.
52. McCully KK, and Faulkner JA. Injury to skeletal muscle fibers of mice following lengthening contractions. *J Appl Physiol* 59: 119-126, 1985.
53. McFarlane C, Plummer E, Thomas M, Hennebry A, Ashby M, Ling N, Smith H, Sharma M, and Kambadur R. Myostatin induces cachexia by activating the ubiquitin proteolytic system through an NF-kappaB-independent, FoxO1-dependent mechanism. *J Cell Physiol* 209: 501-514, 2006.
54. McPherron A, Lawler A, and Lee S. Regulation of skeletal muscle mass in mice by a new TGF-beta superfamily member. *Nature* 387: 83-90, 1997.
55. Monti RJ, Roy RR, Hodgson JA, and Edgerton VR. Transmission of forces within mammalian skeletal muscles. *J Biomech* 32: 371-380, 1999.
56. Moore MJ, and De Beaux A. A quantitative ultrastructural study of rat tendon from birth to maturity. *J Anat* 153: 163-169, 1987.
57. Moustakas A, Souchelnytskyi S, and Heldin C. Smad regulation in TGF-beta signal transduction. *J Cell Sci* 114: 4359-4369, 2001.
58. Muir AR, Kanji AH, and Allbrook D. The structure of the satellite cells in skeletal muscle. *J Anat* 99: 435-444, 1965.
59. Nakagawa Y, Majima T, and Nagashima K. Effect of ageing on ultrastructure of slow and fast skeletal muscle tendon in rabbit Achilles tendons. *Acta Physiol Scand* 152: 307-313, 1994.
60. O'Brien M. Functional anatomy and physiology of tendons. *Clin Sports Med* 11: 505-520, 1992.
61. Paxton JZ, and Baar K. Tendon Mechanics: The Argument Heats Up. *J Appl Physiol* 2007.
62. Philip B, Lu Z, and Gao Y. Regulation of GDF-8 signaling by the p38 MAPK. *Cell Signal* 17: 365-375, 2005.
63. Purslow PP, and Trotter JA. The morphology and mechanical properties of endomysium in series-fibred muscles: variations with muscle length. *J Muscle Res Cell Motil* 15: 299-308, 1994.
64. Rader EP, Song W, Van Remmen H, Richardson A, and Faulkner JA. Raising the antioxidant levels within mouse muscle fibres does not affect contraction-induced injury. *Exp Physiol* 91: 781-789, 2006.
65. Reddy G, Stehno-Bittel L, and Enwemeka C. Glycation-induced matrix stability in the rabbit achilles tendon. *Arch Biochem Biophys* 399: 174-180, 2002.
66. Reisz-Porszasz S, Bhasin S, Artaza J, Shen R, Sinha-Hikim I, Hogue A, Fielder T, and Gonzalez-Cadavid N. Lower skeletal muscle mass in male transgenic mice with muscle-specific overexpression of myostatin. *Am J Physiol Endocrinol Metab* 285: E876-888, 2003.

67. Rybakova IN, Patel JR, and Ervasti JM. The dystrophin complex forms a mechanically strong link between the sarcolemma and costameric actin. *J Cell Biol* 150: 1209-1214, 2000.
68. Sandri M, Sandri C, Gilbert A, Skurk C, Calabria E, Picard A, Walsh K, Schiaffino S, Lecker S, and Goldberg A. Foxo transcription factors induce the atrophy-related ubiquitin ligase atrogin-1 and cause skeletal muscle atrophy. *Cell* 117: 399-412, 2004.
69. Seoane J, Le H, Shen L, Anderson S, and Massagué J. Integration of Smad and forkhead pathways in the control of neuroepithelial and glioblastoma cell proliferation. *Cell* 117: 211-223, 2004.
70. Smith HK, Maxwell L, Martyn JA, and Bass JJ. Nuclear DNA fragmentation and morphological alterations in adult rabbit skeletal muscle after short-term immobilization. *Cell Tissue Res* 302: 235-241, 2000.
71. Solaro RJ, Pang DC, and Briggs FN. The purification of cardiac myofibrils with Triton X-100. *Biochim Biophys Acta* 245: 259-262, 1971.
72. Sommer H. The biomechanical and metabolic effects of a running regime on the Achilles tendon in the rat. *International orthopaedics* 11: 71-75, 1987.
73. Squire JM. Architecture and function in the muscle sarcomere. *Curr Opin Struct Biol* 7: 247-257, 1997.
74. Squire JM. Muscle contraction. *Encyclopedia of Life Sciences* 2005.
75. Tapscott SJ. The circuitry of a master switch: Myod and the regulation of skeletal muscle gene transcription. *Development* 132: 2685-2695, 2005.
76. Tatsumi R, and Allen R. Active hepatocyte growth factor is present in skeletal muscle extracellular matrix. *Muscle Nerve* 30: 654-658, 2004.
77. Tatsumi R, Liu X, Pulido A, Morales M, Sakata T, Dial S, Hattori A, Ikeuchi Y, and Allen R. Satellite cell activation in stretched skeletal muscle and the role of nitric oxide and hepatocyte growth factor. *Am J Physiol, Cell Physiol* 290: C1487-1494, 2006.
78. Turner PR, Fong PY, Denetclaw WF, and Steinhardt RA. Increased calcium influx in dystrophic muscle. *J Cell Biol* 115: 1701-1712, 1991.
79. Viidik A. The effect of training on the tensile strength of isolated rabbit tendons. *Scand J Plast Reconstr Surg* 1: 141-147, 1967.
80. Vilarta R, and Vidal Bde C. Anisotropic and biomechanical properties of tendons modified by exercise and denervation: aggregation and macromolecular order in collagen bundles. *Matrix* 9: 55-61, 1989.
81. Wagner K. Muscle regeneration through myostatin inhibition. *Current opinion in rheumatology* 17: 720-724, 2005.
82. Wang J. Mechanobiology of tendon. *Journal of biomechanics* 39: 1563-1582, 2006.
83. Welle S, Bhatt K, and Pinkert C. Myofibrillar protein synthesis in myostatin-deficient mice. *Am J Physiol Endocrinol Metab* 290: E409-415, 2006.
84. Whittemore L, Song K, Li X, Aghajanian J, Davies M, Girgenrath S, Hill J, Jalenak M, Kelley P, Knight A, Maylor R, O'Hara D, Pearson A, Quazi A, Ryerson S, Tan X, Tomkinson K, Veldman G, Widom A, Wright J, Wudyka S, Zhao L, and Wolfman N. Inhibition of myostatin in adult mice increases skeletal muscle mass and strength. *Biochem Biophys Res Commun* 300: 965-971, 2003.

85. Williams M. Myostatin mutation associated with gross muscle hypertrophy in a child. *N Engl J Med* 351: 1030-1031; author reply 1030-1031, 2004.
86. Woo SL, Gomez MA, Amiel D, Ritter MA, Gelberman RH, and Akeson WH. The effects of exercise on the biomechanical and biochemical properties of swine digital flexor tendons. *J Biomech Eng* 103: 51-56, 1981.
87. Woo SL, Ritter MA, Amiel D, Sanders TM, Gomez MA, Kuei SC, Garfin SR, and Akeson WH. The biomechanical and biochemical properties of swine tendons--long term effects of exercise on the digital extensors. *Connect Tissue Res* 7: 177-183, 1980.
88. Yang W, Chen Y, Zhang Y, Wang X, Yang N, and Zhu D. Extracellular signal-regulated kinase 1/2 mitogen-activated protein kinase pathway is involved in myostatin-regulated differentiation repression. *Cancer Res* 66: 1320-1326, 2006.
89. Yang W, Zhang Y, Li Y, Wu Z, and Zhu D. Myostatin induces cyclin D1 degradation to cause cell cycle arrest through a phosphatidylinositol 3-kinase/AKT/GSK-3 beta pathway and is antagonized by insulin-like growth factor 1. *J Biol Chem* 282: 3799-3808, 2007.
90. Zhu X, Hadhazy M, Wehling M, Tidball J, and McNally E. Dominant negative myostatin produces hypertrophy without hyperplasia in muscle. *FEBS Lett* 474: 71-75, 2000.
91. Zimmers T, Davies M, Koniaris L, Haynes P, Esquela A, Tomkinson K, McPherron A, Wolfman N, and Lee S. Induction of cachexia in mice by systemically administered myostatin. *Science* 296: 1486-1488, 2002.

Chapter II

Contractile Properties of Extensor Digitorum Longus and Soleus Muscles of Myostatin-Deficient Mice

Abstract

Myostatin is a negative regulator of muscle mass. The impact of myostatin deficiency on the contractile properties of healthy muscles has not been determined. We hypothesized that myostatin deficiency would increase the maximum tetanic force (P_o), but decrease the specific P_o (sP_o) of muscles and increase the susceptibility to contraction-induced injury. The *in vitro* contractile properties of EDL and soleus muscles from wild type ($MSTN^{+/+}$), heterozygous-null ($MSTN^{+/-}$) and homozygous-null ($MSTN^{-/-}$) adult male mice were determined. For EDL muscles, the P_o of both $MSTN^{+/-}$ and $MSTN^{-/-}$ mice were greater than the P_o of $MSTN^{+/+}$ mice. For soleus muscles, the P_o of $MSTN^{-/-}$ mice was greater than that of $MSTN^{+/+}$ mice. The sP_o of EDL muscles of $MSTN^{-/-}$ mice was less than $MSTN^{+/+}$ mice. For soleus muscles, however, no difference in sP_o was observed. Following two lengthening contractions, EDL muscles from $MSTN^{-/-}$ mice had a greater force deficit than $MSTN^{+/+}$ or $MSTN^{+/-}$ mice, whereas no differences were observed for the force deficits of soleus muscles. Myostatin deficient EDL muscles had less hydroxyproline, and myostatin directly increased type I collagen mRNA expression and protein content. The difference in the response of EDL and soleus muscles to myostatin may arise from differences in

the levels of a myostatin receptor, ActRIIB. Compared with the soleus, the amount of ActRIIB was approximately two-fold greater in EDL muscles. The results support a significant role for myostatin not only in the mass of muscles, but also in the contractility and the composition of the ECM of muscles.

Introduction

Myostatin (GDF-8) is a member of the transforming growth factor-beta (TGF-β) family of cytokines and functions as a negative regulator of skeletal muscle mass. Inactivation of the myostatin genes and post-natal inhibition of myostatin both result in significant increases in skeletal muscle mass (4, 5, 21, 42, 47, 65, 68, 69). Systemic and skeletal muscle specific overexpression of myostatin induce skeletal muscle atrophy (52, 71). The Belgian Blue and Piedmontese breeds of cattle have a mutated form of the myostatin gene and are characterized by larger skeletal muscles than other breeds (20, 24). At the time of birth, a human child with apparent null mutations in his myostatin genes had a thigh muscle volume two-fold greater in size than ten age-matched controls (54). The child's mother, who is heterozygous for the mutation, was also reported to be hypermuscular (54).

Myostatin circulates through the blood in a latent form bound to its propeptide and to follistatin (2). The myostatin gene (*MSTN*) encodes a precursor protein that undergoes proteolytic processing to generate a propeptide and a mature myostatin dimer (67). The propeptide binds myostatin noncovalently and inhibits the bioactivity of myostatin (42, 57, 67). Cleavage of the propeptide by the BMP-1/tolloid family of metalloproteinases results in the

liberation and activation of myostatin (67). Activated myostatin binds to the activin type IIB (ActRIIB) and IB (ActRIB) receptors to initiate the Smad2/3 and p38 MAPK intercellular signal transduction cascades (29, 46, 50, 70). Myostatin appears to regulate skeletal muscle mass, at least in part, by inhibiting the proliferation, differentiation and self-renewal of myoblasts (28, 39, 56, 58). Type II muscle fibers appear to be more responsive to the myostatin signaling pathway than type I muscles, but the mechanism responsible for this difference is unknown (10, 37, 41, 43).

The inhibition of myostatin may be useful in the treatment of muscle injuries and muscle wasting diseases by improving the contractile properties of muscle (17, 26, 45, 53, 55, 59, 61). Compared with wild type mice, myostatin deficient mice have increased bite force (9) and gross grip strength (65). Treating *mdx* mice with an antibody against myostatin increased the maximum tetanic force (P_o) of EDL muscles, but did not change the specific maximum tetanic force (sP_o) (4). When *mdx* mice were treated with the propeptide of myostatin, both the P_o and sP_o of EDL muscles increased (5).

Myostatin may also be useful in treating muscle injuries and disease by regulating the collagen accumulation and scar tissue formation in the extracellular matrix (ECM) (17, 45). In addition to enhancing the contractile properties of dystrophic muscle, the deficiency of myostatin decreased the accumulation of scar tissue and ECM of *mdx* mice (4, 5, 63). Type I collagen is a major component of muscle ECM (31). The transcripts of two separate genes, *col1α1* and *col1α2*, are used to synthesize the collagen I precursor molecule,

procollagen I. Procollagen I is secreted into the ECM where it undergoes cleavage and assembly to form mature collagen I (27). TGF-β has a well established role as a positive regulator of type I collagen protein synthesis via the Smad2/3 and p38-MAPK signaling pathways (reviewed in (60)). As myostatin is a member of the TGF-β family of cytokines and utilizes similar signal transduction pathways as TGF-β (29, 46, 50, 70), myostatin may have a direct role in the regulation of the type I collagen content of skeletal muscle ECM.

While a few studies have examined the effects of myostatin deficiency on the contractile properties and ECM of dystrophic muscles (4, 5, 63), how myostatin deficiency impacts on healthy, non-dystrophic muscle is unknown. The overall aim of this study was to determine the effect of myostatin deficiency on the contractile properties, susceptibility to contraction-induced injury and collagen composition of skeletal muscle tissue. As increases in P_o due to hypertrophy of muscle fibers often results in a corresponding decrease in sP_o (15, 25, 30), we hypothesized that a deficiency of myostatin would increase the P_o, but decrease the sP_o. Based upon the observations that myostatin deficiency decreased the ECM accumulation in dystrophic muscle (4, 5, 63), and the similarities between the myostatin and TGF-β signal transduction pathways (29, 46, 50, 70), we formed the hypothesis that myostatin deficient mice would have less muscle ECM and that myostatin would directly increase type I collagen expression in skeletal muscle tissue. If these assumptions proved to be correct, we hypothesized that the deficiency of myostatin would increase the force deficits of muscles following a protocol of damaging lengthening contractions.

Methods

Animals. All experiments were conducted in accordance with the guidelines of the University of Michigan Committee on the Use and Care of Animals. Mice were housed in specific-pathogen-free conditions and fed food and water ad libidum. $MSTN^{-/-}$ mice of a C57BL/6 background were a generous gift of Dr. Se-Jin Lee. The MSTN null allele was generated by replacing the portion of the third exon of the MSTN gene that encodes the C-terminal region of the mature myostatin protein with a neo cassette (42). Male $MSTN^{-/-}$ mice were crossed with $MSTN^{+/+}$ C57BL/6 female mice to generate an F1 $MSTN^{+/-}$ generation. The F1 generation was backcrossed to obtain an F2 generation containing all three genotypes. F2 male mice 10 - 12 months of age were used in this study. The genotype of mice was determined by PCR-based analysis of genomic DNA samples obtained via tail biopsy. The MSTN wild type allele was detected using a set of primers that generate a 247 bp amplicon from the third exon of the MSTN gene, and the MSTN null allele was detected using a set of primers that generate a 192 bp amplicon from the neo cassette that replaced the third exon of the MSTN gene. Amplicons from PCR reactions were separated on a 2% agarose gel.

Operative Procedure. Mice were anesthetized with intraperitoneal injection of Avertin (400 mg/kg). Additional doses were provided as required to maintain a deep anesthesia throughout the experiment. The EDL and soleus muscles were removed from both the left and right legs of each mouse. Muscles used for fiber counts, hydroxyproline, histochemistry or protein analysis were

flash frozen in liquid nitrogen and stored at -80°C until use. A 5-0 silk suture was tied to the proximal and distal tendons of muscles used in the contractile properties experiments. These muscles were placed immediately in a bath that contained Kreb's mammalian Ringer solution with 0.25 mM tubocurarine chrloride. The bath was maintained at 25°C and the solution was bubbled with 95% O_2 and 5% CO_2 to stabilize pH at 7.4. Following the removal of muscles, mice were euthanized with an overdose of anesthetic and induction of a pneumothorax.

Fiber Counts of Muscles. To determine the number of fibers present in muscles, the extracellular matrices of muscles were digested as described (38). Briefly, muscles were placed in a 15% HNO_3 solution overnight at room temperature. Following digestion, the HNO_3 solution was replaced with phosphate buffered saline. Individual muscle fibers were teased apart from bundles and counted under a dissecting microscope. The lengths of forty individual fibers per muscle were measured using digital calipers.

Measurement of Maximum Isometric Tetanic Force. Each muscle was immersed in the bath solution and the distal tendon was attached to a servo motor (model 305B, Aurora Scientific, Aurora, ON). The proximal tendon was attached to a force transducer (model BG-50, Kulite Semiconductor Products, Leonia, NJ). The attachment of tendons to the servo motor and force transducer occurred just distal to the myotendinous junctions so that the impact of the tendon on the measurement of contractile properties was minimized. Muscles were stimulated by square pulses delivered by two platinum electrodes

connected to a high-power biphasic current stimulator (model 701B, Aurora Scientific). An IBM-compatible personal computer and custom designed software (LabVIEW 7.1, National Instruments, Austin, TX) controlled electrical pulse properties and servo motor activity and recorded data from the force transducer. The voltage of pulses was increased and muscle length (L_o) was subsequently adjusted to the length that resulted in maximum twitch force (P_t) (6). The L_o was measured with digital calipers. Muscles were held at L_o and subjected to trains of pulses to generate an isometric contraction. Pulse trains were 300 ms for EDL muscles and 900 ms for soleus muscles. Stimulus frequency was increased until the P_o was achieved (6). The general shape of the force traces during twitch and isometric contractions were not different between the three genotypes of mice for EDL and soleus muscles, respectively. The sP_o was determined by dividing P_o by the cross sectional area (CSA). Following nitric acid digestion, both EDL and soleus muscles showed no difference in the ratio of fiber lengths to whole muscle lengths among any of the three genotypes. Therefore the L_f/L_o ratios of 0.44 for EDL muscles and 0.70 for soleus muscles were used to calculate L_f (6). The physiological CSA of muscles was determined by dividing the mass of the muscle by the product of L_f and 1.06 g/cm^3, the density of mammalian skeletal muscle.

Contraction-Induced Injury. Following measurement of P_t and P_o, a mechanical injury to muscles was produced by two 40% lengthening contractions (7, 11, 14). Muscles were stimulated and held at L_o for 100 ms for EDL muscles and 300 ms for soleus muscles to allow muscles to develop P_o. Following the

isometric contraction, muscles were stretched through a 40% strain relative to L_f. A 40% strain of the EDL plantarflexes the ankle by 12º and the soleus dorsiflexes by 16º. The velocity of the stretch was 1 L_f/s. The total time of stimulation was 500 ms. Following stimulation, muscles were returned to L_o, remained quiescent for 1 min, then were subjected to a second 40% strain. Following 1 min of rest the P_o was measured. The general shape of the force traces during lengthening contractions were not different for any of the three genotypes of mice. The average force produced during a stretch was calculated by integrating the force-time curve and dividing this value by the duration of the stretch. Work was calculated by multiplying the average force produced during a stretch by the length of the displacement and normalized by the wet mass of the muscle.

Measurement of Lengths of Tibias. Hindlimbs from euthanized mice were stripped of gross muscle and connective tissue and placed in 20% hydrogen peroxide at 55°C overnight to remove remaining soft tissue. Photographic images of tibias were analyzed with ImageJ (version 1.34, NIH, Bethesda, MD) to determine length.

Hydroxyproline Assay. Hydroxyproline content of muscles was measured as described by Woessner (66). Muscles were dried for 90 min at 110ºC and hydrolyzed in 500 µL of 6 M hydrochloric acid for 3.5 hours. The hydrolysate was neutralized with an equal volume of 6 M sodium hydroxide. Known amounts of purified L-hydroxyproline (Sigma, St. Louis, MO) were used to construct a standard curve. Samples were assayed in triplicate using a Genios plate reader (Tecan, Mannedorf, Switzerland) at an absorbance of 560 nm.

Histology. Muscles were cryosectioned at their mid-belly and stained with Masson's Trichrome. The areas of 100 muscle fibers randomly selected from sections of three muscles of each of the three genotypes were measured using ImageJ.

ActRIIB Immunoblot. Muscles that did not undergo assessments of the contractile properties were homogenized in cold Laemmli's sample buffer with 1:20 β-mercaptoethanol and 1:20 protease inhibitor cocktail (Sigma) and then placed in boiling water for 5 minutes. Protein concentration of the samples was determined using an RC DC Protein Assay (Bio-Rad, Hercules, CA). Equal amounts of protein were loaded into two 4% stacking, 7.5% separating polyacrylamide gels and subjected to electrophoresis. To verify equal protein loading, gels that were not used in immunoblotting were stained with Coomassie Brilliant Blue (Bio-Rad). Proteins were transferred to a 0.45 μm nitrocellulose membrane and stained with Ponceau S to verify equal protein transfer. Membranes were blocked using casein and an avidin-biotin blocking kit (Vector Labs, Burlingame, CA), rinsed and incubated with a biotinylated monoclonal antibody against ActRIIB (R & D Systems, Minneapolis, MN) and an avidin-HRPO conjugate (Vector Labs). Membranes were developed with SuperSignal West Dura enhanced chemiluminescent reagents (Pierce Biotechnology, Rockford, IL) and visualized using a chemiluminescent documentation system (Bio-Rad).

Satellite Cell Isolation and Culture. Satellite cells were isolated from adult male $MSTN^{+/+}$ mice as described by Allen and his colleagues (1). Mice were

anesthetized with intraperitoneal injection of Avertin (400 mg/kg) and sacrificed by cervical dislocation. The hindlimb muscles were quickly removed, minced and digested in protease solution (1.25 mg/mL of Pronase E in PBS, Sigma) for 1 hour at 37ºC. Satellite cells were separated from muscle fiber fragments and from tissue debris by differential centrifugation and then plated on fibronectin coated 60mm tissue culture plates (BD Biosciences, San Jose, CA). Cultures were maintained in a humidified environment maintained at 37ºC and 5% CO_2. Satellite cells were grown in DMEM + 20% FBS + 1% antibiotic-antimycotic (AbAm) until reaching 80% confluence, at which time the media was changed to DMEM + 2% horse serum + 1% AbAm to induce differentiation into myotubes.

RT-qPCR. Myotubes were treated with different concentrations of recombinant murine myostatin (R & D Systems, Minneapolis, MN) in DMEM + 1% AbAm for 2 hours. RNA was isolated from myotubes using an RNeasy Mini kit (Qiagen, Valencia, CA), treated with DNase I and reverse transcribed using an Omniscript RT kit (Qiagen) and oligo$(dT)_{15}$ primers. cDNA was amplified using primers for col1α2 (forward: 5'-CCAGCGAAGAACTCATACAGC-3'; reverse: 5'-GGACACCCCTTCTACGTTGT-3') and β2-microglobulin (forward: 5'-ATGGGAAGCCGAACATACTG-3'; reverse: 5'-CAGTCTCAGTGGGGGTGAAT-3') using a SYBR Green I PCR system (Qiagen) with Uracil DNA Glycosylase (Invitrogen) in an Opticon 2 real-time thermal cycler (Bio-Rad). qPCR reactions were conducted in triplicate for each sample. C(t) values for col1α2 were normalized to β2-microglobulin (β2m) using the $2^{-\Delta\Delta C(t)}$ method (32). β2m was chosen as a housekeeping gene based on its stable expression in skeletal

muscle tissue (35) and because β2m expression did not differ between treatment groups. The presence of single amplicons from qPCR reactions were verified by melting curve analysis as well as electrophoresis using a 2% agarose gel. Primers for col1α2 generate a 105 bp amplicon from exons 46 and 47 of the col1α2 gene. Intron 46 - 47 of the col1α2 gene is 320 bp which would allow us to detect the presence of genomic DNA in qPCR reactions using gel electrophoresis. Genomic DNA contamination was not detected in qPCR reactions.

Procollagen I Immunoblot. Myotubes were treated with different concentrations of recombinant murine myostatin (R & D Systems) in DMEM + 1% AbAm for 8 hours, rinsed with PBS and 0.5M EDTA, scraped and homogenized in Laemmli's sample buffer with 1:20 β-mercaptoethanol and 1:20 protease inhibitor cocktail (Sigma) and subsequently placed in boiling water for 5 minutes. Protein concentration, electrophoresis and blotting occurred as described above. Membranes were blocked in 10% powdered milk, rinsed and incubated with a polyclonal antibody against procollagen I (Santa Cruz Biotechnology, Santa Cruz, CA) and an HRPO conjugated secondary antibody (Pierce Biotechnology), and developed as described above. Following detection of procollagen I, membranes were stripped and reprobed using a monoclonal antibody against β-tubulin (Developmental Studies Hybridoma Bank, Iowa City, IA).

Statistical Analyses. Results are presented as mean ± SEM. KaleidaGraph 4.02 software (Synergy Software, Reading, PA) was used to conduct statistical analyses. Differences between groups were tested using a

one-way ANOVA with α=0.05. Fisher's LSD post-hoc test was used to identify specific differences when significance was detected.

Results

Morphology. The body mass, body length, tibial length, muscle mass, absolute numbers of fibers per muscle, fiber areas, L_o, L_f, and CSA values of EDL and soleus muscles from each of the three groups of mice are shown in Table 2.1. Although no differences were observed for body masses or body lengths of the *MSTN*$^{+/+}$, *MSTN*$^{+/-}$ or *MSTN*$^{-/-}$ mice, the mean mass of the EDL muscles of *MSTN*$^{-/-}$ mice was 66% greater than that of the *MSTN*$^{+/+}$ mice and 51% greater than that of the *MSTN*$^{+/-}$ mice. For *MSTN*$^{-/-}$ mice, the mass of the soleus was 36% greater soleus muscle mass than that of the *MSTN*$^{+/+}$ mice.

Conflicting reports have been published regarding the role of myostatin in determining the number of fibers per muscle (21, 36, 42, 47, 51, 68, 69). Each of these reports counted the number of muscle fibers present in a cross section of muscle. The counting of the number of fibers present in a cross section of a muscle does not necessarily provide an accurate indication of the total number of fibers present in that muscle (38). To address this issue, the absolute number of fibers in muscles from *MSTN*$^{+/+}$, *MSTN*$^{+/-}$ and *MSTN*$^{-/-}$ mice were counted. The EDL muscles of *MSTN*$^{-/-}$ mice had 60% more muscle fibers than *MSTN*$^{+/+}$ mice and 39% more fibers than *MSTN*$^{+/-}$ mice, and the *MSTN*$^{+/-}$ mice had 16% more fibers than *MSTN*$^{+/+}$ mice (Table 2.1). For soleus muscles, *MSTN*$^{-/-}$ mice had 31% more fibers than *MSTN*$^{+/+}$ mice and 9% more than *MSTN*$^{+/-}$ mice, and the *MSTN*$^{+/-}$ mice had 20% more fibers than *MSTN*$^{+/+}$ mice (Table 2.1).

The mean fiber areas and CSA of EDL muscles of *MSTN*$^{+/-}$ and *MSTN*$^{-/-}$ mice were greater than *MSTN*$^{+/+}$ mice. For soleus muscles, the mean fiber areas and CSA of *MSTN*$^{-/-}$ mice were greater than *MSTN*$^{+/+}$ mice (Table 2.1).

The EDL and soleus muscles of mice both originate on the proximal tibia and run the entire length of the tibia before inserting on the phalanges or calcaneus, respectively. No differences in the lengths of tibias of *MSTN*$^{+/+}$, *MSTN*$^{+/-}$ and *MSTN*$^{-/-}$ mice were observed (Table 2.1). Furthermore, the L_o and L_f values of EDL and soleus muscles, respectively, were not different among the three genotypes.

Collagen Content of Muscles. The amino acid hydroxyproline makes up ~14% of the dry mass of fibrillar collagens (44) and is commonly used as an indicator of collagen content. The relative hydroxyproline content of EDL muscles of MSTN$^{-/-}$ was 75% less than MSTN$^{+/+}$ mice (Table 2.1 and Figure 2.1). MSTN$^{+/-}$ mice had 59% less hydroxyproline than MSTN$^{+/+}$ mice. For soleus muscles, no difference was observed for the relative amounts of hydroxyproline amongst the three genotypes (Table 2.1 and Figure 2.1).

Myostatin Mediated Type I Collagen Synthesis. The marked decrease in the collagen content of the EDL muscles from myostatin deficient mice lead us to hypothesize that myostatin induces the expression of type I collagen in muscle tissue. We found a dose dependent increase in col1α2 expression (Figure 2.2) and procollagen I protein content (Figure 2.2) of primary myotubes treated with myostatin. Similar results were observed in C_2C_{12} myotubes and primary fibroblasts isolated from mouse tendon (data not shown).

Contractile Properties. Myostatin deficiency had a more profound impact on the contractile properties of EDL muscles than soleus muscles (Table 2.2 and Figure 2.3). The P_o of $MSTN^{-/-}$ mice was 34% greater than the P_o of $MSTN^{+/+}$ mice and 19% greater than the P_o of $MSTN^{+/-}$ mice. $MSTN^{+/-}$ mice had a 13% greater P_o than $MSTN^{+/+}$ mice. When P_o was normalized by the CSA, $MSTN^{-/-}$ mice had an 18% lower value for sP_o than either $MSTN^{+/+}$ or $MSTN^{+/-}$ mice. For soleus muscles, the P_o of $MSTN^{-/-}$ mice was 30% greater than $MSTN^{+/+}$ mice, but the values for sP_o were not different.

Contraction-Induced Injury. During lengthening contractions, the average force developed by EDL muscles was not different, but compared with $MSTN^{+/+}$ mice, the work done to lengthen the muscles was 12% and 37% less for $MSTN^{+/-}$ and $MSTN^{-/-}$ mice, respectively (Table 2.3), indicating a decrease in the stiffness of these muscles. After the lengthening contraction protocol (LCP), muscles from $MSTN^{-/-}$ mice had a force deficit that was 15% greater than $MSTN^{+/+}$ mice (Table 2.3 and Figure 2.4). During stretches of soleus muscles, the average force developed by $MSTN^{-/-}$ mice was approximately 18% greater than that of $MSTN^{+/+}$ mice. During lengthening contractions of soleus muscles, no differences in the work done to stretch the muscles were observed. Following the LCP, the force deficits of soleus muscles were not different.

ActRIIB Content of EDL and Soleus Muscles. The deficiency of myostatin had a more profound impact on the morphological and contractile properties of EDL muscles than soleus muscles. Since myostatin appears to act systemically (71), the difference in the amount of ActRIIB present in EDL and soleus muscles

was determined. Compared with soleus muscles, the amount of ActRIIB was greater in EDL muscles (Figure 2.5).

Discussion

The P_o of skeletal muscle can be increased by either hypertrophy of existing fibers or by hyperplasia. In either case, as whole muscle CSA increases, the angle of pennation of muscle fibers (θ) also increases (38). The transmission of the force developed by single muscle fibers from tendon to tendon along the line of tension development of the muscle is proportional to the cosine of θ. As θ increases from 0º to 90º, the cosine of θ decreases from 1 to 0. Therefore, as a muscle undergoes hypertrophy or hyperplasia, the net force per CSA is expected to decrease. Our hypothesis that myostatin deficiency would increase the P_o but decrease the sP_o of muscles is supported by the observations of the contractile properties of the EDL muscles of *MSTN*$^{-/-}$ mice. In contrast, for soleus muscles, the complete deficiency of myostatin increased the P_o less than that of the EDL muscle and had no effect on the sP_o. Furthermore, EDL muscles of *MSTN*$^{+/-}$ mice displayed a greater P_o than *MSTN*$^{+/+}$ mice, but showed no change in sP_o. While θ was not measured directly, using a model of muscle architecture that estimates θ based upon the number of fibers in a muscle, L_f, L_o and fiber areas (38), compared with *MSTN*$^{+/+}$ mice, we estimate that *MSTN*$^{-/-}$ mice had a 38% greater θ for EDL muscles, and a 17% greater θ for soleus muscles, respectively. The greater increase in θ for EDL than soleus muscles may explain the observed decrease in sP_o for EDL muscles and the lack of change in sP_o for soleus muscles. In terms of the magnitude of the increases in muscle CSA, mass and

P_o, a threshold appears to exist for initiating a decrease in sP_o, wherein large increases in muscle CSA, mass and P_o initiate decreases in sP_o, whereas with small increases, sP_o does not change.

Following contraction-induced injury to muscles, the immediate force deficit results from the mechanical disruption of the ultrastructure of sarcomeres (8, 18, 33, 34). The magnitude of this force deficit is a function of strain and the work done to stretch the contractile component (CC) of muscle (8). The aponeurosis (intramuscular tendon) and the tendon, composed chiefly of type I and III collagen (12, 22, 27), form the series elastic component (SEC) of muscle (23). A positive correlation exists between the collagen content and stiffness of a muscle (16, 19, 48). During a lengthening contraction, the total displacement of the muscle is the sum of the displacement of the CC and the SEC, therefore displacement of the SEC protects the CC from contraction-induced injury. During a lengthening contraction, the protection afforded to the CC by the SEC increases as the displacement of the SEC relative to the CC increases. Despite this potential for protection, if the strain and work done during a lengthening contraction are great enough, the SEC can become damaged and no longer provide protection for the CC. Consequently, an advantageous arrangement for a muscle is to have an SEC with a stiffness that allows for a moderate amount of displacement during a lengthening contraction, but not too compliant as to become damaged during a lengthening contraction. Our results suggest that for EDL muscles, the complete deficiency of myostatin decreases the stiffness of the

SEC in such a way that the susceptibility to contraction-induced injury is increased.

The effect of myostatin deficiency on the structure and function of EDL and soleus muscles was quite different. Compared with the content of the primary myostatin receptor, ActRIIB, in the soleus muscles of *MSTN*$^{+/+}$ mice, the content in the EDL muscles was ~ two-fold greater. The greater quantity of ActRIIB in the EDL muscles of *MSTN*$^{+/+}$ mice appeared to make the EDL muscles more responsive than soleus muscles to the presence of myostatin. Consequently, with the absence of myostatin in the *MSTN*$^{-/-}$ mice, the EDL muscles experience a much greater relative increase in mass and number of fibers than experienced by the soleus muscles.

The treatment of muscle injuries and disease often involves a two-pronged therapeutic regimen of improving the strength of muscle and decreasing the formation of collagenous scar tissue (13, 49). Much of the interest behind the potential use of myostatin inhibitors is the ability of these inhibitors to enhance the regeneration of skeletal muscle and also decrease the accumulation of scar tissue in murine models of muscle injuries and disease (17, 40, 45, 61-63). Myostatin inhibitors may therefore be a useful therapeutic adjunct to traditional athletic training and physical therapy by directly improving contractility and decreasing fibrosis. The enhanced regenerative capacity of myostatin-deficient muscle is likely due to an increase in satellite cell activity, as myostatin is a negative regulator of satellite cell proliferation and migration (28, 39, 40, 56, 58, 62). The increased satellite cell activity produced by the deficiency of myostatin

does not explain how myostatin deficiency decreases the fibrosis normally present in dystrophic muscle (4, 5, 63) and following snake venom-induced muscle injury (40, 62). The decreased content of collagen in otherwise healthy myostatin-deficient muscles, along with the observation that myostatin increases directly the expression of type I collagen in cultured muscle tissue, suggest a direct role for myostatin in the signal transduction pathways that regulate the collagen content of the ECM of skeletal muscle tissue.

Pharmaceutical inhibition of myostatin likely suppresses, but does not eliminate myostatin signaling completely. The haploinsufficient *MSTN*$^{+/-}$ mouse provides a useful model for the investigation of the effects of partial suppression of myostatin signaling. In the present study, compared with their *MSTN*$^{+/+}$ littermates, the EDL muscles of *MSTN*$^{+/-}$ mice developed a greater P_o, but unlike the *MSTN*$^{-/-}$ mice had no difference in sP_o or force deficit after injury. The collagen content and stiffness of the EDL muscles of *MSTN*$^{+/-}$ mice was less than that of *MSTN*$^{+/+}$ mice, but this did not increase the susceptibility of these muscles to contraction-induced injury. Such a decrease in the stiffness of muscle might be beneficial in the treatment of diseases that involve severe muscle fibrosis, such as Duchenne muscular dystrophy (DMD). Patients with DMD suffer from respiratory insufficiency due to impaired contractility of the diaphragm muscle and to the increased stiffness of the diaphragm muscle (3, 64). Therefore, partial inhibition of myostatin may provide a useful treatment for fibrotic muscle diseases through an increase in the contractile forces and a decrease in the stiffness of the muscles.

Acknowledgements

We would like to acknowledge the generosity of Dr. Se-Jin Lee for providing transgenic mice for this study, Cheryl Hassett for providing assistance with animal surgeries and Kimberly Gates for assistance with animal breeding. This work was supported by grants AG13283 and AG020591 from the National Institute on Aging. This chapter represents previously published work: Mendias C.M., Marcin J.E., Calderon D.R., and Faulkner J.A. Contractile properties of EDL and soleus muscles of myostatin-deficient mice. J Appl Physiol 101: 898-905, 2006.

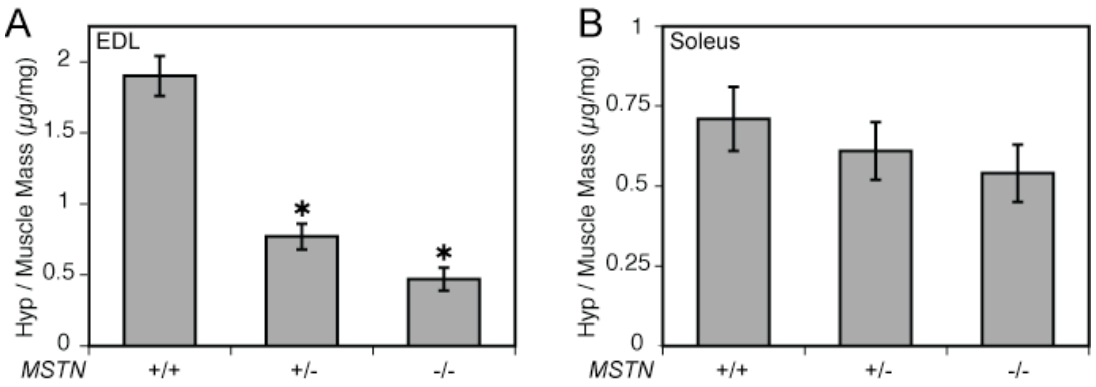

Figure 2.1. Relative hydroxyproline content of EDL (A) and soleus (B) muscles from *MSTN*$^{+/+}$, *MSTN*$^{+/-}$ and *MSTN*$^{-/-}$ mice. (A) Compared with *MSTN*$^{+/+}$ mice, the amount of hydroxyproline per mg of dry EDL muscle mass was less for *MSTN*$^{+/-}$ and *MSTN*$^{-/-}$ mice. (B) There was no difference in the amount of hydroxyproline per mg of dry soleus muscle mass between *MSTN*$^{+/+}$, *MSTN*$^{+/-}$ and *MSTN*$^{-/-}$ mice. Values are means ± SE. N = 5 muscles per genotype. *Significantly different from *MSTN*$^{+/+}$ at $P < 0.05$.

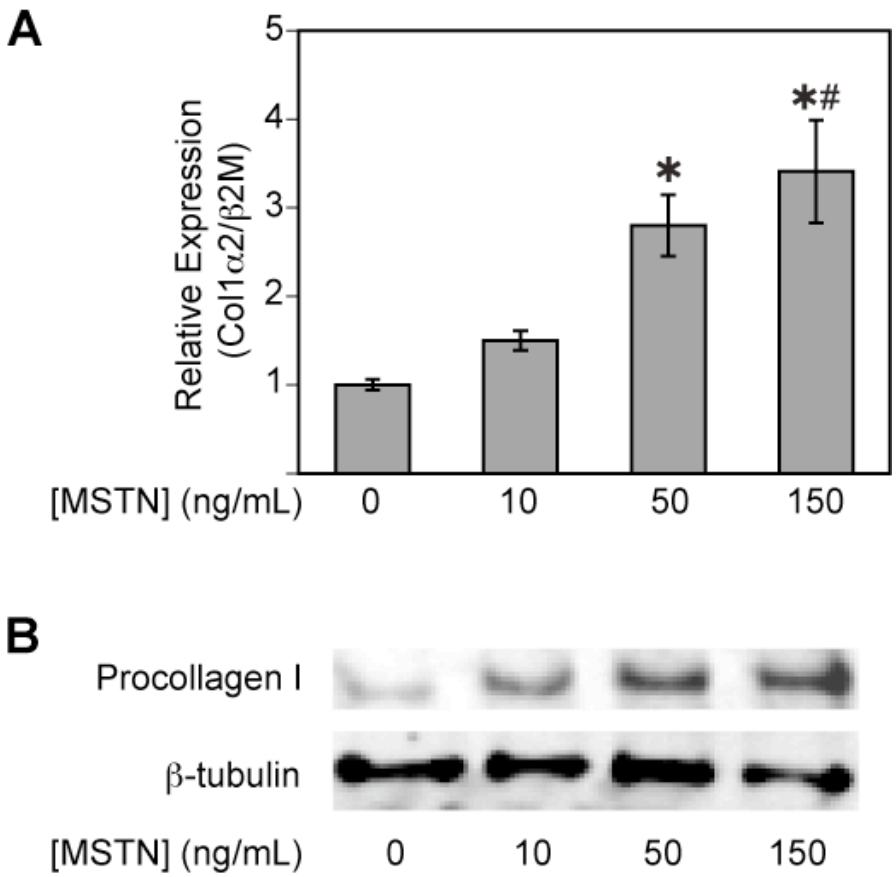

Figure 2.2. Myostatin increases (A) *col1α2* expression and (B) procollagen I content of primary skeletal muscle myotubes. (A) RT-qPCR: Myostatin increases the expression of *col1α2* normalized to *β2m* in a dose-dependant fashion. Values are means ± SE. *Significantly different from the 0 ng/mL group at P < 0.05. #Significantly different from the 10ng/mL group at P < 0.05. (B) Immunoblot: Myostatin increases the procollagen I protein content of myotubes in a dose-dependant fashion. β-tubulin is shown as a loading control.

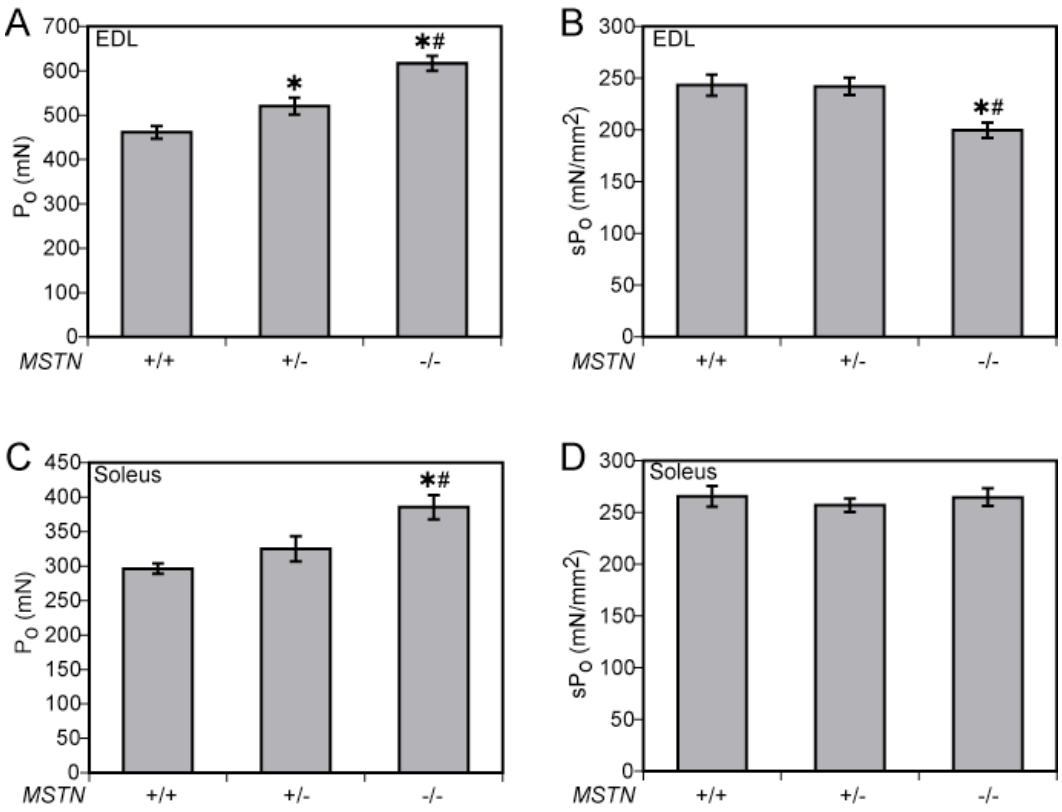

Figure 2.3. Force values for EDL muscles (A, B) and soleus muscles (C,D) from *MSTN*$^{+/+}$, *MSTN*$^{+/-}$ and *MSTN*$^{-/-}$ mice. (A) The P_o of EDL muscles of *MSTN*$^{-/-}$ mice is greater than the P_o of *MSTN*$^{+/+}$ and *MSTN*$^{+/-}$ mice. (B) When P_o is normalized to CSA, the sP_o of EDL muscles of *MSTN*$^{-/-}$ mice is less than the sP_o of *MSTN*$^{+/+}$ and *MSTN*$^{+/-}$ mice. (C) The P_o of soleus muscles of *MSTN*$^{-/-}$ mice is greater than the P_o of *MSTN*$^{+/+}$ and *MSTN*$^{+/-}$ mice. (D) When P_o is normalized to CSA, there is no difference in sP_o of soleus muscles. Values are means ± SE. N = 6 muscles per genotype. *Significantly different from *MSTN*$^{+/+}$ at $P < 0.05$. #Significantly different from *MSTN*$^{+/-}$ at $P < 0.05$.

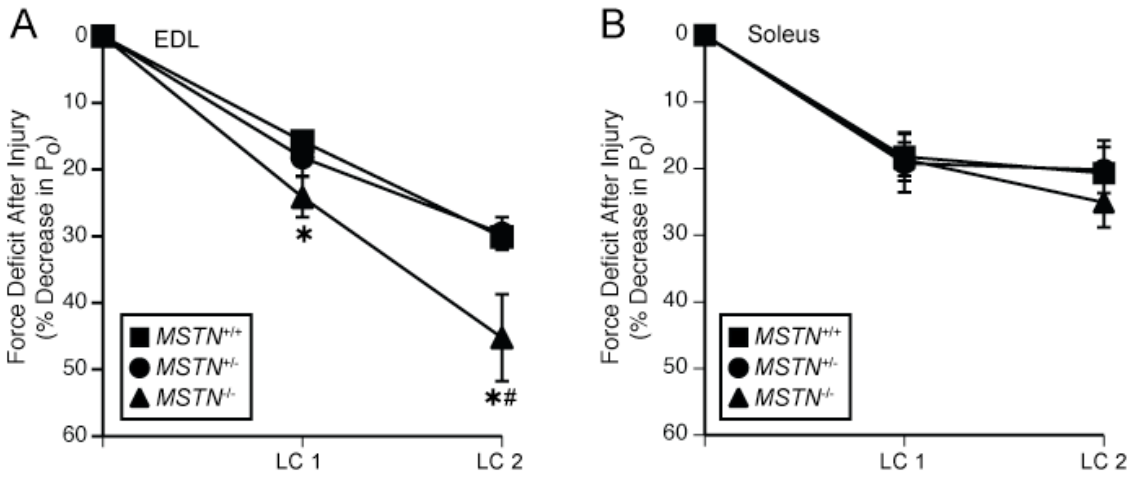

Figure 2.4. Force deficits following contraction-induced injury to EDL muscles (A) and soleus muscles (B). (A) Muscles from $MSTN^{-/-}$ mice had a force deficit that was greater than $MSTN^{+/+}$ mice after the first lengthening contraction, and a force deficit that was greater than $MSTN^{+/+}$ and $MSTN^{+/-}$ mice after the second lengthening contraction. (B) There was no difference in the force deficits between soleus muscles following the lengthening contractions. LC = Lengthening contraction. Values are means ± SE. N = 6 muscles per genotype. *Significantly different from $MSTN^{+/+}$ at $P < 0.05$. #Significantly different from $MSTN^{+/-}$ at $P < 0.05$.

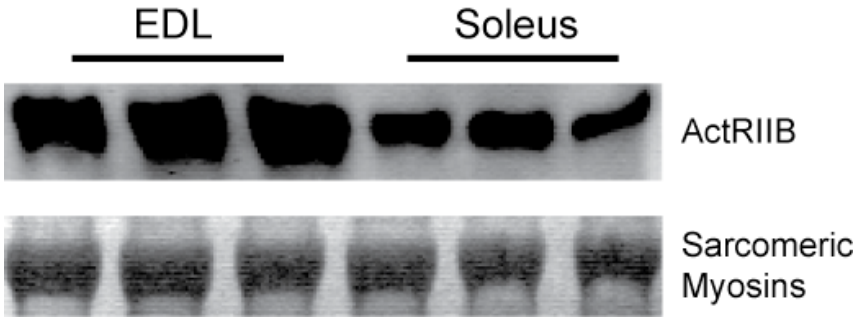

Figure 2.5. ActRIIB protein content of EDL and soleus muscles from *MSTN*$^{+/+}$ mice. Compared with soleus muscles, the amount of ActRIIB protein is greater in EDL muscles (immunoblot). Sarcomeric myosin proteins are shown as loading controls (Coomassie Brilliant Blue staining).

	$MSTN^{+/+}$	$MSTN^{+/-}$	$MSTN^{-/-}$
Body Mass (g)	32.39±1.32	36.63±1.11	35.01±1.27
Body Length (mm)	93.33±0.53	95.00±0.59	92.75±0.92
Tibia Length (mm)	17.91±0.10	17.74±0.13	18.07±0.15
EDL Muscles			
Wet Mass (mg)	11.62±0.29	12.82±0.25*	19.32±0.52*#
Fibers per muscle	1462±12	1693±58*	2351±87*#
Fiber area (μm^2)	1231.12±28.64	1315.38±24.55*	1512.14±29.00*#
L_o (mm)	13.13±0.43	12.78±0.22	13.38±0.23
L_f (mm)	5.78±0.19	5.63±0.10	5.89±0.10
CSA (mm^2)	1.90±0.04	2.15±0.05*	3.10±0.07*#
Hyp / Muscle Mass (µg/mg)	1.90±0.14	0.77±0.09*	0.47±0.08*
Soleus Muscles			
Wet Mass (mg)	10.45±0.44	11.97±0.78	14.22±0.73*
Fibers per muscle	985±37	1185±33*	1292±34*#
Fiber area (μm^2)	1148.99±20.89	1162.28±20.66	1316.45±36.12*#
L_o (mm)	12.42±0.30	12.55±0.25	12.98±0.46
L_f (mm)	8.82±0.21	8.91±0.18	9.22±0.33
CSA (mm^2)	1.12±0.06	1.27±0.07	1.45±0.03*
Hyp / Muscle Mass (µg/mg)	0.71±0.10	0.61±0.09	0.54±0.09

Table 2.1. Anatomical properties of animals. Values are means ± SE. N = 12 for tibia length and body length. N = 300 fibers from 3 muscles for each genotype. N = 5 muscles per genotype for fibers per muscle and hydroxyproline. N = 6 muscles per genotype for all other values. *Significantly different from $MSTN^{+/+}$ at $P < 0.05$. #Significantly different from $MSTN^{+/-}$ at $P < 0.05$.

	MSTN$^{+/+}$	*MSTN*$^{+/-}$	*MSTN*$^{-/-}$
EDL Muscles			
P_t (mN)	110.78±4.84	136.76±12.33	160.87±8.07*
sP_t (mN/mm^2)	58.20±1.75	63.27±5.10	52.25±3.38
TTPT (ms)	23.68±2.80	20.91±1.32	23.86±2.46
½RT (ms)	22.56±1.48	20.80±1.02*	15.51±0.25*#
dP/dt (mN/ms)	13.07±0.05	15.64±1.29	19.00±1.24*#
P_o (mN)	461.19±14.69	520.53±18.48*	616.93±17.10*#
sP_o (mN/mm^2)	243.32±10.04	242.12±8.22	199.86±7.37*#
Soleus Muscles			
P_t (mN)	47.12±2.78	60.43±5.00	65.52±5.85*
sP_t (mN/mm^2)	42.08±1.90	47.51±2.30	45.06±3.81
TTPT (ms)	40.61±4.68	32.41±0.99	27.38±3.75
½RT (ms)	50.10±5.42	47.55±2.13	37.57±1.92
dP/dt (mN/ms)	4.20±0.21	4.91±0.33	6.08±0.80
P_o (mN)	295.84±7.49	324.94±18.52	385.06±17.57*#
sP_o (mN/mm^2)	265.81±10.10	257.15±6.34	264.84±8.50

Table 2.2. Contractile Properties of EDL and Soleus Muscles. Values are means ± SE. N = 6 muscles per genotype. P_t = peak twitch force; sP_t = specific P_t; TTPT = time to peak twitch tension; ½RT = half-relaxation time; dP/dt = maximum rise in tension. *Significantly different from *MSTN*$^{+/+}$ at $P < 0.05$. #Significantly different from *MSTN*$^{+/-}$ at $P < 0.05$.

	MSTN$^{+/+}$	*MSTN*$^{+/-}$	*MSTN*$^{-/-}$
EDL Muscles			
Stretch 1			
Average Force (mN)	648.07±8.21	644.48±15.74	664.56±8.63
Work (J/kg)	129.00±3.66	113.05±1.85*	81.31±2.65*#
Force Deficit (% of Pre-injury P_o)	15.74±0.81	18.19±2.78	24.14±3.03*
Stretch 2			
Average Force (mN)	631.03±8.43	632.78±14.93	651.86±9.00
Work (J/kg)	125.58±3.39	111.01±1.76*	79.76±2.65*#
Force Deficit (% of Pre-injury P_o)	30.10±1.71	29.59±2.46	45.23±6.52*#
Soleus Muscles			
Stretch 1			
Average Force (mN)	509.53±26.93	537.37±33.60	620.89±28.49*
Work (J/kg)	173.21±11.68	160.60±5.56	161.15±5.39
Force Deficit (% of Pre-injury P_o)	18.21±3.63	19.18±4.38	18.60±2.52
Stretch 2			
Average Force (mN)	455.83±14.49	480.13±29.67	569.29±31.98*#
Work (J/kg)	154.89±8.35	143.33±3.96	147.60±6.21
Force Deficit (% of Pre-injury P_o)	20.68 ± 4.93	20.21 ± 3.45	25.08 ± 3.76

Table 2.3. Mechanical Injury of EDL and Soleus Muscles. Values are means ± SE. N = 6 muscles per genotype. *Significantly different from *MSTN*$^{+/+}$ at $P < 0.05$. #Significantly different from *MSTN*$^{+/-}$ at $P < 0.05$.

References

1. Allen RE, Temm-Grove CJ, Sheehan SM, and Rice G. Skeletal muscle satellite cell cultures. *Methods Cell Biol* 52: 155-176, 1997.
2. Amthor H, Nicholas G, McKinnell I, Kemp CF, Sharma M, Kambadur R, and Patel K. Follistatin complexes Myostatin and antagonises Myostatin-mediated inhibition of myogenesis. *Dev Biol* 270: 19-30, 2004.
3. Bernasconi P, Torchiana E, Confalonieri P, Brugnoni R, Barresi R, Mora M, Cornelio F, Morandi L, and Mantegazza R. Expression of transforming growth factor-beta 1 in dystrophic patient muscles correlates with fibrosis. Pathogenetic role of a fibrogenic cytokine. *J Clin Invest* 96: 1137-1144, 1995.
4. Bogdanovich S, Krag TO, Barton ER, Morris LD, Whittemore LA, Ahima RS, and Khurana TS. Functional improvement of dystrophic muscle by myostatin blockade. *Nature* 420: 418-421, 2002.
5. Bogdanovich S, Perkins KJ, Krag TO, Whittemore LA, and Khurana TS. Myostatin propeptide-mediated amelioration of dystrophic pathophysiology. *Faseb J* 19: 543-549, 2005.
6. Brooks SV and Faulkner JA. Contractile properties of skeletal muscles from young, adult and aged mice. *J Physiol* 404: 71-82, 1988.
7. Brooks SV and Faulkner JA. The magnitude of the initial injury induced by stretches of maximally activated muscle fibres of mice and rats increases in old age. *J Physiol* 497 (Pt 2): 573-580, 1996.
8. Brooks SV, Zerba E, and Faulkner JA. Injury to muscle fibres after single stretches of passive and maximally stimulated muscles in mice. *J Physiol* 488 (Pt 2): 459-469, 1995.
9. Byron CD, Hamrick MW, and Wingard CJ. Alterations of temporalis muscle contractile force and histological content from the myostatin and Mdx deficient mouse. *Arch Oral Biol*, 2005.
10. Carlson CJ, Booth FW, and Gordon SE. Skeletal muscle myostatin mRNA expression is fiber-type specific and increases during hindlimb unloading. *Am J Physiol* 277: R601-606, 1999.
11. Consolino CM and Brooks SV. Susceptibility to sarcomere injury induced by single stretches of maximally activated muscles of mdx mice. *J Appl Physiol* 96: 633-638, 2004.
12. Contri MB, Guerra D, Vignali N, Taparelli F, Marcuzzi A, Caroli A, and Ronchetti IP. Ultrastructural and immunocytochemical study on normal human palmar aponeuroses. *Anat Rec* 240: 314-321, 1994.
13. Delforge G. *Musculoskeletal Trauma : implications for sports injury management*. Champaign, IL: Human Kinetics, 2002.
14. Dellorusso C, Crawford RW, Chamberlain JS, and Brooks SV. Tibialis anterior muscles in mdx mice are highly susceptible to contraction-induced injury. *J Muscle Res Cell Motil* 22: 467-475, 2001.
15. Donovan CM and Faulkner JA. Muscle grafts overloaded by ablation of synergistic muscles. *J Appl Physiol* 61: 288-292, 1986.

16. Ducomps C, Mauriege P, Darche B, Combes S, Lebas F, and Doutreloux JP. Effects of jump training on passive mechanical stress and stiffness in rabbit skeletal muscle: role of collagen. *Acta Physiol Scand* 178: 215-224, 2003.
17. Engvall E and Wewer UM. The new frontier in muscular dystrophy research: booster genes. *Faseb J* 17: 1579-1584, 2003.
18. Friden J and Lieber RL. Segmental muscle fiber lesions after repetitive eccentric contractions. *Cell Tissue Res* 293: 165-171, 1998.
19. Gosselin LE, Adams C, Cotter TA, McCormick RJ, and Thomas DP. Effect of exercise training on passive stiffness in locomotor skeletal muscle: role of extracellular matrix. *J Appl Physiol* 85: 1011-1016, 1998.
20. Grobet L, Martin LJ, Poncelet D, Pirottin D, Brouwers B, Riquet J, Schoeberlein A, Dunner S, Menissier F, Massabanda J, Fries R, Hanset R, and Georges M. A deletion in the bovine myostatin gene causes the double-muscled phenotype in cattle. *Nat Genet* 17: 71-74, 1997.
21. Grobet L, Pirottin D, Farnir F, Poncelet D, Royo LJ, Brouwers B, Christians E, Desmecht D, Coignoul F, Kahn R, and Georges M. Modulating skeletal muscle mass by postnatal, muscle-specific inactivation of the myostatin gene. *Genesis* 35: 227-238, 2003.
22. Hanyu T, Tajima T, Takagi T, Sasaki S, Fujimoto D, Isemura M, and Yosizawa Z. Biochemical studies on the collagen of the palmar aponeurosis affected with Dupuytren's disease. *Tohoku J Exp Med* 142: 437-443, 1984.
23. Huijing P. Muscular force transmission: a unified, dual or multiple system? A review and some explorative experimental results. *Arch Physiol Biochem* 107: 292-311, 1999.
24. Kambadur R, Sharma M, Smith TP, and Bass JJ. Mutations in myostatin (GDF8) in double-muscled Belgian Blue and Piedmontese cattle. *Genome Res* 7: 910-916, 1997.
25. Kandarian SC and White TP. Mechanical deficit persists during long-term muscle hypertrophy. *J Appl Physiol* 69: 861-867, 1990.
26. Khurana TS and Davies KE. Pharmacological strategies for muscular dystrophy. *Nat Rev Drug Discov* 2: 379-390, 2003.
27. Kjaer M. Role of extracellular matrix in adaptation of tendon and skeletal muscle to mechanical loading. *Physiol Rev* 84: 649-698, 2004.
28. Langley B, Thomas M, Bishop A, Sharma M, Gilmour S, and Kambadur R. Myostatin inhibits myoblast differentiation by down-regulating MyoD expression. *J Biol Chem* 277: 49831-49840, 2002.
29. Lee SJ and McPherron AC. Regulation of myostatin activity and muscle growth. *Proc Natl Acad Sci U S A* 98: 9306-9311, 2001.
30. Lesch M, Parmley WW, Hamosh M, Kaufman S, and Sonnenblick EH. Effects of acute hypertrophy on the contractile properties of skeletal muscle. *Am J Physiol* 214: 685-690, 1968.
31. Light N and Champion AE. Characterization of muscle epimysium, perimysium and endomysium collagens. *Biochem J* 219: 1017-1026, 1984.
32. Livak KJ and Schmittgen TD. Analysis of relative gene expression data using real-time quantitative PCR and the 2(-Delta Delta C(T)) Method. *Methods* 25: 402-408, 2001.

33. Macpherson PC, Dennis RG, and Faulkner JA. Sarcomere dynamics and contraction-induced injury to maximally activated single muscle fibres from soleus muscles of rats. *J Physiol* 500 (Pt 2): 523-533, 1997.
34. Macpherson PC, Schork MA, and Faulkner JA. Contraction-induced injury to single fiber segments from fast and slow muscles of rats by single stretches. *Am J Physiol* 271: C1438-1446, 1996.
35. Mahoney DJ, Carey K, Fu MH, Snow R, Cameron-Smith D, Parise G, and Tarnopolsky MA. Real-time RT-PCR analysis of housekeeping genes in human skeletal muscle following acute exercise. *Physiol Genomics* 18: 226-231, 2004.
36. Martyn JK, Bass JJ, and Oldham JM. Skeletal muscle development in normal and double-muscled cattle. *Anat Rec A Discov Mol Cell Evol Biol* 281: 1363-1371, 2004.
37. Matsakas A, Friedel A, Hertrampf T, and Diel P. Short-term endurance training results in a muscle-specific decrease of myostatin mRNA content in the rat. *Acta Physiol Scand* 183: 299-307, 2005.
38. Maxwell LC, Faulkner JA, and Hyatt GJ. Estimation of number of fibers in guinea pig skeletal muscles. *J Appl Physiol* 37: 259-264, 1974.
39. McCroskery S, Thomas M, Maxwell L, Sharma M, and Kambadur R. Myostatin negatively regulates satellite cell activation and self-renewal. *J Cell Biol* 162: 1135-1147, 2003.
40. McCroskery S, Thomas M, Platt L, Hennebry A, Nishimura T, McLeay L, Sharma M, and Kambadur R. Improved muscle healing through enhanced regeneration and reduced fibrosis in myostatin-null mice. *J Cell Sci* 118: 3531-3541, 2005.
41. McMahon CD, Popovic L, Oldham JM, Jeanplong F, Smith HK, Kambadur R, Sharma M, Maxwell L, and Bass JJ. Myostatin-deficient mice lose more skeletal muscle mass than wild-type controls during hindlimb suspension. *Am J Physiol Endocrinol Metab* 285: E82-87, 2003.
42. McPherron AC, Lawler AM, and Lee SJ. Regulation of skeletal muscle mass in mice by a new TGF-beta superfamily member. *Nature* 387: 83-90, 1997.
43. Mendler L, Zador E, Ver Heyen M, Dux L, and Wuytack F. Myostatin levels in regenerating rat muscles and in myogenic cell cultures. *J Muscle Res Cell Motil* 21: 551-563, 2000.
44. Neuman RE and Logan MA. The determination of hydroxyproline. *J Biol Chem* 184: 299-306, 1950.
45. Patel K and Amthor H. The function of Myostatin and strategies of Myostatin blockade-new hope for therapies aimed at promoting growth of skeletal muscle. *Neuromuscul Disord* 15: 117-126, 2005.
46. Philip B, Lu Z, and Gao Y. Regulation of GDF-8 signaling by the p38 MAPK. *Cell Signal* 17: 365-375, 2005.
47. Pirottin D, Grobet L, Adamantidis A, Farnir F, Herens C, Daa Schroder H, and Georges M. Transgenic engineering of male-specific muscular hypertrophy. *Proc Natl Acad Sci U S A* 102: 6413-6418, 2005.
48. Prado LG, Makarenko I, Andresen C, Kruger M, Opitz CA, and Linke WA. Isoform diversity of giant proteins in relation to passive and active contractile properties of rabbit skeletal muscles. *J Gen Physiol* 126: 461-480, 2005.

49. Prentice WE. *Rehabilitation techniques in sports medicine and athletic training*. New York: McGraw-Hill, 2004.
50. Rebbapragada A, Benchabane H, Wrana JL, Celeste AJ, and Attisano L. Myostatin signals through a transforming growth factor beta-like signaling pathway to block adipogenesis. *Mol Cell Biol* 23: 7230-7242, 2003.
51. Rehfeldt C, Ott G, Gerrard DE, Varga L, Schlote W, Williams JL, Renne U, and Bunger L. Effects of the Compact mutant myostatin allele Mstn (Cmpt-dl1Abc) introgressed into a high growth mouse line on skeletal muscle cellularity. *J Muscle Res Cell Motil*, 2005.
52. Reisz-Porszasz S, Bhasin S, Artaza JN, Shen R, Sinha-Hikim I, Hogue A, Fielder TJ, and Gonzalez-Cadavid NF. Lower skeletal muscle mass in male transgenic mice with muscle-specific overexpression of myostatin. *Am J Physiol Endocrinol Metab* 285: E876-888, 2003.
53. Roth SM and Walsh S. Myostatin: a therapeutic target for skeletal muscle wasting. *Curr Opin Clin Nutr Metab Care* 7: 259-263, 2004.
54. Schuelke M, Wagner KR, Stolz LE, Hubner C, Riebel T, Komen W, Braun T, Tobin JF, and Lee SJ. Myostatin mutation associated with gross muscle hypertrophy in a child. *N Engl J Med* 350: 2682-2688, 2004.
55. Sharma M, Langley B, Bass J, and Kambadur R. Myostatin in muscle growth and repair. *Exerc Sport Sci Rev* 29: 155-158, 2001.
56. Taylor WE, Bhasin S, Artaza J, Byhower F, Azam M, Willard DH, Jr., Kull FC, Jr., and Gonzalez-Cadavid N. Myostatin inhibits cell proliferation and protein synthesis in C2C12 muscle cells. *Am J Physiol Endocrinol Metab* 280: E221-228, 2001.
57. Thies RS, Chen T, Davies MV, Tomkinson KN, Pearson AA, Shakey QA, and Wolfman NM. GDF-8 propeptide binds to GDF-8 and antagonizes biological activity by inhibiting GDF-8 receptor binding. *Growth Factors* 18: 251-259, 2001.
58. Thomas M, Langley B, Berry C, Sharma M, Kirk S, Bass J, and Kambadur R. Myostatin, a negative regulator of muscle growth, functions by inhibiting myoblast proliferation. *J Biol Chem* 275: 40235-40243, 2000.
59. Tobin JF and Celeste AJ. Myostatin, a negative regulator of muscle mass: implications for muscle degenerative diseases. *Curr Opin Pharmacol* 5: 328-332, 2005.
60. Verrecchia F and Mauviel A. TGF-beta and TNF-alpha: antagonistic cytokines controlling type I collagen gene expression. *Cell Signal* 16: 873-880, 2004.
61. Wagner KR. Muscle regeneration through myostatin inhibition. *Curr Opin Rheumatol* 17: 720-724, 2005.
62. Wagner KR, Liu X, Chang X, and Allen RE. Muscle regeneration in the prolonged absence of myostatin. *Proc Natl Acad Sci U S A* 102: 2519-2524, 2005.
63. Wagner KR, McPherron AC, Winik N, and Lee SJ. Loss of myostatin attenuates severity of muscular dystrophy in mdx mice. *Ann Neurol* 52: 832-836, 2002.

64. Wanke T, Toifl K, Merkle M, Formanek D, Lahrmann H, and Zwick H. Inspiratory muscle training in patients with Duchenne muscular dystrophy. *Chest* 105: 475-482, 1994.
65. Whittemore LA, Song K, Li X, Aghajanian J, Davies M, Girgenrath S, Hill JJ, Jalenak M, Kelley P, Knight A, Maylor R, O'Hara D, Pearson A, Quazi A, Ryerson S, Tan XY, Tomkinson KN, Veldman GM, Widom A, Wright JF, Wudyka S, Zhao L, and Wolfman NM. Inhibition of myostatin in adult mice increases skeletal muscle mass and strength. *Biochem Biophys Res Commun* 300: 965-971, 2003.
66. Woessner JF, Jr. The determination of hydroxyproline in tissue and protein samples containing small proportions of this imino acid. *Arch Biochem Biophys* 93: 440-447, 1961.
67. Wolfman NM, McPherron AC, Pappano WN, Davies MV, Song K, Tomkinson KN, Wright JF, Zhao L, Sebald SM, Greenspan DS, and Lee SJ. Activation of latent myostatin by the BMP-1/tolloid family of metalloproteinases. *Proc Natl Acad Sci U S A* 100: 15842-15846, 2003.
68. Yang J, Ratovitski T, Brady JP, Solomon MB, Wells KD, and Wall RJ. Expression of myostatin pro domain results in muscular transgenic mice. *Mol Reprod Dev* 60: 351-361, 2001.
69. Zhu X, Hadhazy M, Wehling M, Tidball JG, and McNally EM. Dominant negative myostatin produces hypertrophy without hyperplasia in muscle. *FEBS Lett* 474: 71-75, 2000.
70. Zhu X, Topouzis S, Liang LF, and Stotish RL. Myostatin signaling through Smad2, Smad3 and Smad4 is regulated by the inhibitory Smad7 by a negative feedback mechanism. *Cytokine* 26: 262-272, 2004.
71. Zimmers TA, Davies MV, Koniaris LG, Haynes P, Esquela AF, Tomkinson KN, McPherron AC, Wolfman NM, and Lee SJ. Induction of cachexia in mice by systemically administered myostatin. *Science* 296: 1486-1488, 2002.

Chapter III

Tendons of Myostatin-Deficient Mice are Small, Brittle and Hypocellular

Abstract

Tendons play a significant role in the modulation of forces transmitted between bones and skeletal muscles and consequently protect muscle fibers from contraction-induced, or high strain, injuries. Myostatin (GDF-8) is a negative regulator of muscle mass. Inhibition of myostatin not only increases the mass and maximum isometric force of muscles, but also increases the susceptibility of muscle fibers to contraction-induced injury. Furthermore, the expression of myostatin and the myostatin receptors, ACVR2B and ACVRB, were detectable in the tendons. We hypothesized that myostatin would regulate the morphology and mechanical properties of tendons. Surprisingly, compared with wild type (*MSTN*$^{+/+}$) mice, the tendons of myostatin-null mice (*MSTN*$^{-/-}$) were smaller, had a decrease in fibroblast density and a decrease in the expression of type I collagen. Tendons of *MSTN*$^{-/-}$ mice also had a decrease in the expression of two genes that promote tendon fibroblast proliferation, scleraxis and tenomodulin. Treatment of tendon fibroblasts with myostatin activated the p38 MAPK and Smad2/3 signaling cascades, increased cell proliferation and increased the expression of type I collagen, scleraxis and tenomodulin. Compared with the tendons of *MSTN*$^{+/+}$ mice, the mechanical properties of tibialis

anterior tendons from *MSTN*$^{-/-}$ mice had a greater peak stress, lower peak strain and a increased stiffness. We conclude that in addition to the regulation of muscle mass and force, myostatin regulates the structure and function of tendon tissues.

Introduction

Tendons are a critical component of the musculoskeletal system. Situated, as tendons are, between bones and skeletal muscles, tendons are in a position to transmit forces generated within skeletal muscle fibers to bone and conversely transmit to skeletal muscle external loads placed on bone. The extracellular matrix (ECM) of tendon tissue is composed primarily of type I collagen, as well as type III collagen, elastin and various proteoglycans and mucopolysaccharides. Tendons are in series with both the contractile and non-contractile elements of skeletal muscles as well as with bone. Consequently, tendons are able to both store elastic energy during locomotion and protect muscle fibers from stretch-induced and contraction-induced injuries (15, 28). While considerable research has been conducted on the effects of exercise, immobilization and aging on the structure and function of tendons (19, 20), much less is known about the specific cytokines that regulate the structure and function of tendons.

During embryonic development of the limb, early tendon development can be categorized into three phases, with each phase corresponding to an upregulation of the bHLH transcription factor scleraxis (13, 40). Scleraxis is a marker of the tendon cell lineage (38, 40) and mice deficient in scleraxis display

severe tendon defects, have impaired locomotion and a complete inability to use their tails (34). Scleraxis promotes the formation of tendon ECM by inducing the expression of type I collagen (23) and increases tendon fibroblast proliferation by the upregulation of the expression of the type II transmembrane protein, tenomodulin (41). During the final stages of early tendon development, FGF-4 and FGF-8, are secreted by adjacent myogenic cells and induce the expression of scleraxis (5, 14). While FGF-4 and FGF-8 can induce scleraxis expression in the final phase of early tendon development, they do not appear to be responsible for the first and second phases of scleraxis expression (13). In fact, another member of the GDF family may be a candidate for the regulation of scleraxis expression during the first and second phases of early tendon development (13), but the specific member of the GDF family has not been identified.

Three members of the GDF family have been reported to influence the development of tendon tissue. The placement of matrices coated with GDF-5, GDF-6 and GDF-7 into skeletal muscle induce the ectopic formation of tendon-like tissue (50). The tendons of *GDF5*$^{-/-}$ mice are smaller and display decreases in type I collagen content, peak stress, stiffness and energy absorption to yield (32). The *GDF5*$^{-/-}$ mice also have severe bone and joint defects (32), but whether these changes in tendon mechanical properties arise due to a direct effect of GDF-5 on tendon cells or the associated skeletal defects is not clear. Compared with wild type mice, *GDF7*$^{-/-}$ mice have a minor tendon phenotype, with a decrease in proteoglycan content and smaller collagen fibrils, but no

differences in Achilles tendon mechanical properties, type I collagen content, or gross morphology (31). Some evidence supports roles for GDF-5, GDF-6 and GDF-7 in tendon development, but whether other members of the GDF family influence tendon development has not been established.

Myostatin (GDF-8) is a member of the TGF-ß superfamily of cytokines and is a negative regulator of skeletal muscle mass. Myostatin binds to the activin type IIB (ACVR2B) and type IB (ACVRB) receptors and activates the Smad2/3, p38 MAPK and Erk1/2 signal transduction pathways (22, 37, 39, 51, 53). Myostatin regulates muscle mass by inhibiting the proliferation and differentiation of satellite cells (21, 26, 45), in addition to decreasing myofibrillar protein synthesis (49) and increasing the expression of the E3 ubiquitin ligase atrogin-1/MAFbx (27). Myostatin has a well established role in regulation of the structure and function of skeletal muscle, but the contribution of myostatin to the regulation of the structure and function of tendon has not been established.

In addition to the regulation of muscle mass, myostatin has a profound impact on the contractile properties of skeletal muscles. Inhibition of myostatin increases the maximum isometric force of skeletal muscles (3, 4, 30) and the susceptibility of muscles to contraction-induced injury (30). During a lengthening contraction, the series elastic component (aponeurosis and tendon) of a muscle protects muscle fibers from damage by reducing the strain on fibers (15). The *MSTN*$^{-/-}$ mice are much more susceptible to contraction-induced injury than the *MSTN*$^{+/+}$ mice, an observation that is consistent with the possibility that myostatin might play a role in the regulation of the structural and functional properties of the

tendons. Our prior study (30) focused on the mechanical and contractile properties of the muscle and aponeurosis, but did not investigate the mechanical properties of the tendons of *MSTN*$^{-/-}$ mice directly. The overall aim of this investigation was to determine the role of myostatin in regulation of the mechanical and morphological properties of tendons. We hypothesized that a deficiency in myostatin results in smaller, stiffer, and more brittle tendons.

Methods

Animals. All experiments were conducted in accordance with the guidelines of the University of Michigan Committee on the Use and Care of Animals. Mice were housed in specific-pathogen-free conditions and were provided food and water *ad libidum*. The line of *MSTN*$^{-/-}$ mice used in this study are of a C57Bl/6 background and were a kind gift of Dr. Se-Jin Lee. The null *MSTN* allele was generated by replacing a portion of the third exon of the *MSTN* gene that encodes the C-terminal region of the mature myostatin protein with a *neo* cassette (29). The wild type (*MSTN*$^{+/+}$) littermates of the *MSTN*$^{-/-}$ mice served as controls. The genotype of mice was determined by PCR-based analysis of DNA samples obtained via tail biopsy.

Mechanical Testing of Tendons. To evaluate the mechanical properties of the tibialis anterior tendon, the entire tendon unit (from the myotendinous junction to the base of the first metatarsal bone) was used. The tibialis anterior tendon was chosen based on its relative uniformity of diameter, minimal aponeurosis and long gauge length (2). Six month old male mice were anesthetized with intraperitoneal injection of Avertin (400 mg/kg). Braded silk sutures were tied

around the distal end of the tibialis anterior muscle just superior to the myotendinous junction and at the very distal end of the tendon, just superior to the first metatarsal. The length (L_o) of the tibialis anterior tendon was measured using digital calipers while the ankle was placed in maximal plantarflexion. The tendon was removed by cutting the muscle just superior to the proximal suture and by removing the first metatarsal bone that was inferior to the distal suture. The tendon was immediately submerged in PBS maintained at 25º C. The tendon was held at L_o and cross-sectional area (CSA) was calculated from 10 evenly spaced width and depth measurements from high resolution digital photographs of both top and side views of the tendon. Side views were obtained using a 90º prism embedded in the side of the bath. These measurements were fitted to an ellipse and the ellipse area was used as the tendon CSA.

The proximal end of the tendon was attached to a dual-mode servo motor/force transducer (model 305C, Aurora Scientific) and the distal end was attached to a fixed post. Custom designed software (LabVIEW 7.1, National Instruments) controlled the servo motor motion and recorded force and strain data at a sampling rate of 20 kHz. The tendon was stretched to a 100% strain relative to L_o at a velocity of 1 $L_o \times s^{-1}$. Peak stress was defined as the stress that further increases in length resulted in a rupture of the tendon or the point at which yield strength had been reached without a frank rupture of the tendon. Peak strain was defined as the strain at which peak stress was reached. The data were fitted by either a fourth or fifth order polynomial function with an $R^2 \geq 0.9995$. Peak tendon stiffness was calculated by differentiating the fitted

polynomial and then determining its maximum value between L_o and peak strain. Average tendon stiffness was calculated as the mean value of the differentiated polynomial between L_o and peak strain. The energy absorption to the yield point was calculated by integrating the force-displacement function from L_o through peak strain and normalizing this value by the mass of the tendon.

Histology. To determine the density of fibroblasts in tendon tissue, tibialis anterior tendons were removed from 6 month old anesthetized mice, placed in embedding media and snap frozen in using isopentane cooled with dry ice. Sections were obtained from the proximal, middle and distal thirds of the tendon and stained with hematoxylin and eosin. Fibroblast density for the entire tendon was calculated by taking the mean value of the counts from each of the three regions of the tendon.

Tendon Fibroblast Isolation, Culture And Treatment With Myostatin. Hindlimb and forelimb tendons were isolated from anesthetized 4 month old male *MSTN*$^{+/+}$ mice, carefully trimmed of muscle and fat tissue, finely minced and placed in DMEM + 0.05% Type II Collagenase (Invitrogen) in a shaking water bath for 2 h at 37º C. Following dissociation, fibroblasts were pelleted by centrifugation, resuspended in DMEM + 2% fetal bovine serum (FBS) + 1% antibiotic-antimycotic (AbAm) and expanded in 100 mm culture dishes coated with type I collagen (BD Biosciences). Fibroblasts were passaged twice upon reaching 70% confluence. Following the last passage, 2×10^4 fibroblasts were plated in 35 mm culture dishes coated with type I collagen and expanded until reaching 80% confluence. Fibroblasts were then starved of serum for 24 hours

prior to treatment by replacing serum containing media with DMEM + 1% AbAm + 1× Insulin-Transferrin-Selenium supplement (ITS, Invitrogen). Recombinant murine myostatin, produced in NS0 mouse myeloma cells (R & D Systems), was dissolved into the serum-free media at a final concentration of 500 or 1000 ng/mL. Stock solutions of the p38 MAPK inhibitor SB-203580 (10) and the Smad2/3 inhibitor SB-431542 (17) were prepared by dissolving these solid anhydrous compounds in DMSO at a concentration of 10mM. These stock solutions were then added to serum-free media containing 1% DMSO at a final concentration of 10μM for SB-203580 and 5μM for SB-431542. Fibroblasts were pretreated with SB-203580 or SB-431542 for 1 hour prior to treatment with myostatin.

Cell Proliferation and Immunocytochemistry. Following serum starvation, fibroblasts were incubated in serum free media containing 20μM of the thymidine analog 5-bromo-2′-deoxyuridine (BrdU, Sigma) for 3 hours. Fibroblasts were rinsed twice with serum free media and treated with myostatin, SB-203580 and SB-431542 as described above. Following 24 hours of treatment, fibroblasts were rinsed with PBS, fixed in ice cold methanol and permeabilized with 0.5% Triton X-100. The BrdU epitope was exposed by digesting DNA with 200U/mL of EcoRI and denaturing DNA with 2N HCl. BrdU was visualized using an anti-BrdU antibody (G3G4, SJ Kaufman, Developmental Studies Hybridoma Bank) and a Cy3-conjugated secondary antibody (Jackson ImmunoResearch). DAPI (Sigma) was used as a non-specific nuclear stain. Twenty five random fields

were counted per dish. Cell proliferation data presented are the mean ± SE values of three independent experiments.

RT-PCR. RNA was isolated from samples using an RNeasy Mini Kit (Qiagen). When isolating RNA from whole tendons, the tissue was treated with type II collagenase and proteinase K prior to vigorous homogenization in guanidine thiocyanate buffer. Due to the smaller size of the tibialis anterior tendons, we were unable to consistently obtain adequate quantities of RNA with an A_{260}/A_{280} ratio between 1.8 and 2.0. We instead used RNA from Achilles tendons, as we were able to obtain RNA with A_{260}/A_{280} ratios between 1.8 and 2.0 from these tendons. RNA was treated with DNase I and reverse transcribed using an Omniscript RT kit (Qiagen) and oligo$(dT)_{15}$ primers. Primers for PCR reactions (Table 3.1) were designed to generate amplicons that span multiple exons. For standard PCR, 250ng of cDNA underwent 42 rounds of amplification using GoTaq Green (Promega). PCR products were separated using a 2% agarose gel. For real-time PCR, cDNA was amplified using a QuantiTect SYBR Green I PCR system (Qiagen) with Uracil-N-Glycosylase (Invitrogen) in an Opticon 2 real-time thermal cycler (Bio-Rad). qPCR reactions were conducted in quadruplicate for each sample. We used the methods of Livak and Schmittgen (25) to determine optimal loading quantities of cDNA and in the validation of GAPDH as a housekeeping gene. Gene expression was normalized to GAPDH expression using the $2^{-\Delta\Delta C(t)}$ method (25). The presence of single amplicons from qPCR reactions was verified by melting curve analysis as

well as electrophoresis using a 2% agarose gel. qPCR data presented is the combined means ± SE of three independent experiments.

Immunoblot. Tendon fibroblasts, prepared as described above and starved of serum for 24 hours, were treated for two hours with myostatin, SB-203580 and SB-431542 for 2 hours. Following treatment, cells were rinsed with PBS and scraped and homogenized in Laemmli's sample buffer with 1:20 ß-mercaptoethanol, 1:20 protease inhibitor cocktail (Sigma) and 1:40 phosphatase inhibitor cocktail (Sigma), and then placed in boiling water for 5 minutes. Protein concentration of the samples was determined using an RC DC Protein Assay (Bio-Rad). Equal amounts of protein were loaded into polyacrylamide gels and subjected to electrophoresis using a 4% stacking, 10% resolving gel. Proteins were transferred to a 0.45 µm nitrocellulose membrane, stained with Ponceau S to verify equal protein transfer and blocked using casein (Vector Labs). Antibodies against p38 MAPK and phospho-p38 MAPK were purchased from Cell Signaling. Primary antibodies against Smad2/3 and phospho-Smad2/3 were purchased from Millipore. Biotinylated secondary antibodies were purchased from Pierce Biotechnology. Avidin-HRPO conjugates were purchased from Vector Labs. Membranes were developed using SuperSignal West Dura enhanced chemiluminescent reagents (Pierce Biotechnology) and visualized using a FluorChem chemiluminescent documentation system (Alpha Innotech).

Statistical Analysis. Results are presented as means ± SE. KaleidaGraph 4.02 software was used to conduct statistical tests. For gene expression and cell proliferation data from cell culture experiments, differences between groups were

tested with a one-way ANOVA with α = 0.05. Fisher's least significant post hoc test was used to identify specific differences when significance was tested. For all other data, differences between *MSTN*$^{+/+}$ and *MSTN*$^{-/-}$ mice was tested with Student's t-test with α = 0.05.

Results

MSTN$^{-/-}$ *mice have greater muscle masses but smaller tendons.* We first determined the impact of myostatin deficiency on the mass of tendons. Although the mass of the tibialis anterior (TA) muscles of *MSTN*$^{-/-}$ mice were 72% greater than *MSTN*$^{+/+}$ mice, the TA tendons of the *MSTN*$^{-/-}$ mice were 40% smaller (Table 3.2). When the tendon mass was normalized by the muscle mass, the *MSTN*$^{-/-}$ mice had a 64% decrease in the tendon/muscle mass ratio. Similar results were observed for soleus muscles and Achilles tendons. The mass of the soleus muscles of *MSTN*$^{-/-}$ mice were 82% greater than *MSTN*$^{+/+}$ mice, but the Achilles tendons of the soleus muscles of *MSTN*$^{-/-}$ mice were 44% smaller than those of *MSTN*$^{+/+}$ mice. Consequently, for *MSTN*$^{-/-}$ mice the Achilles tendon/soleus muscle mass ratio was decreased by 69%. Furthermore, for the *MSTN*$^{-/-}$ mice, the CSA of the TA tendons were 50% smaller than those of the *MSTN*$^{+/+}$ mice (Table 3.3). The lengths and densities of the TA tendons of *MSTN*$^{-/-}$ and *MSTN*$^{+/+}$mice were not different. CSA and the lengths and densities of Achilles tendons were not determined, as the Achilles tendons were not used in testing of mechanical properties.

Tendon fibroblasts express the myostatin receptors and activate the p38 MAPK and Smad2/3 signaling pathways in response to myostatin treatment.

Subsequently, the expression of the myostatin receptors, ACVR2B and ACVRB, was examined in tendon fibroblasts. Transcripts for both ACVR2B and ACVRB were identified in whole tendon tissue, as well as in cultured tendon fibroblasts (Figure 3.1A). The myostatin transcript was also detected in tendon tissue and in cultured fibroblasts. Due to the close anatomical proximity between muscle and tendon tissue, the purity of tendon samples was verified by probing for the presence of type IIa myosin heavy chain and MyoD. Neither muscle specific gene was detected in tendon samples.

The next step was to determine whether cultured tendon fibroblasts activate intracellular signaling cascades in response to myostatin treatment. Myostatin induced the phosphorylation of both p38 MAPK and Smad2/3 (Figure 3.1B). When cells were treated with myostatin in the presence of the p38 MAPK inhibitor SB-203580 (10), the phosphorylation of p38 MAPK did not occur. Consequently, SB-203580 was specific to the p38 MAPK pathway, as this inhibitor did not block the phosphorylation of Smad2/3. For cells that were treated with myostatin in the presence of the Smad2/3 inhibitor SB-431542 (17), the phosphorylation of Smad2/3 was blocked with no effect on the phosphorylation of p38 MAPK. These results indicated that tendon fibroblasts expressed the myostatin receptors, were responsive to myostatin treatment and this response could be blocked by the use of SB-203580 and SB-431542.

Myostatin induces the proliferation of tendon fibroblasts. To determine whether myostatin induced the proliferation of tendon fibroblasts, fibroblasts were pulsed with BrdU and the cells were subsequently treated with myostatin, SB-

203580 and SB-431542 for 24h. Treatment with 1000 ng/mL of myostatin increased tendon cell proliferation by 37% over controls (Figure 3.2A). While the inhibition of the p38 MAPK pathway was sufficient to decrease the myostatin-mediated increase in fibroblast proliferation, the inhibition of the Smad2/3 pathway did not block the myostatin-mediated increase in fibroblast proliferation. Compared with *MSTN*$^{+/+}$ mice, the density of fibroblasts in whole tendon tissue was 47% less than for the *MSTN*$^{-/-}$ mice (Figure 3.2B). These results indicated that myostatin was a potent regulator of tendon cell proliferation.

Myostatin induces the expression of scleraxis, tenomodulin and type I collagen in tendon fibroblasts. The next step was to determine if myostatin regulated the expression of scleraxis and tenomodulin, the two genes that induce the proliferation of tendon fibroblasts. Treatment with 1000 ng/mL of myostatin resulted in a greater than two-fold increase in scleraxis expression (Figure 3.3A). Inhibiting the p38 MAPK pathway resulted in a 70% decrease in scleraxis expression, while the inhibition of the Smad2/3 pathway resulted in a 50% increase in scleraxis expression. Myostatin treatment doubled the expression of tenomodulin, and inhibition of both the p38 MAPK and Smad2/3 pathways to blocked the myostatin-mediated increase in tenomodulin expression (Figure 3.3B). Compared with *MSTN*$^{+/+}$ mice, *MSTN*$^{-/-}$ mice had a 64% decrease in scleraxis expression (Figure 3.3D) and a 63% decrease in tenomodulin expression (Figure 3.3E). These results indicated that the mechanisms responsible for the myostatin-mediated increase in fibroblast proliferation were due to an upregulation of scleraxis and tenomodulin.

Due to the smaller mass and CSA of the tendons of *MSTN*$^{-/-}$ mice, the impact of myostatin on the major structural protein of tendon, type I collagen, was determined. Treatment with 1000 ng/mL of myostatin resulted in a 67% increase in the expression of type I collagen (Figure 3.3C). The inhibition of either the p38 MAPK, or the Smad2/3 pathway was sufficient to block this increase in type I collagen expression. Compared with *MSTN*$^{+/+}$ mice, a 54% decrease in type I collagen expression was observed in the tendons of *MSTN*$^{-/-}$ mice (Figure 3.3F). Taken together, the cell proliferation and gene expression data indicated that the smaller tendons of the *MSTN*$^{-/-}$ mice depended on a decrease in tendon fibroblast proliferation and on the production of the constituents of the ECM.

MSTN$^{-/-}$ *mice have stiff, brittle tendons*. The profound impact of myostatin on the structure of tendons indicated that myostatin-deficiency likely influenced the mechanical properties of tendons. Consequently, the stress-strain relationships of tendons from *MSTN*$^{+/+}$ and *MSTN*$^{-/-}$ mice were measured (Figure 3.4A). Compared with the tendons of *MSTN*$^{+/+}$ mice, those of *MSTN*$^{-/-}$ mice reached a greater than two-fold higher peak stress before yielding, but reached less than half of the peak strain before yielding (Table 3.3). Tendons of *MSTN*$^{-/-}$ mice also demonstrated a fourteen-fold greater peak stiffness and average stiffness values than those of *MSTN*$^{+/+}$ mice (Figure 3.4B and Table 3.3). Despite the different stress-strain and stiffness properties of tendons from *MSTN*$^{+/+}$ and *MSTN*$^{-/-}$ mice, the tendons absorbed the same amount of energy before reaching the yield point (Figure 3.4C and Table 3.3). These results

indicated that the loss of myostatin had a major impact on the mechanical properties of tendons.

Discussion

Myostatin has a well characterized role in the regulation of the structure and function of skeletal muscles. Although the myostatin transcript has been detected previously in tendons (16), our results provide the first evidence that myostatin regulates directly the structure and function of tendons. For the *MSTN*$^{-/-}$ mice, the deficiency in myostatin resulted in small, brittle, hypocellular tendons. The difference in tendon phenotypes between the *MSTN*$^{-/-}$ and *MSTN*$^{+/+}$ mice is clearly not attributable to any indirect influence of a greater muscle mass of the *MSTN*$^{-/-}$ mice, as both genotypes were limited to cage sedentary activity levels and the two genotypes showed no differences in body masses. Consequently, the tendons of both groups of mice experienced very similar mechanical loads throughout their lifespan and the dramatic change in the structure and function of tendons could be attributed directly to the effect of myostatin on tendon fibroblasts. In addition, this conclusion is supported further by the concurrent cell culture experiments.

While myostatin promotes the synthesis of intramuscular collagen content and skeletal muscle fibroblast proliferation (30, 52), whether myostatin regulated the collagen content and proliferation of fibroblasts of tendon was not immediately evident. The inhibition of myostatin in *mdx* mice, a murine model of Duchenne muscular dystrophy, decreased fibrosis and increased maximum isometric force production (3, 4, 48). Compared with *MSTN*$^{+/+}$ mice, a decrease

in the type I collagen content of EDL muscles of *MSTN*$^{-/-}$ mice was observed (30). Myostatin also induced the expression of type I collagen in skeletal muscle myotubes (30) and muscle-derived fibroblasts (52) and increased the proliferation of cultured muscle-derived and NIH/3T3 fibroblasts (52). The current investigation indicated that myostatin also promotes fibroblast proliferation and type I collagen synthesis in tendons, both *in vivo* and *in vitro*.

A rapidly growing body of literature supports the role of scleraxis and tenomodulin in the embryonic development of tendons (5, 12-14, 23, 34, 38, 40, 41), but little is known regarding their function in adult tendons. FGF-4 and FGF-8 directly induced the expression of scleraxis in tendon fibroblasts (5, 6, 14, 43). Furthermore, TGF-ß induced the expression of scleraxis in osteosarcoma cells (24) . Overexpression of scleraxis in tendon fibroblasts either directly or indirectly resulted in the upregulation of tenomodulin (41). The relative expression of scleraxis and tenomodulin in the tendons of *MSTN*$^{+/+}$ and *MSTN*$^{-/-}$ mice in this study were in good agreement with the data on tendon mass and cell density. Similar to tenomodulin deficient mice, the tendons of *MSTN*$^{-/-}$ mice were hypocellular (12). The results from the current study indicate that scleraxis and tenomodulin are expressed in adult tendons and that both genes are downstream targets of myostatin, that activates similar signal transduction cascades as TGF-ß and FGF.

During several stages of embryonic development, myogenic cells and tendon precursor cells interact with each other to ensure proper spatial alignment and proper timing of differentiation events (13, 18). While myostatin was

expressed in myogenic cells and decreased the expression of the myogenic genes *MyoD*, *Myf-5* and *Pax3* in these cells, myostatin was also expressed in non-myogenic cells of the ectoderm (1) but the reason for the expression of myostatin in non-muscle cells was not known. Scleraxis expression occurred in three phases of tendon development (13, 40), with the final phase initiated by FGF-4 and FGF-8 (5, 14) produced in adjacent myogenic cells. The signal that initiated the first phase of scleraxis expression in tendon progenitor cells is not known, but this signal does not come from muscle cells, as removal of myogenic cells does not alter scleraxis expression (14). The ectoderm appeared critical to the induction of the first stage of scleraxis expression, as ablation of the ectoderm abolished the first phase of scleraxis expression (40). Myostatin was expressed in the ectoderm around the time of the first phase of scleraxis expression (1) and removal of the ectoderm resulted in a downregulation of scleraxis. Consequently, myostatin may play a direct role in the development of tendons by regulating the initial expression of scleraxis.

One of the most striking differences between the mechanical properties of $MSTN^{+/+}$ and $MSTN^{-/-}$ mice was the fourteen-fold increase in the stiffness of tendons in $MSTN^{-/-}$ mice. The stiffness of tendons is a critical factor in determining the damage to muscle fibers during lengthening contractions. Immediately following a two-stretch lengthening contraction protocol, the EDL muscles of $MSTN^{-/-}$ mice had a 15% greater force deficit than $MSTN^{+/+}$ mice (30). The force deficit following a contraction-induced injury is directly related to the strain on the muscle fibers during the lengthening contraction (7). Consequently,

the series elastic component of a muscle protects the sarcomeres from damage by limiting the strain of the muscle fibers during the contraction (15). Similarly, the increased stiffness of tendons increases the strain on the muscle fibers plays a direct role in the greater force deficit observed for the muscles of *MSTN*$^{-/-}$ mice compared with *MSTN*$^{+/+}$ mice following a lengthening contraction protocol (30). While the mechanisms responsible for the increased stiffness of tendons from *MSTN*$^{-/-}$ mice are not known, the stiffening of tendons is thought to arise as a result of the increased crosslinking between type I collagen molecules (47). Future studies that evaluate the biochemical and molecular differences between the tendons of *MSTN*$^{+/+}$ and *MSTN*$^{-/-}$ mice are necessary to determine the mechanisms behind the regulation of tendon mechanical properties by myostatin.

Considerable interest has focused on the potential use of myostatin inhibitors in the treatment of muscle wasting diseases such as Duchenne muscular dystrophy (8, 35, 46). Muscles of *mdx* mice (9, 11, 33, 36, 44) and patients with Duchenne muscular dystrophy (42) are highly susceptible to contraction-induced injury. A profound increase in the stiffness of tendons would likely further increase the susceptibility of dystrophic muscles to contraction-induced injury and exacerbate the symptoms of muscular dystrophy. A careful evaluation of the long term impact of myostatin suppression on the mechanical properties of tendons of dystrophic muscles, and the susceptibility of dystrophic muscles to contraction-induced injury, is warranted.

Acknowledgements

The authors wish to thank Dennis Claflin, Keith Baar, Cheryl Hassett and Kimberly Gates for providing technical assistance. This work was supported by the grants AG-13283 and AG-20591 from the National Institute on Aging.

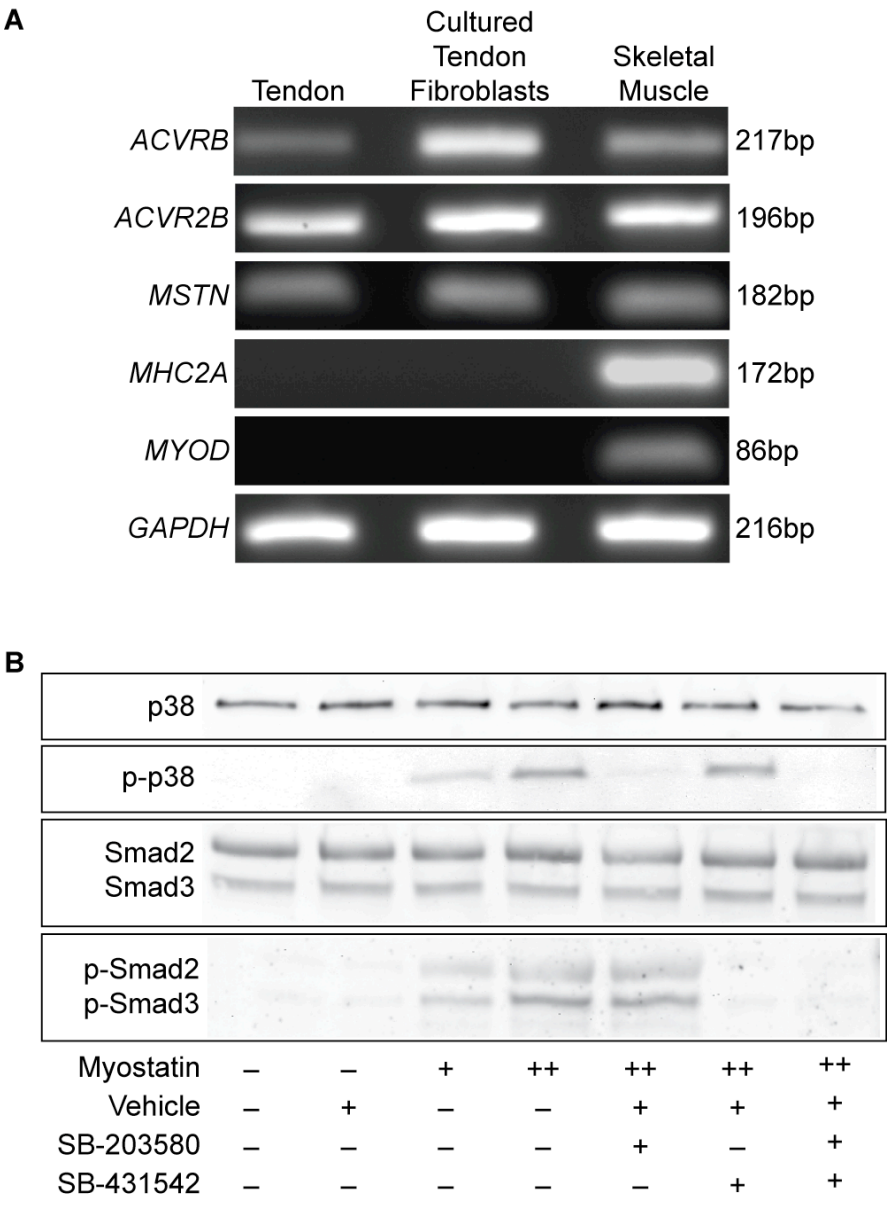

Figure 3.1. Tendon fibroblasts expressed the myostatin receptors and activated signal transduction cascades in the presence of myostatin. (A) PCR analysis of cDNA libraries from whole tendon tissue and cultured tendon fibroblasts indicated that tendon fibroblasts expressed both of the myostatin receptors (*ACVRB* and *ACVR2B*) as well as myostatin (*MSTN*) itself. *MHC2A* and *MyoD* were used as negative controls to indicate purity of tendon samples. (B) Treatment of tendon fibroblasts with myostatin for 2h results in the phosphorylation of both p38 MAPK and Smad2/3. The p38 MAPK inhibitor SB-203580 was able to specifically block the myostatin-mediated phosphorylation of p38 MAPK, and the Smad2/3 inhibitor SB-431542 was able to specifically block the myostatin-mediated phosphorylation of Smad2/3. +, 500ng/mL of myostatin. ++, 1000ng/mL of myostatin.

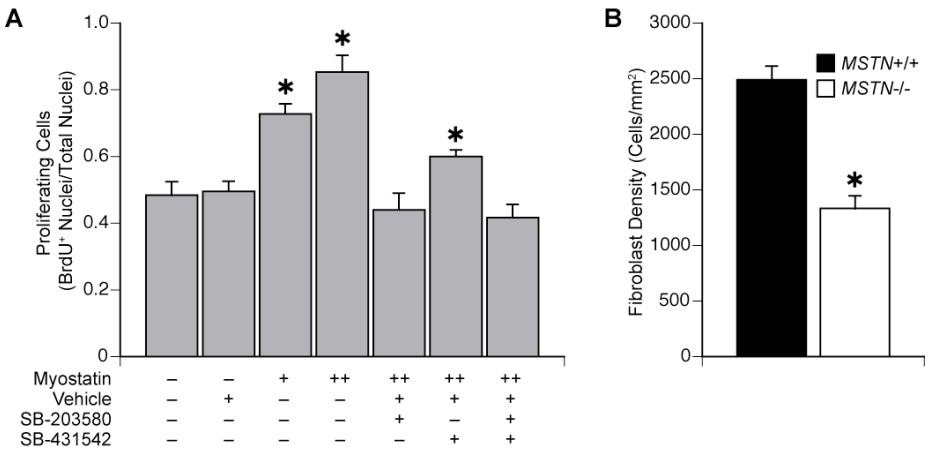

Figure 3.2. Myostatin induced the proliferation of tendon fibroblasts. (A) Treatment of tendon fibroblasts for 24h with myostatin increases cell proliferation as measured by the relative incorporation of the thymidine analog BrdU. N = 3 independent experiments. +, 500ng/mL of myostatin. ++, 1000ng/mL of myostatin. *, significantly different from control group at $P < 0.05$. (B) Cell density data from tibialis anterior tendon sections stained with H&E. *MSTN*$^{-/-}$ mice a lower fibroblast density than *MSTN*$^{+/+}$ mice. N = 6 tendons per genotype. *, significantly different from *MSTN*$^{+/+}$ at $P < 0.05$.

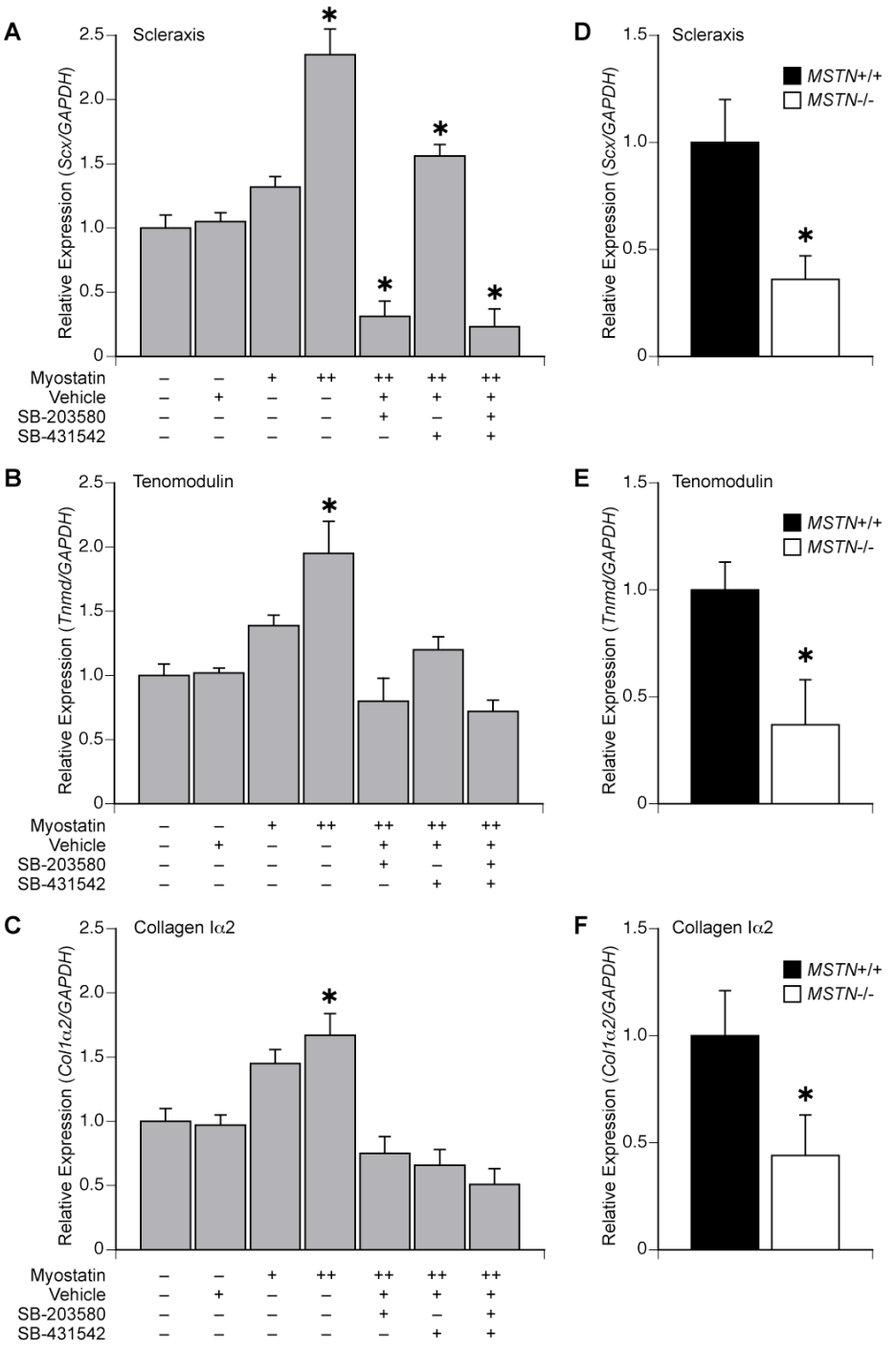

Figure 3.3. Myostatin induces the expression of scleraxis, tenomodulin and collagen Iα2 genes in tendon fibroblasts. Treatment of cells with myostatin for 24h increases the relative expression of scleraxis (A), tenomodulin (B) and collagen Iα2 (C) normalized to GAPDH. +, 500ng/mL of myostatin. ++, 1000ng/mL of myostatin. *, significantly different from control group at $P < 0.05$. There is a decrease in the expression of scleraxis (D), tenomodulin (E) and collagen Iα2 (F) normalized to GAPDH in tendons of *MSTN*$^{-/-}$ mice. N = 4 tendons per genotype. *, significantly different from *MSTN*$^{+/+}$ at $P < 0.05$.

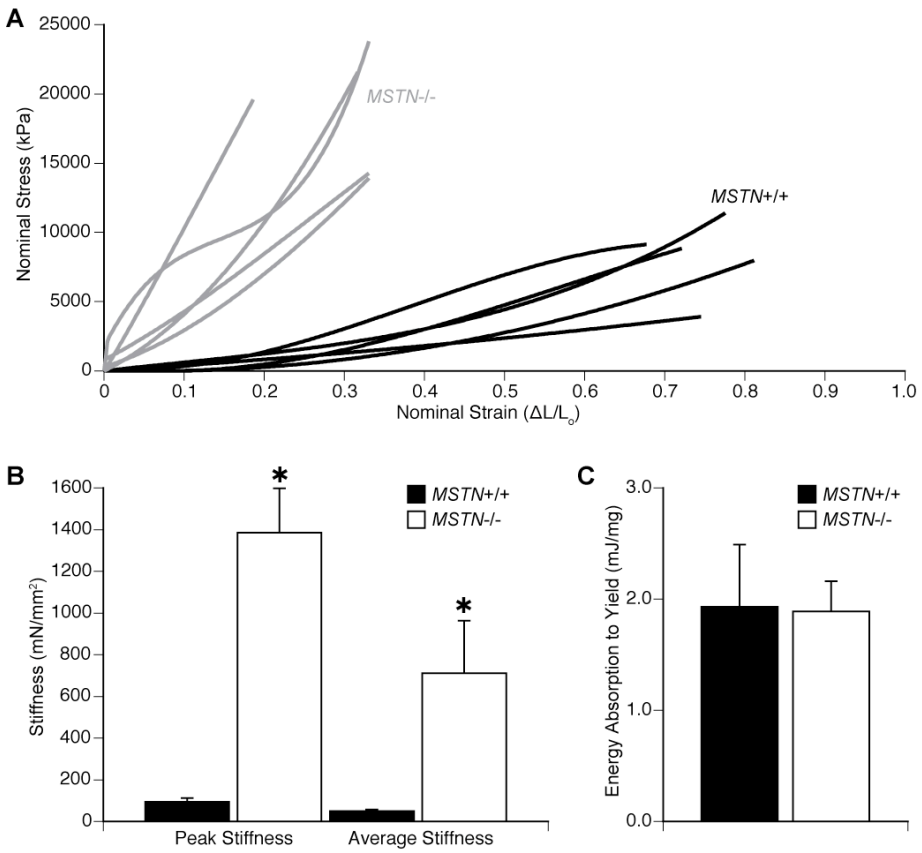

Figure 3.4. Mechanical properties of tibialis anterior tendons of MSTN$^{+/+}$ and MSTN$^{-/-}$ mice. (A) The stress-strain relationship of tendons from *MSTN*$^{+/+}$ and *MSTN*$^{-/-}$ mice indicate that *MSTN*$^{-/-}$ mice develop a higher peak stress but have a lower peak strain. (B) *MSTN*$^{-/-}$ mice have a greater peak stiffness and average stiffness than *MSTN*$^{+/+}$ mice. (C) The energy absorbed to the yield point is not different between *MSTN*$^{+/+}$ and *MSTN*$^{-/-}$ mice. N = 5 tendons per genotype. *, significantly different from *MSTN*$^{+/+}$ at $P < 0.05$.

Gene	Forward Primer (5' - 3')	Reverse Primer (5' - 3')
ACVRB	GCTGGAAAGCCCTTCTACTG	TGATGACCAGGAAGACGATG
ACVR2B	GAAGATGAGGCCCACGATTA	GGAGGTCACCAGAGAGACGA
COL1A2	CCAGCGAAGAACTCATACAGC	GGACACCCCTTCTACGTTGT
GAPDH	TGGAAAGCTGTGGCGTGAT	TGCTTCACCACCTTCTTGAT
MHC2A	CCAAGTCAGAGGCAAAGAGG	TCTTTGATTTTGGCCTCCAG
MSTN	TGCAAAATTGGCTCAAACAG	GCAGTCAAGCCCAAAGTCTC
MYOD	CGCTCCAACTGCTCTGATG	TAGTAGGCGGTGTCGTAGCC
TNMD	TGTACTGGATCAATCCCACTCT	GCTCATTCTGGTCAATCCCCT

Table 3.1. PCR primer sequences. Primers for RT-PCR and RT-qPCR. Primers are designed to generate an amplicon which spans two or more exons and can discriminate cDNA from genomic DNA.

	***MSTN*$^{+/+}$**	***MSTN*$^{-/-}$**
Mouse Mass (g)	33.8±1.1	36.8±1.1
TA Tendon Mass (mg)	1.30±0.10	0.78±0.05*
TA Muscle Mass (mg)	51.84±1.58	89.34±3.92*
TA Tendon/Muscle Mass Ratio	0.025±0.002	0.009±0.001*
Achilles Tendon Mass (mg)	2.34±0.10	1.32±0.10*
Soleus Mass (mg)	8.10±0.29	14.80±0.21*
Achilles Tendon/Soleus Muscle Mass Ratio	0.291±0.005	0.090±0.008*

Table 3.2. Whole animal, muscle and tendon masses. Values are means ± SE. N = 5 for each genotype. *Significantly different from *MSTN*$^{+/+}$ at $P < 0.05$.

	***MSTN*$^{+/+}$**	***MSTN*$^{-/-}$**
L_o (mm)	6.78±0.28	6.12±0.10
CSA (mm^2)	0.16±0.03	0.08±0.01*
Density (mg/mm^3)	1.54±0.42	1.63±0.06
Peak Strain ($\Delta L/L_o$)	0.75±0.02	0.33±0.04*
Peak Stress (kPa)	8250±1223	20300±1067*
Peak Stiffness (mN/mm^2)	95.0±17.1	1386±212*
Average Stiffness (mN/mm^2)	49.6±8.3	711±253*
Energy Absorption (mJ/mg)	1.93±0.56	1.89±0.27

Table 3.3. Morphological and mechanical properties of tibialis anterior tendons. Values are means ± SE. N = 5 for each genotype. *Significantly different from *MSTN*$^{+/+}$ at $P < 0.05$.

References

1. Amthor H, Huang R, McKinnell I, Christ B, Kambadur R, Sharma M, and Patel K. The regulation and action of myostatin as a negative regulator of muscle development during avian embryogenesis. *Dev Biol* 251: 241-257, 2002.
2. Arruda E, Calve S, Dennis R, Mundy K, and Baar K. Regional variation of tibialis anterior tendon mechanics is lost following denervation. *J Appl Physiol* 101: 1113-1117, 2006.
3. Bogdanovich S, Krag T, Barton E, Morris L, Whittemore L, Ahima R, and Khurana T. Functional improvement of dystrophic muscle by myostatin blockade. *Nature* 420: 418-421, 2002.
4. Bogdanovich S, Perkins K, Krag T, Whittemore L, and Khurana T. Myostatin propeptide-mediated amelioration of dystrophic pathophysiology. *FASEB J* 19: 543-549, 2005.
5. Brent A, Schweitzer R, and Tabin C. A somitic compartment of tendon progenitors. *Cell* 113: 235-248, 2003.
6. Brent A, and Tabin C. FGF acts directly on the somitic tendon progenitors through the Ets transcription factors Pea3 and Erm to regulate scleraxis expression. *Development* 131: 3885-3896, 2004.
7. Brooks SV, Zerba E, and Faulkner JA. Injury to muscle fibres after single stretches of passive and maximally stimulated muscles in mice. *J Physiol* 488 (Pt 2): 459-469, 1995.
8. Chakkalakal JV, Thompson J, Parks RJ, and Jasmin BJ. Molecular, cellular, and pharmacological therapies for Duchenne/Becker muscular dystrophies. *Faseb J* 19: 880-891, 2005.
9. Consolino CM, and Brooks SV. Susceptibility to sarcomere injury induced by single stretches of maximally activated muscles of mdx mice. *J Appl Physiol* 96: 633-638, 2004.
10. Cuenda A, Rouse J, Doza Y, Meier R, Cohen P, Gallagher T, Young P, and Lee J. SB 203580 is a specific inhibitor of a MAP kinase homologue which is stimulated by cellular stresses and interleukin-1. *FEBS Lett* 364: 229-233, 1995.
11. Dellorusso C, Crawford RW, Chamberlain JS, and Brooks SV. Tibialis anterior muscles in mdx mice are highly susceptible to contraction-induced injury. *J Muscle Res Cell Motil* 22: 467-475, 2001.
12. Docheva D, Hunziker E, Fässler R, and Brandau O. Tenomodulin is necessary for tenocyte proliferation and tendon maturation. *Mol Cell Biol* 25: 699-705, 2005.
13. Edom-Vovard F, and Duprez D. Signals regulating tendon formation during chick embryonic development. *Dev Dyn* 229: 449-457, 2004.
14. Edom-Vovard F, Schuler B, Bonnin M, Teillet M, and Duprez D. Fgf4 positively regulates scleraxis and tenascin expression in chick limb tendons. *Dev Biol* 247: 351-366, 2002.
15. Griffiths RI. Shortening of muscle fibres during stretch of the active cat medial gastrocnemius muscle: the role of tendon compliance. *J Physiol* 436: 219-236, 1991.

16. Heinemeier K, Olesen J, Schjerling P, Haddad F, Langberg H, Baldwin K, and Kjaer M. Short-term strength training and the expression of myostatin and IGF-I isoforms in rat muscle and tendon: differential effects of specific contraction types. *J Appl Physiol* 102: 573-581, 2007.
17. Inman G, Nicolás F, Callahan J, Harling J, Gaster L, Reith A, Laping N, and Hill C. SB-431542 is a potent and specific inhibitor of transforming growth factor-beta superfamily type I activin receptor-like kinase (ALK) receptors ALK4, ALK5, and ALK7. *Mol Pharmacol* 62: 65-74, 2002.
18. Kardon G. Muscle and tendon morphogenesis in the avian hind limb. *Development* 125: 4019-4032, 1998.
19. Kjaer M. Role of extracellular matrix in adaptation of tendon and skeletal muscle to mechanical loading. *Physiol Rev* 84: 649-698, 2004.
20. Kjaer M, Magnusson P, Krogsgaard M, Boysen Møller J, Olesen J, Heinemeier K, Hansen M, Haraldsson B, Koskinen S, Esmarck B, and Langberg H. Extracellular matrix adaptation of tendon and skeletal muscle to exercise. *J Anat* 208: 445-450, 2006.
21. Langley B, Thomas M, Bishop A, Sharma M, Gilmour S, and Kambadur R. Myostatin inhibits myoblast differentiation by down-regulating MyoD expression. *J Biol Chem* 277: 49831-49840, 2002.
22. Lee S, and McPherron A. Regulation of myostatin activity and muscle growth. *Proc Natl Acad Sci USA* 98: 9306-9311, 2001.
23. Léjard V, Brideau G, Blais F, Salingcarnboriboon R, Wagner G, Roehrl M, Noda M, Duprez D, Houillier P, and Rossert J. Scleraxis and NFATc regulate the expression of the pro-alpha 1(I) collagen gene in tendon fibroblasts. *J Biol Chem* 2007.
24. Liu Y, Cserjesi P, Nifuji A, Olson E, and Noda M. Sclerotome-related helix-loop-helix type transcription factor (scleraxis) mRNA is expressed in osteoblasts and its level is enhanced by type-beta transforming growth factor. *J Endocrinol* 151: 491-499, 1996.
25. Livak K, and Schmittgen T. Analysis of relative gene expression data using real-time quantitative PCR and the 2(-Delta Delta C(T)) Method. *Methods* 25: 402-408, 2001.
26. McCroskery S, Thomas M, Maxwell L, Sharma M, and Kambadur R. Myostatin negatively regulates satellite cell activation and self-renewal. *J Cell Biol* 162: 1135-1147, 2003.
27. McFarlane C, Plummer E, Thomas M, Hennebry A, Ashby M, Ling N, Smith H, Sharma M, and Kambadur R. Myostatin induces cachexia by activating the ubiquitin proteolytic system through an NF-kappaB-independent, FoxO1-dependent mechanism. *J Cell Physiol* 209: 501-514, 2006.
28. McHugh M, and Pasiakos S. The role of exercising muscle length in the protective adaptation to a single bout of eccentric exercise. *Eur J Appl Physiol* 93: 286-293, 2004.
29. McPherron A, Lawler A, and Lee S. Regulation of skeletal muscle mass in mice by a new TGF-beta superfamily member. *Nature* 387: 83-90, 1997.

30. Mendias C, Marcin J, Calerdon D, and Faulkner J. Contractile properties of EDL and soleus muscles of myostatin-deficient mice. *J Appl Physiol* 101: 898-905, 2006.
31. Mikic B, Bierwert L, and Tsou D. Achilles tendon characterization in GDF-7 deficient mice. *J Orthop Res* 24: 831-841, 2006.
32. Mikic B, Schalet B, Clark R, Gaschen V, and Hunziker E. GDF-5 deficiency in mice alters the ultrastructure, mechanical properties and composition of the Achilles tendon. *J Orthop Res* 19: 365-371, 2001.
33. Moens P, Baatsen PH, and Marechal G. Increased susceptibility of EDL muscles from mdx mice to damage induced by contractions with stretch. *J Muscle Res Cell Motil* 14: 446-451, 1993.
34. Murchison N, Price B, Conner D, Keene D, Olson E, Tabin C, and Schweitzer R. Regulation of tendon differentiation by scleraxis distinguishes force-transmitting tendons from muscle-anchoring tendons. *Development* 2007.
35. Patel K, Macharia R, and Amthor H. Molecular mechanisms involving IGF-1 and myostatin to induce muscle hypertrophy as a therapeutic strategy for Duchenne muscular dystrophy. *Acta Myol* 24: 230-241, 2005.
36. Petrof BJ, Shrager JB, Stedman HH, Kelly AM, and Sweeney HL. Dystrophin protects the sarcolemma from stresses developed during muscle contraction. *Proc Natl Acad Sci U S A* 90: 3710-3714, 1993.
37. Philip B, Lu Z, and Gao Y. Regulation of GDF-8 signaling by the p38 MAPK. *Cell Signal* 17: 365-375, 2005.
38. Pryce B, Brent A, Murchison N, Tabin C, and Schweitzer R. Generation of transgenic tendon reporters, ScxGFP and ScxAP, using regulatory elements of the scleraxis gene. *Dev Dyn* 236: 1677-1682, 2007.
39. Rebbapragada A, Benchabane H, Wrana J, Celeste A, and Attisano L. Myostatin signals through a transforming growth factor beta-like signaling pathway to block adipogenesis. *Mol Cell Biol* 23: 7230-7242, 2003.
40. Schweitzer R, Chyung J, Murtaugh L, Brent A, Rosen V, Olson E, Lassar A, and Tabin C. Analysis of the tendon cell fate using Scleraxis, a specific marker for tendons and ligaments. *Development* 128: 3855-3866, 2001.
41. Shukunami C, Takimoto A, Oro M, and Hiraki Y. Scleraxis positively regulates the expression of tenomodulin, a differentiation marker of tenocytes. *Dev Biol* 298: 234-247, 2006.
42. Siegel IM. The management of muscular dystrophy: a clinical review. *Muscle Nerve* 1: 453-460, 1978.
43. Smith T, Sweetman D, Patterson M, Keyse S, and Münsterberg A. Feedback interactions between MKP3 and ERK MAP kinase control scleraxis expression and the specification of rib progenitors in the developing chick somite. *Development* 132: 1305-1314, 2005.
44. Stevens ED, and Faulkner JA. The capacity of mdx mouse diaphragm muscle to do oscillatory work. *J Physiol* 522 Pt 3: 457-466, 2000.
45. Thomas M, Langley B, Berry C, Sharma M, Kirk S, Bass J, and Kambadur R. Myostatin, a negative regulator of muscle growth, functions by inhibiting myoblast proliferation. *J Biol Chem* 275: 40235-40243, 2000.

46. Tobin J, and Celeste A. Myostatin, a negative regulator of muscle mass: implications for muscle degenerative diseases. *Current opinion in pharmacology* 5: 328-332, 2005.
47. Tuite D, Renström P, and O'Brien M. The aging tendon. *Scandinavian journal of medicine & science in sports* 7: 72-77, 1997.
48. Wagner K, McPherron A, Winik N, and Lee S. Loss of myostatin attenuates severity of muscular dystrophy in mdx mice. *Ann Neurol* 52: 832-836, 2002.
49. Welle S, Bhatt K, and Pinkert C. Myofibrillar protein synthesis in myostatin-deficient mice. *Am J Physiol Endocrinol Metab* 290: E409-415, 2006.
50. Wolfman N, Hattersley G, Cox K, Celeste A, Nelson R, Yamaji N, Dube J, DiBlasio-Smith E, Nove J, Song J, Wozney J, and Rosen V. Ectopic induction of tendon and ligament in rats by growth and differentiation factors 5, 6, and 7, members of the TGF-beta gene family. *J Clin Invest* 100: 321-330, 1997.
51. Yang W, Chen Y, Zhang Y, Wang X, Yang N, and Zhu D. Extracellular signal-regulated kinase 1/2 mitogen-activated protein kinase pathway is involved in myostatin-regulated differentiation repression. *Cancer Res* 66: 1320-1326, 2006.
52. Zhu J, Li Y, Shen W, Qiao C, Ambrosio F, Lavasani M, Nozaki M, Branca M, and Huard J. Relationships between TGF-beta -1, myostatin, and decorin: Implications for skeletal muscle fibrosis. *J Biol Chem* 2007.
53. Zhu X, Topouzis S, Liang L, and Stotish R. Myostatin signaling through Smad2, Smad3 and Smad4 is regulated by the inhibitory Smad7 by a negative feedback mechanism. *Cytokine* 26: 262-272, 2004.

Chapter IV

Summary and Conclusion

Overview

Prior to the studies described in this dissertation, myostatin was known to be a negative regulator of muscle mass. What was not clear was whether or not the deficiency of myostatin had an impact on the function of either skeletal muscles or the structure of function of tendons. To clarify the role of myostatin deficiency on the function of skeletal muscles the structure and function of tendons, a combined approach was utilized that involved the use of transgenic animals for structural and functional studies and of cell culture work to establish the molecular mechanisms responsible for the structural and functional changes. The studies described in the previous three chapters indicate that myostatin regulates the structure and function of both skeletal muscles and tendons.

Discussion of Findings and Future Directions - Skeletal Muscle

Prior to the preliminary studies described in Chapter I and the study described in Chapter II, the deficiency of myostatin was known to increase the mass of skeletal muscles (10, 17). Furthermore, although myostatin deficiency improved the function of dystrophic muscles (1), the role of myostatin in the regulation of the function of healthy, non-dystrophic muscle tissue had not been determined. Consequently, the findings from the first and second chapters can be divided into two separate categories – structure and function.

Structure. The genetic deficiency of myostatin leads to both hypertrophy and hyperplasia of fast-fibered muscles (17). In prior studies, the measurements of the number of fibers in the skeletal muscles were determined from cross sections of muscles that might not provide an accurate indication of the true number of fibers (15). By digesting the ECM of EDL and soleus muscles and counting all of the fibers present in the muscle, we have now demonstrated that the deficiency of myostatin leads to a bona fide hyperplasia.

In addition to a greater number of fibers, myostatin deficiency leads to an increase in the CSAs of fibers. While myostatin inhibition increases satellite cell proliferation (12, 16, 27), this satellite cell inhibition does not appear to be wholly sufficient to explain the hypertrophic response that occurs with the inhibition of myostatin. Administering mice an inhibitory antibody against myostatin resulted in a 14% increase in muscle mass in only two weeks (29). This increase in muscle mass is unlikely to occur simply by modulating satellite cell activity. The preliminary study presented in Chapter I demonstrated that the deficiency of myostatin leads to a marked decrease in ubiquitinated myosin heavy chain and a decrease in atrogin-1 expression. No difference in relative myofibrillar protein content was observed between the muscles of $MSTN^{+/+}$ and $MSTN^{-/-}$ mice. These results suggest that the inhibition of myostatin leads to muscle fiber hypertrophy by the inhibition of protein degradation.

The deficiency of myostatin reduced collagenous fibrosis in *mdx* mice (1, 2, 28), but whether myostatin regulate the expression of type I collagen directly was not clear. The cell culture studies from Chapter II demonstrated that

myostatin increased directly the expression of type I collagen. Additionally, myostatin-deficient EDL muscles showed a decrease in whole muscle collagen content. These results indicated that, in addition to regulating the numbers of fibers in a muscle, myostatin regulated the ECM of skeletal muscle.

Function. In addition to the profound impact on the structure of skeletal muscle, myostatin had an impact on the function of skeletal muscle through the hypertrophy and hyperplasia present in the skeletal muscles of myostatin-deficient mice, and the impact these changes had on the contractile properties of muscles. The studies from Chapter II demonstrated that the deficiency of myostatin increased the P_o of both EDL and soleus muscles. When P_o was normalized to the CSA of the muscles to calculate sP_o, an unexpected finding was observed. As a muscle undergoes hypertrophy and is able to generate a greater P_o, the sP_o will usually decrease due to the increase in θ (15). Despite having a greater number of fibers, fiber CSA, P_o and θ, the EDL muscles from *MSTN*$^{+/-}$ and soleus muscles from *MSTN*$^{-/-}$ mice did not show a decrease in sP_o. In contrast, the EDL muscles of the *MSTN*$^{-/-}$ mice, that had a greater number of fibers, fiber CSA, P_o and θ did suffer from a decrease in sP_o. For a muscle that undergoes hypertrophy, a threshold appears to exist above which a decrease in sP_o occurs. In contrast, for small increases in muscle CSA, mass and P_o, sP_o does not change.

Furthermore, the deficiency of myostatin was found to increase the susceptibility of muscles to contraction-induced injury. Following contraction-induced injury, the EDL muscles of *MSTN*$^{-/-}$ mice had greater relative force

deficits than those of *MSTN*$^{+/+}$ mice. Despite having a greater force deficit following injury, the work done to stretch the muscles of *MSTN*$^{-/-}$ mice was less than *MSTN*$^{+/+}$ and *MSTN*$^{+/-}$ mice. As the series elastic component of muscles can protect fibers from injury (9), we initially hypothesized that the series elastic component of muscles of the *MSTN*$^{-/-}$ mice were more compliant, exceeded their elastic limit during the lengthening contractions, and therefore no longer acted as mechanical springs. This lead to a subsequent study of tendon structure and function, presented in Chapter III. After completion of the investigation of the properties of tendon structure and function, the initial hypothesis as to why the EDL muscles of *MSTN*$^{-/-}$ mice are more susceptible to contraction-induced injury was rejected. The rejection was based on the observation that the tendons of *MSTN*$^{-/-}$ mice were fourteen times stiffer than the tendons of *MSTN*$^{+/+}$ mice and the peak stiffness occurred at an early strain value. These findings suggested that the series elastic component of the tendons of the *MSTN*$^{-/-}$ mice were so stiff that they acted as a rigid body and did not take up much, if any, strain as the muscle was stretched. Extremely stiff tendons appear to be the reason why the deficiency of myostatin increases the susceptibility of the fast-fibered EDL muscles to contraction-induced injury.

Future Studies. An interesting finding from the studies presented in Chapter II is that the EDL muscles of *MSTN*$^{+/-}$ mice developed a greater P_o than the *MSTN*$^{+/+}$ mice, but unlike the *MSTN*$^{-/-}$ mice, no difference was observed in sP_o, or force deficit, after the injury. Even though the collagen content of the EDL muscles of *MSTN*$^{+/-}$ mice was less than that of *MSTN*$^{+/+}$ mice, this did not

increase the susceptibility of these muscles to contraction-induced injury. As the *MSTN*$^{+/-}$ mice have a 20% decrease in circulating myostatin levels compared to *MSTN*$^{+/+}$ mice, this suggests that the partial suppression of myostatin is able to increase force production of muscles without making the muscles more susceptible to injury. Based on the preliminary data in Chapter I that showed that myostatin increased protein degradation and the data in Chapter II that showed that myostatin increased type I collagen expression, the use of a pharmaceutical inhbitor of myostatin might be beneficial in the treatment of severe contraction-induced injuries. Following the induction of a severe lengthening contraction injury to the muscles of a mouse, the administration of a pharmaceutical inhibitor such as a monoclonal antibody against myostatin, the propeptide of myostatin, or a small peptide that blocks the interaction of myostatin with its receptors, the effect of myostatin inhibition on the recovery from a severe contraction induced injury could be determined. Based on the findings from Chapters I and II, the hypothesis that inhibition of myostatin promotes the long-term recovery of muscle from severe injury by blocking protein degradation and reducing fibrosis appears promising.

Discussion of Findings and Future Directions - Tendon

The study described in Chapter III demonstrated, for the first time, that myostatin has a profound impact on the structure and function of tendon tissue. The study not only described and characterized the phenotype of tendons from myostatin-deficient mice, but also demonstrated that myostatin can directly activate intracellular signal transduction cascades in tendon fibroblasts and

explored the possible cellular and molecular mechanisms behind the tendon phenotype. In addition to showing that myostatin can directly regulate tendon structure and function, Chapter III demonstrated for the first time that the bHLH transcription factor scleraxis continues to be expressed in adult tendon fibroblasts and that myostatin increases the expression of scleraxis directly. Tenomodulin was also shown to be a downstream target of myostatin signaling. While tenomodulin deficient mice displayed hypocellular tendons with no change in ECM structure or size (3), the mechanisms behind the control of cell proliferation by tenomodulin are not known. Three future studies are suggested that would provide further insight into the regulation of tendon physiology.

Study 1 – Myostatin-mediated regulation of scleraxis expression during development. During the development of tendon structures in the limb, tendon development can be categorized into three phases, each phase corresponding to an upregulation of scleraxis (4, 25). While FGF appears to be responsible for the third phase of scleraxis expression, FGF does not appear to be responsible for the first and second phases of scleraxis expression (4). Edom-Vovard and Duprez (4) suggested that a member of the GDF family is a likely candidate for the regulation of scleraxis expression during the first and second phases of early tendon development. To determine if myostatin induces the expression of scleraxis during the first and second phases of early tendon development, a double transgenic animal model could be utilized. Crossing the myostatin deficient mice with the *ScxGFP* line of mice that contain a GFP reporter linked to the scleraxis promoter (23) to obtain *MSTN*$^{-/-}$*ScxGFP* mice would create a model

organism that would allow for the visualization of scleraxis expression in the absence of myostatin at various stages of development. Comparing GFP intensity between *MSTN*$^{+/+}$*ScxGFP* and *MSTN*$^{-/-}$*ScxGFP* mice would be a useful first step to determine if myostatin is the cytokine that induces the first two phases of scleraxis expression. The most likely interpretation is that compared with *MSTN*$^{+/+}$*ScxGFP* mice, the GFP intensity in the tendon primordia of *MSTN*$^{-/-}$ *ScxGFP* mice is severely depressed.

Study 2 – *Myostatin-mediated biochemical modifications of tendons.* Compared with *MSTN*$^{+/+}$ mice, the tendons of *MSTN*$^{-/-}$ mice had a two-fold greater peak stress, less than half of the peak strain, and a fourteen-fold greater peak stiffness. Furthermore, the fibroblast density of the tendons of the *MSTN*$^{-/-}$ mice was only half that of the *MSTN*$^{+/+}$ mice. While the hypocellularity may explain the increase in stiffness, as fibroblasts can break the spontaneous cross-links that form between collagen molecules, changes in the activities of other enzymes might also occur that regulate tendon mechanical properties. Lysyl oxidase is the chief enzyme that can form cross-links between collagen molecules (6). In addition, elastin is a structural protein that allows tendon to have a greater peak stress (8). Determining the expression of lysyl oxidase and elastin in tendon might reveal the molecular mechanism behind the myostatin-mediated regulation of tendon mechanical properties. Based on the stiffness and peak strain data, myostatin might promote the expression of lysyl oxidase and elastin in tendon tissue.

Study 3 – Regulation of Tendon Fibroblast Proliferation by Tenomodulin. Tenomodulin is a type II transmembrane protein that promotes the proliferation of tendon fibroblasts (3), but the molecular mechanisms behind the actions of tenomodulin are not known. The tenomodulin protein consists of two domains, an N-terminal transmembrane anchor domain and a C-terminal extracellular domain (26). The C-terminal peptide is cleaved and presumably interacts with other receptors on the plasma membrane, but the identities of these receptors are not known. To determine if the C-terminal peptide of tenomodulin interacts with receptors on the plasma membrane, recombinant c-myc tagged C-terminal tenomodulin peptide could be incubated with tendon fibroblast cells followed by treatment with a crosslinking reagent. The cell homogenates would then be subjected to immunoprecipitation with an antibody against c-myc. The pull down would then be treated with a reagent to reverse the crosslinking and samples would be separated using 2D SDS-PAGE. Proteins would be removed from the gel and subjected to N-terminal sequencing. The amino acid sequence data could then be used to search for possible receptors with which the C-terminal peptide of tenomodulin interacts. The underlying mechanism could be that the C-terminal tenomodulin peptide interacts with a receptor that controls cell proliferation, but currently there is no basis for the selection of a particular receptor. Identifying the receptors with which tenomodulin interacts is the first step in determining the molecular mechanisms behind the tenomodulin-mediated increase in tendon fibroblast proliferation.

Summary

The studies described in this thesis demonstrate that myostatin not only has a profound impact on the structure and function of muscle tissue, but also on the structure and function of tendon tissue. While initially characterized as a cytokine that regulates skeletal muscle function, myostatin also has important roles in tendon, cardiac, bone, mammary and adipose tissue (5, 11, 18, 20, 30).

From an evolutionary perspective, an interesting question is: Why is there a gene for myostatin? The presence of larger, stronger muscles would appear to be beneficial for many aspects of everyday life. All vertebrate species have a myostatin gene (22), and fish have two copies (14). While myostatin has a controversial role in metabolism, one potential role of myostatin in metabolism is to divert food energy to fat, instead of to muscle (5, 7, 13, 18, 19, 30, 31). Diverting food energy to fat instead of muscle would presumptively better enable an animal to survive during periods of low food availability. A recent study explored the adaptive evolution of myostatin in the human genome (24). The authors of this study concluded that positive natural selection has acted on the myostatin gene, but acknowledged that the amount and rate of polymorphisms at the myostatin locus may suggest an evolutionarily recent decline in natural selective pressure for myostatin. While not all polymorphisms lead to a loss of function mutation, the greater the rate of polymorphisms, the greater the chance of developing a loss of function mutation. The authors rejected this decline in selective pressure at the myostatin locus based entirely on the long history of conservation of the myostatin gene across all vertebrate species (24). The

results of this thesis argue against a decline in the natural selective pressure at the myostatin gene. The studies in Chapter II indicate that the *MSTN*$^{+/-}$ mice generate greater forces, without incurring an increased susceptibility to injury. In the Whippet breed of racing dogs, a natural loss of the functional mutation in the myostatin gene has arisen (21). The *MSTN*$^{+/-}$ and *MSTN*$^{-/-}$ whippets are known as "Bully Whippets" and are considerably faster than their *MSTN*$^{+/+}$ counterparts (21). While we did not directly assess the amount of adipose tissue, the *MSTN*$^{+/-}$ mice appear to be leaner than their *MSTN*$^{+/+}$ littermates. We are currently conducting a longevity study of *MSTN*$^{+/+}$, *MSTN*$^{+/-}$, and *MSTN*$^{-/-}$ mice. While the study is still ongoing, our preliminary results indicate that the *MSTN*$^{+/-}$ mice have an 8 month longer maximum longevity than either the *MSTN*$^{+/+}$ or *MSTN*$^{-/-}$ mice. While the long history of selective pressure being applied at the myostatin locus may have helped our ancestors survive through periods of famine, in the developed world, currently most humans have access to a virtually unlimited source of food energy. The increased rate of polymorphisms does suggest a decline in selective pressure at the myostatin locus. With an unlimited access to food energy, the "larger, faster, stronger, leaner, longer-lived" phenotype of *MSTN*$^{+/-}$ organisms has clear advantages over the wild type phenotype. A pharmaceutical inhibitor of myostatin, Stamulumab (Myo-029, Wyeth), is currently in clinical trials in the USA and Europe. Stamulumab is not yet available for prescription in the USA, but is available for purchase in China and Korea. Inhibition of myostatin appears to be a practical and potentially useful treatment for many muscle wasting conditions and to counteract the decline in

muscle mass that occurs with aging. Future studies that determine the long term safety and efficacy of the use of myostatin inhibitors are warranted. Doping control policies and procedures for myostatin inhibitors must also be developed to ensure equality in athletic performance.

References

1. Bogdanovich S, Krag T, Barton E, Morris L, Whittemore L, Ahima R, and Khurana T. Functional improvement of dystrophic muscle by myostatin blockade. *Nature* 420: 418-421, 2002.
2. Bogdanovich S, Perkins K, Krag T, Whittemore L, and Khurana T. Myostatin propeptide-mediated amelioration of dystrophic pathophysiology. *FASEB J* 19: 543-549, 2005.
3. Docheva D, Hunziker E, Fässler R, and Brandau O. Tenomodulin is necessary for tenocyte proliferation and tendon maturation. *Mol Cell Biol* 25: 699-705, 2005.
4. Edom-Vovard F, and Duprez D. Signals regulating tendon formation during chick embryonic development. *Dev Dyn* 229: 449-457, 2004.
5. Feldman B, Streeper R, Farese R, and Yamamoto K. Myostatin modulates adipogenesis to generate adipocytes with favorable metabolic effects. *Proc Natl Acad Sci USA* 103: 15675-15680, 2006.
6. Gerriets J, Curwin S, and Last J. Tendon hypertrophy is associated with increased hydroxylation of nonhelical lysine residues at two specific cross-linking sites in type I collagen. *J Biol Chem* 268: 25553-25560, 1993.
7. Gonzalez-Cadavid N, and Bhasin S. Role of myostatin in metabolism. *Current opinion in clinical nutrition and metabolic care* 7: 451-457, 2004.
8. Gosline J, Lillie M, Carrington E, Guerette P, Ortlepp C, and Savage K. Elastic proteins: biological roles and mechanical properties. *Philos Trans R Soc Lond, B, Biol Sci* 357: 121-132, 2002.
9. Griffiths RI. Shortening of muscle fibres during stretch of the active cat medial gastrocnemius muscle: the role of tendon compliance. *J Physiol* 436: 219-236, 1991.
10. Grobet L, Martin L, Poncelet D, Pirottin D, Brouwers B, Riquet J, Schoeberlein A, Dunner S, Ménissier F, Massabanda J, Fries R, Hanset R, and Georges M. A deletion in the bovine myostatin gene causes the double-muscled phenotype in cattle. *Nat Genet* 17: 71-74, 1997.
11. Hamrick M, Pennington C, Webb C, and Isales C. Resistance to body fat gain in 'double-muscled' mice fed a high-fat diet. *International journal of obesity (2005)* 30: 868-870, 2006.
12. Langley B, Thomas M, Bishop A, Sharma M, Gilmour S, and Kambadur R. Myostatin inhibits myoblast differentiation by down-regulating MyoD expression. *J Biol Chem* 277: 49831-49840, 2002.
13. Lin J, Arnold HB, Della-Fera MA, Azain MJ, Hartzell DL, and Baile CA. Myostatin knockout in mice increases myogenesis and decreases adipogenesis. *Biochem Biophys Res Commun* 291: 701-706, 2002.
14. Maccatrozzo L, Bargelloni L, Cardazzo B, Rizzo G, and Patarnello T. A novel second myostatin gene is present in teleost fish. *FEBS Lett* 509: 36-40, 2001.
15. Maxwell L, Faulkner J, and Hyatt G. Estimation of number of fibers in guinea pig skeletal muscles. *Journal of applied physiology* 37: 259-264, 1974.

16. McCroskery S, Thomas M, Maxwell L, Sharma M, and Kambadur R. Myostatin negatively regulates satellite cell activation and self-renewal. *J Cell Biol* 162: 1135-1147, 2003.
17. McPherron A, Lawler A, and Lee S. Regulation of skeletal muscle mass in mice by a new TGF-beta superfamily member. *Nature* 387: 83-90, 1997.
18. McPherron A, and Lee S. Suppression of body fat accumulation in myostatin-deficient mice. *J Clin Invest* 109: 595-601, 2002.
19. Milan G, Dalla Nora E, Pilon C, Pagano C, Granzotto M, Manco M, Mingrone G, and Vettor R. Changes in muscle myostatin expression in obese subjects after weight loss. *J Clin Endocrinol Metab* 89: 2724-2727, 2004.
20. Morissette M, Cook S, Foo S, McKoy G, Ashida N, Novikov M, Scherrer-Crosbie M, Li L, Matsui T, Brooks G, and Rosenzweig A. Myostatin regulates cardiomyocyte growth through modulation of Akt signaling. *Circ Res* 99: 15-24, 2006.
21. Mosher D, Quignon P, Bustamante C, Sutter N, Mellersh C, Parker H, and Ostrander E. A mutation in the myostatin gene increases muscle mass and enhances racing performance in heterozygote dogs. *PLoS Genet* 3: e79, 2007.
22. Pie M, and Alvares L. Evolution of myostatin in vertebrates: is there evidence for positive selection? *Mol Phylogenet Evol* 41: 730-734, 2006.
23. Pryce B, Brent A, Murchison N, Tabin C, and Schweitzer R. Generation of transgenic tendon reporters, ScxGFP and ScxAP, using regulatory elements of the scleraxis gene. *Dev Dyn* 236: 1677-1682, 2007.
24. Saunders M, Good J, Lawrence E, Ferrell R, Li W, and Nachman M. Human adaptive evolution at Myostatin (GDF8), a regulator of muscle growth. *Am J Hum Genet* 79: 1089-1097, 2006.
25. Schweitzer R, Chyung J, Murtaugh L, Brent A, Rosen V, Olson E, Lassar A, and Tabin C. Analysis of the tendon cell fate using Scleraxis, a specific marker for tendons and ligaments. *Development* 128: 3855-3866, 2001.
26. Shukunami C, Oshima Y, and Hiraki Y. Molecular cloning of tenomodulin, a novel chondromodulin-I related gene. *Biochem Biophys Res Commun* 280: 1323-1327, 2001.
27. Thomas M, Langley B, Berry C, Sharma M, Kirk S, Bass J, and Kambadur R. Myostatin, a negative regulator of muscle growth, functions by inhibiting myoblast proliferation. *J Biol Chem* 275: 40235-40243, 2000.
28. Wagner K, McPherron A, Winik N, and Lee S. Loss of myostatin attenuates severity of muscular dystrophy in mdx mice. *Ann Neurol* 52: 832-836, 2002.
29. Whittemore L, Song K, Li X, Aghajanian J, Davies M, Girgenrath S, Hill J, Jalenak M, Kelley P, Knight A, Maylor R, O'Hara D, Pearson A, Quazi A, Ryerson S, Tan X, Tomkinson K, Veldman G, Widom A, Wright J, Wudyka S, Zhao L, and Wolfman N. Inhibition of myostatin in adult mice increases skeletal muscle mass and strength. *Biochem Biophys Res Commun* 300: 965-971, 2003.
30. Zhao B, Wall R, and Yang J. Transgenic expression of myostatin propeptide prevents diet-induced obesity and insulin resistance. *Biochem Biophys Res Commun* 337: 248-255, 2005.

31. Zimmers T, Davies M, Koniaris L, Haynes P, Esquela A, Tomkinson K, McPherron A, Wolfman N, and Lee S. Induction of cachexia in mice by systemically administered myostatin. *Science* 296: 1486-1488, 2002.